A PROBLEM ASSOCIATED WITH THE DESIGN OF RADIO TELEMETRIC EQUIPMENT.

PRESENTED FOR THE DEGREE OF DOCTOR OF PHILOSOPHY OF GLASGOW UNIVERSITY.

IAN COCHRANE, B.Sc., D.R.T.C.
10 ROTHMAN AVENUE
GREAT BADDOW
CHELMSFORD
ESSEX.

P R E F A C E.

This thesis presents the results of an experimental investigation of the concept of a transient fluctuation of frequency. Consideration of an oscillator subjected to continuous cisoidal variations in capacitance shows that its output contains a large number of harmonics; if the frequency with which the capacitance is varied is high enough, instability occurs with a change in the harmonic content of the output. Therefore, if the capacitance is varied as a step-function of time, it is to be expected that at least all the harmonics of the steady-state case will occur, each multiplied by some attenuation constant, with perhaps a rapidly damped instability. Under these conditions it would appear that the frequency would not change instantly from one value to another, but would pass through a transient condition. No published account of work either experimental or theoretical could be found on this subject, and therefore it is claimed that the concept of transient frequency is original. The method of experimentally analysing the waveform to obtain the frequency transient is also claimed as original. The various circuits used are all well described in the literature, although it is thought that the type of reactor valve used is an original application of a well-known effect; the literature on circuits is so extensive, however, that no positive claim of originality may be made.

The results of this investigation were analysed empirically, design criteria being evolved; no theoretical

analysis of the frequency-modulated oscillator is given, since the conditions which apply to the oscillator herein invalidate the assumptions required to obtain a solution. Since the method of waveform analysis was very laborious and time-consuming, the work was restricted to an investigation of one type of oscillator and reactor unit, refinements of the method being suggested for future work. This investigation arose from, and the results are particularly applicable to, sequence-sampler frequency-modulated telemetric systems, although the results may be extended to any Frequency-modulated system in which the modulating waveform consists of a pulse train.

Thanks are due to Drs. Fairley and Lamont of the Royal Technical College, Glasgow, for their constructive criticism of the experimental work, and to Mr. R.G. Hulse of Marconi College, Chelmsford, for helpful discussions. In particular, the author is indebted to Professor F.M. Bruce of the Royal Technical College, Glasgow, for his generous assistance and advice throughout the whole of this investigation, and for his permission to carry out the experimental work in his department.

I.C.

CHAPTER 1.

THE CONCEPT OF FREQUENCY TRANSIENTS.

1.1. Origin of subject.

The concept of frequency transients arose from past work carried out by the author on a radio telemetric system utilising frequency modulation. The art of radio telemetry is concerned with the automatic transmission of suitably transformed physical data from a remote object to a base station by means of a radio link. The term physical data is used to denote physical quantities such as temperature, pressure, acceleration, strain etc., as distinct from intelligence as transmitted by telegraphy or telephony. In most cases, radio telemetry is used under circumstances which do not permit the presence of an operator to observe the required data, as in a rocket projectile or a controlled torpedo.

Thus, the condition to be measured in the remote object is transformed into a voltage, which is then used to modulate an U.H.F. transmitter either in amplitude or frequency. The base station demodulates the signal, and since the system can be calibrated, the value of the original condition may be ascertained at any instant of time. By using a cathode ray tube display with a drum-camera, a continuous record of the fluctuation of the condition may be obtained.

In the frequency modulated system referred to in

the first paragraph, it was desired to obtain information on the fluctuation of strains, temperatures, pressures, acceleration and fuel consumption from a rocket-type guided projectile in flight. The projectile carried 24 different sources of information, hereinafter called 'channels', each channel being recurrently sampled. During the sampling period for any one channel, the output of that channel was used to vary the frequency of an oscillator about a centre or zero modulation frequency of 400 Kc/s by an amount determined by the level of the quantity being sampled. The output from this oscillator was frequency multiplied by normal means and radiated at a carrier frequency of 469 Mc/s. In this case, the sampling device consisted of a motor driven rotary switch, each channel being connected to a separate stator stud and for the purposes of channel recognition at the base station, there was one synchronising channel which transmitted a distinctive signal, once every revolution of the switch, making the total number of channels 25.

At the base station, the received signal was demodulated in a manner which is of no concern here and by a system of gating, each channel was separated out and displayed on separate oscilloscopes, a continuous film record being taken over the time of flight - in this case, about 3 minutes. The gating system was so arranged that of the transmission time of each channel, the first and last portions were not recorded because of a certain amount of instability produced by the

switch arms bouncing at make, and towards break, as the contact slid partially clear of the stud.

This system produced fairly good and consistent results, but there were limitations to the accuracy obtainable. To obtain high accuracy the channel recurrence frequency should be as high as possible. This infers a short sampling period per channel and hence the total allowable instability period must be decreased accordingly. The same problem exists if more than the 25 channels used in this system are required.

The first step towards a solution was an electronic commutating device, and it was known before the commencement of this investigation that the Germans had successfully used such a device in the telemetering of V2 rockets and that another similar system had been used in the U.S.A.[1,2.] The details of these systems are not relevant here, but, with the knowledge that fast commutation was possible, it was the author's opinion that the final upper limit to commutation speed would be imposed by the frequency modulated oscillator itself.

Thus, the problem appeared to be a consideration of the factors affecting the rate of change of frequency of an oscillator, when the modulating signal varied in a time of the same order as the period of one cycle at the unmodulated frequency. It was thought that under these conditions of modulation, the oscillator frequency would go through some transient condition before settling down to the new

steady value. Assuming there is a frequency transient, it is required to investigate its duration and the effect of the oscillator circuit parameters upon it. Also, under these conditions, the definition to be given to the term 'frequency' requires modification.

In an attempt to gain information on these problems, a library search failed to reveal any published experimental work on this subject. Van der Pol[3,4], McLachlan[5], Maginnis[6] and others[7-15] have explored various aspects of the theoretical field, dealing with resonant circuits whose parameters varied by a small amount with respect to their mean value as continuous functions of time.

Again, Barrow[16-18], in 1932-34 completed a mathematical analysis of such a circuit, and carried out experimental work at low audio frequency to support his theory. However, Barrow did not measure the frequency changes which occurred, but was only concerned with the amplitude of the oscillation, and with the coincidence of the unstable regions with those predicted by his theory. Further, his equipment was crude by modern techniques, using a mechanically switched capacitor to give the required variation in capacitance.

More recently, Barber[19] has examined experimentally the response of variable parameter resonant circuits with a signal of constant frequency applied to them. The rate of resonant frequency variation was of the order of 1,000 c/s/s, which is very slow, as can be seen by comparison with the figures given in 1.2.

Thus it appeared that no attempt had been made to investigate experimentally the frequency variation resulting from a very fast rate of change of parameter. This thesis embodies the results of an experimental investigation into the behaviour of the frequency of a self-sustaining oscillatory system modulated in frequency by a waveform which is approximately a step function of time. The fundamental meaning of the term 'frequency' was examined and a new method of instantaneous frequency measurement was developed.

1.2 General Outline of Method.

To carry out this investigation, an L - C oscillator was chosen, since most of the relevant published mathematical analyses had been on this type of circuit. Secondly, an L - C oscillator permits of an electronic method of varying the parameters by means of a reactor stage. The reactor stage is equivalent to a variable reactance in parallel with a variable resistance, the variation being controlled by a modulating signal at the input terminals of the reactor stage. If the reactor stage is placed across the tuned circuit of an L - C oscillator, it varies not only the frequency but also the amplitude of the oscillator output. In this investigation, the reactor and oscillator were considered as one integral unit, and the frequency transient measured was the resultant transient behaviour of this unit, since it is the overall response that is required in practice.

It was thought that a modulating signal consisting of a

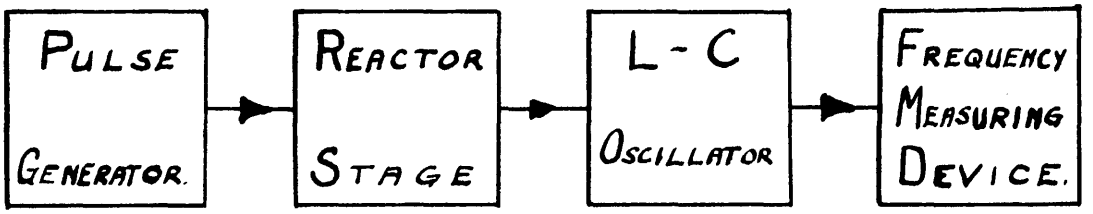
PULSE GENERATOR.
REACTOR STAGE
L - C OSCILLATOR
FREQUENCY MEASURING DEVICE.

FIG. 1.1.

step function pulse of voltage would represent the worst possible modulating conditions, that is, the best condition for the production of a frequency transient. Hence the modulating signal used consisted of a train of similar rectangular pulses of known rise-time. The block diagram of the basic scheme is shown in Fig. 1.1.

Ideally, each pulse should have an infinitely short rise-time, but there are practical limits to the speed of rise of a pulse. Since the centre frequency of the L - C oscillator used in the practical system was in the region of 500 Kc/s, this frequency was chosen for this investigation and a rise time of 0.2 μsec. was considered satisfactory. Thus, the oscillator frequency should change in 1/10th of a cycle of the unmodulated frequency, and for a frequency change of 5% the rate of change of frequency is 125 Kc/s per μsec. For all practical purposes this frequency variation may be considered as a very close approach to that resulting from the ideal of a step function modulating voltage. It is to be noted that a rate of change of frequency of 125 Kc/s/μsec. is far in excess of that met with in commercial F.M. systems. By law, in the U.S.A. the maximum frequency deviation is $\pm$ 75 Kc/s about a carrier frequency of 40 Mc/s or over. Thus, the total frequency swing is 150 Kc/s and corresponds to the 'loudest' note transmitted. It is certain that the maximum audio frequency in the modulating signal will never exceed 20 Kc/s.

This gives a maximum rate of change of frequency of 150 Kc/s. in 50 μsec. or 3 Kc/s per μsec.

Various means of measuring a frequency that varied with time were considered and from the results of this investigation a novel method of frequency measurement was derived. The main investigation was carried out by this means.

CHAPTER 2.

METHODS OF MEASURING FREQUENCY VARIATION.

Of the devices for measuring frequency in the range of frequency between 100 Kc/s and 1 Mc/s., bridge circuits, beat frequency oscillators, Lissajou figures, etc., are all well-known methods. Some can be used to measure a slowly varying frequency, but there appears to be nothing known on the transient response of these methods to a fast frequency variation, and some, such as the Lissajou figure and beat-frequency methods are obviously unsuited for measuring such a variation. A very few are deliberately designed to measure a fast frequency change, such as the Foster-Seeley Phase Discriminator and Ratio Detector but the upper limit to the rate of frequency variation is restricted.

2.1. Requirements of Measuring Equipment.

Frequency measuring equipment may be divided into two broad categories -

(a) Equipment which gives a voltage output proportional to the frequency of the input signal.

(b) Oscilloscope techniques.

Dealing first with category (a) equipment and in terms of an extremely fast and erratic frequency fluctuation, there are two fundamental requirements.

Firstly, the output voltage of the circuit must follow faithfully the frequency variations of the input signal; the

frequency/voltage transfer function should not contain any exponential or cisoidal term which is not a function of the input frequency only. Secondly, variation in the amplitude of the input signal must not produce variation of the output voltage. The sensitivity $\delta v / \delta f$ should be as high as possible, for the sake of accuracy, and there must be no ambiguity with respect to increasing and decreasing frequencies. The mechanical inertia of an indicating meter is too great for use in measuring the output from this type of equipment.

For category (b) techniques, the fundamental requirements are rather different, and each technique tends to have different conditions imposed upon it. In general, all methods are comparative, and the one essential requirement is that the standard signal must have no deleterious effect whatever on the waveform under inspection - in particular, the standard signal must not 'pull' the frequency of the test signal. Nearly all oscillograph techniques measure the time per cycle, rather than the cycles per unit time, and no very small percentage differences in lengths of time are readily discernible and mensurable.

2.2. Unsuitable Methods.

The following methods of frequency measurement were discarded as unsuitable for the reasons stated.

(a) All methods in which a standard signal generator is required to 'follow' the varying frequency to be measured.

For example, the Beat Frequency principle could not be used

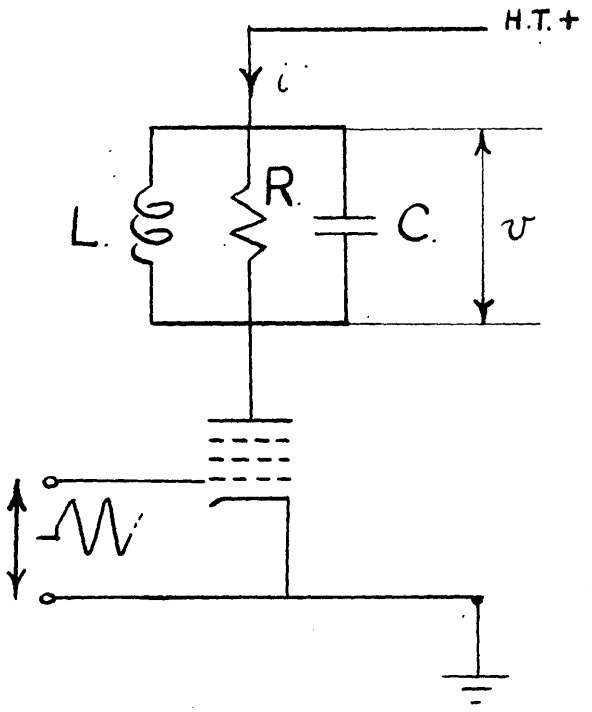

FIG. 2.1.

to follow the deviation of a frequency modulated signal, due not only to the number of side bands produced but also to the physical impossibility of following the frequency deviation quickly enough.

Any form of Lissajou figure could not be employed for exactly the same reasons.

(b) Any method dependent upon the variable impedance of a resonant R, L, C, circuit was deemed unsuitable for the purpose of measuring a varying frequency. Consider a parallel R, L, C, circuit connected in the anode circuit of a pentode, and let a step function pulse of form $E \sin(\omega t + \theta)U(t)$ arrive at the grid of the pentode at time $t = 0$, as shown in Fig. 2.1.

The solution for the resultant anode voltage is shown in Appendix 1. Consider only the transient part of the solution obtained there, i.e.

$$\frac{Ie^{-\alpha t}}{\omega_o C} \cdot \sin\theta . \sin\omega_o t . - I|Z|e^{-\alpha t}\left[\cos\omega_o t . \sin(\theta+\phi)\right.$$

$$\left. + \frac{\omega}{\omega_o}\sin\omega_o t . \cos(\theta+\phi) + \frac{\alpha}{\omega_o}\sin\omega_o t . \sin(\theta+\phi)\right].$$

From this it is obvious that the magnitude and phasing of the transient with respect to the applied signal depends on the initial phase angle. In the above work, ω_o is now taken as the frequency for maximum impedance for simplicity and consideration of two special cases which are of particular interest here shows the effects of the transient term. Let

the signal frequency ω be removed from ω_0 in each case, and firstly let θ be zero, and secondly let θ be $\pi/2$. For the first case

$$\theta = 0 \ , \quad \varphi \approx \pm \pi/2 \ , \ and$$

$$v_t \approx I|Z| e^{-\alpha t}\left[\pm \cos \omega_0 t \pm \frac{\alpha}{\omega_0} \sin \omega_0 t\right].$$

But $\frac{\alpha}{\omega_0} \ll 1$, hence the second term in the brackets may be ignored with respect to the first, at least, as a first approximation. Thus, for v(t)

$$v(t) \approx \pm I|Z|\left[\cos \omega t - e^{-\alpha t} \cos \omega_0 t\right].$$

Now consider the result obtained with $\theta = \frac{\pi}{2}$. $(\varphi \approx \pm \frac{\pi}{2})$. For this case

$$v_t \approx I|Z| . e^{-\alpha t}\left[-\sin 0 . \cos \omega_0 t - \left\{\left(\frac{\omega_0}{\omega} - \frac{\omega}{\omega_0}\right) \mp \frac{\omega}{\omega_0}\right\} \sin \omega_0 t\right],$$

since, ignoring α, $Z = \frac{j\omega}{C(\omega_0^2 - \omega^2)}$; $|Z| = \frac{\omega}{C(\omega_0^2 - \omega^2)}$.

$$\therefore v(t) \approx \pm I|Z|\left[\sin \omega t - e^{-\alpha t} \frac{\omega_0}{\omega} \sin \omega_0 t\right].$$

Therefore from these two equations, it is seen that in the first case the magnitude of the transient term is equal to the steady state amplitude, whereas in the second the magnitude of the transient depends on the ratio ω_0/ω. Thus the transient term is very dependent on the initial phase angle and the ratio ω_0/ω. This result shows the effect of a suddenly applied cisoidal waveform on a tuned circuit which was initially

quiescent. If the circuit was already oscillating say, at its natural frequency, when a signal of frequency ω is impressed upon it, the resultant transient would again depend upon the initial phase angle φ, and also upon the charge and current associated with C and L respectively at the instant of application of ω[20,21].

For these reasons, such a circuit, or any equipment containing such a circuit, was thought to be unsuitable for the measurement of a varying frequency.

2.3 Bridge Methods.

There exists an almost limitless number of bridge circuits which could be used for frequency determination. In the range of frequencies considered here, the Wien Bridge[22] is one circuit which has received considerable attention, mainly because no arm contains inductance and its response curve is similar to that of a parallel resonant circuit. For these reasons this circuit was considered a possible means of measuring a frequency variation, provided the amplitude variation associated with the frequency variation is small, since all bridge circuits give an output proportional to the input amplitude. But this type of bridge circuit has

the undesirable feature of requiring either a transformer coupled input circuit, or some form of balanced push-pull output. Further, the selectivity of the bridge is rather poor. However, the Wien Bridge is equivalent, electrically, to a Parallel-T Network, but the latter has the advantage of having one side of both its input and output common; this is an advantage if an amplifier is to be used. Therefore, the Parallel-T network was preferred.

2.4 The Parallel-T Net and Feed-Back Amplifier.

(a) Parallel-T Filter.

A typical Parallel-T filter section is shown in Fig.2.2 This network appears to have been first suggested by H.H. Scott[23] as a frequency selective circuit, and is important because its common input and output point facilitates its inclusion as a feed-back loop in frequency sensitive amplifiers. The mathematical analysis of this filter section is amply described in the literature,[24-27] and a summary of the results of such an analysis is included here for reference in the subsequent design of a frequency sensitive amplifier. Each T-section is transformed to an equivalent π-section and putting the two derived π-sections in parallel yields, with reference to Fig. 2.2.

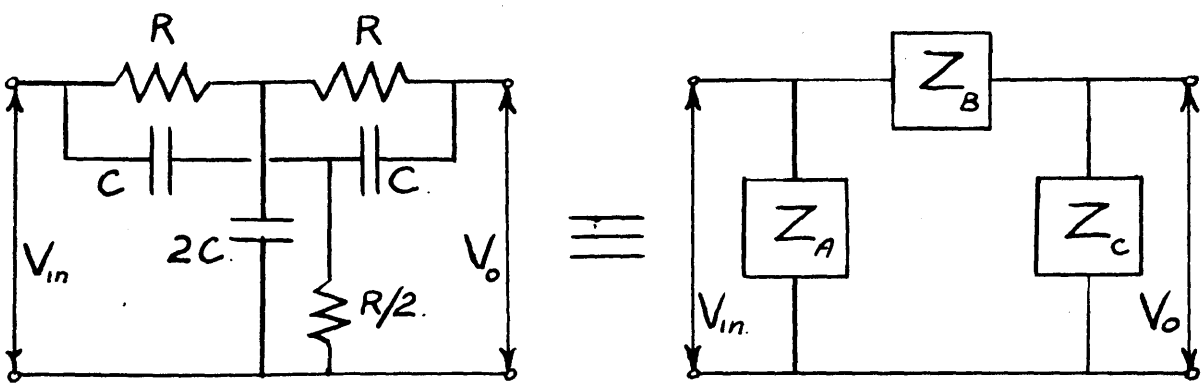

FIG. 2.2.

$$Z_A = Z_C = \tfrac{1}{2}\left(R - \frac{j}{\omega C}\right),$$

$$Z_B = 2R(1 + j\omega CR)/(1 - \omega^2 C^2 R^2).$$

At some value of $\omega = \omega_0$, Z_B will become infinite, the output voltage being then zero, and for this null point,

$$\omega_0 = \frac{1}{RC}.$$

Also, the input and output impedance become equal,

$$Z_A = Z_C = \tfrac{1}{2}(R - jR),$$

and

$$|Z_A| = R/\sqrt{2}.$$

If the filter section is nowloaded by an impedance Z comprised of a parallel combination of resistance (aR) and capacitance (C/a), where $a > 0$, the transfer function $S(\omega) = V_{out}/V_{in}$ can be shown to be

$$S(\omega) = \frac{1}{1 + \frac{2}{a} + j4\left(\frac{1 + 1/a}{K - 1/K}\right)},$$

for any ω, where $K = \omega_0/\omega$. This expression is symmetrical about $K = 1$ when plotted against log K, since inversion of K does not affect $|S(\omega)|$; for symmetry Z must be complex, and of the form given above. The effect of loading the filter section is to decrease the rate of change of $S(\omega)$ with K,

and therefore (a) is normally made as large as possible. With (a) infinite, the selectivity $\frac{\partial}{\partial K}(S(\omega))$ is still too low for some purposes, and the selectivity of the practical loaded section may be increased greatly by incorporating the filter section as the feed-back loop in a valve amplifier.

A skeleton circuit of such an arrangement is shown in Fig. 2.3 . At the balance frequency the output is maximum, since the feed-back is zero. The general considerations of design are :-

(a) The feed-back from output to input terminals of the amplifier must always be in the correct phase, for if the feed-back becomes positive, instability will occur.

(b) The load impedance across the terminals of the bridge must be as high as possible, as it affects the selectivity both in amplitude and phase, with the possibility of instability. The preference will be for feed-back to the grid-circuit of a valve, rather than to the cathode.

(c) The input impedance of the bridge must have negligible shunting effect upon the anode load, R_L in Fig. 2.3. R_L must not be too high, or the bridge resistive elements become so great that the fulfilment of condition (b) is very difficult. Also, for large values of ω_0 the required bridge

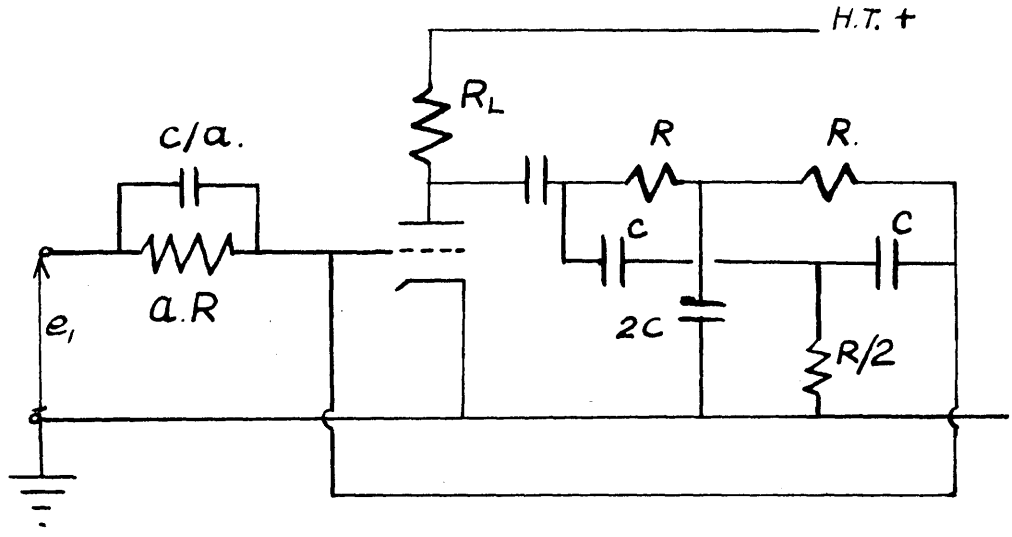
H.T. +
R_L
c/a.
R
R.
C
C
2C
a.R
e_1
R/2

FIG. 2.3.

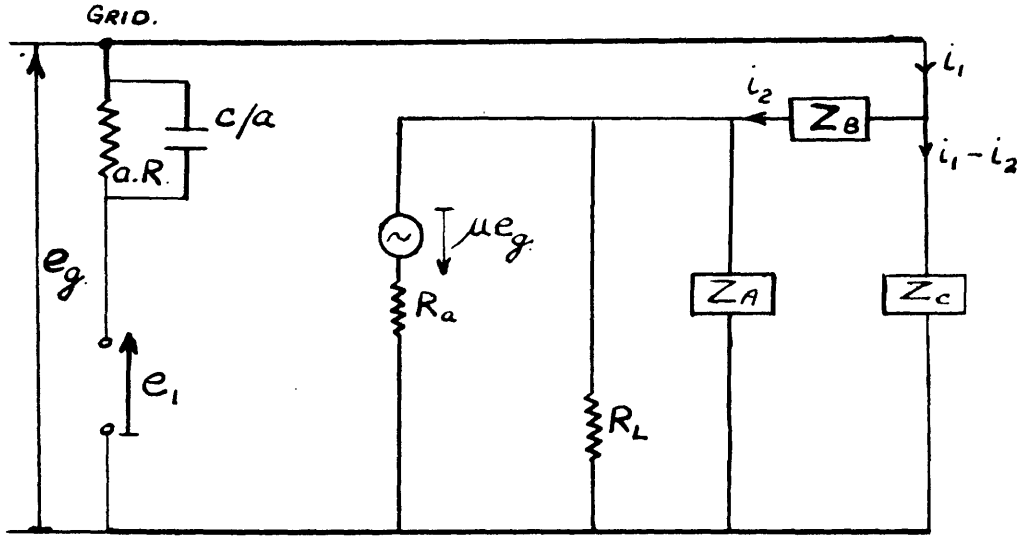
GRID.
c/a
a.R
e_g
e_1
μe_g
R_a
R_L
Z_A
Z_B
Z_C
i_1
i_2
$i_1 - i_2$

FIG. 2.4.

capacitance C would become extremely small.

(d) The source impedance of the input signal must be negligible compared to the bridge load comprised of (aR) in parallel with C/a.

(e) The stray capacitance between the output and input of the complete amplifier must be a minimum.

To obtain negative feed-back an amplifier containing an odd number of stages is preferred to permit feed-back to the input grid as required by condition (b). The limit to the number of stages is one of stability, for as the number of stages, and hence the total gain, increases, the overall stability will tend to decrease. For increased selectivity, it is preferable to use two or more complete selective amplifiers in series, each of moderate gain, rather than one frequency selective bridge looped between the output and input of a high-gain amplifier chain. A typical circuit of such an amplifier and feed-back loop is shown in Fig.2.3. The overall gain of this amplifier as a function of frequency or K, may be derived from its equivalent circuit in Fig.2.4., giving,

$$G(\omega) = 2M\left[\frac{(1-\frac{1}{K^2}) + j\frac{3}{K}}{(1-\frac{1}{K^2})\{2+a(1+M)\} + j\frac{4}{K}(a+1)}\right]$$

where $G(\omega)$ = gain from input to output terminals,

M = available grid to anode gain

$$= -\mu \cdot \frac{R_L}{R_a + R_L}$$

At the balance, or null, frequency, ω_o, of the Parallel-T section, the overall gain reduces to,

$$G(\omega)_{\omega=\omega_o} = \frac{M}{a+1},$$

since K = 1.

This is the maximum gain attainable, and shows the conflicting limitations placed on the parameter (a). For the filter section alone (a) must be large to prevent the load reducing the selectivity; for the feed-back amplifier (a) must not be too large or the attainable gain is reduced, hence reducing selectivity. Therefore, the practical range of (a) is usually between 3 and 10.

Using these results a feed-back amplifier was designed. Since a variation in frequency is to be measured, the balance frequency must be kept above or below the maximum or minimum frequency to be measured, respectively, to avoid ambiguity of result. Thus,

$$f_o > f_c + \delta f \quad \text{or} \quad f_o < f_c - \delta f,$$

where f_c is the unmodulated frequency.

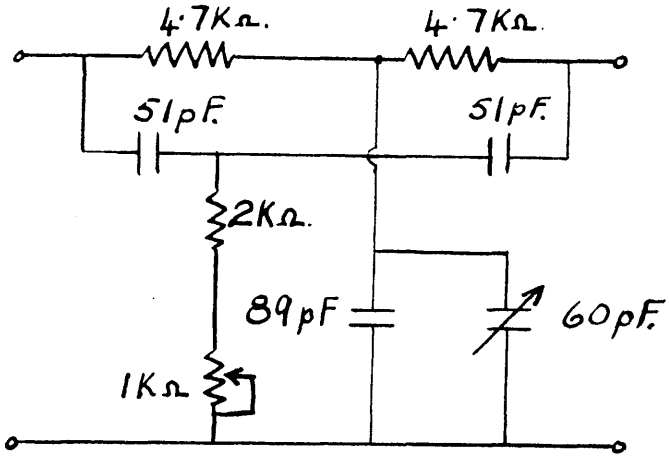
4·7KΩ.
4·7KΩ.
51pF.
51pF.
2KΩ.
89pF
60pF.
1KΩ

FIG. 2.5.

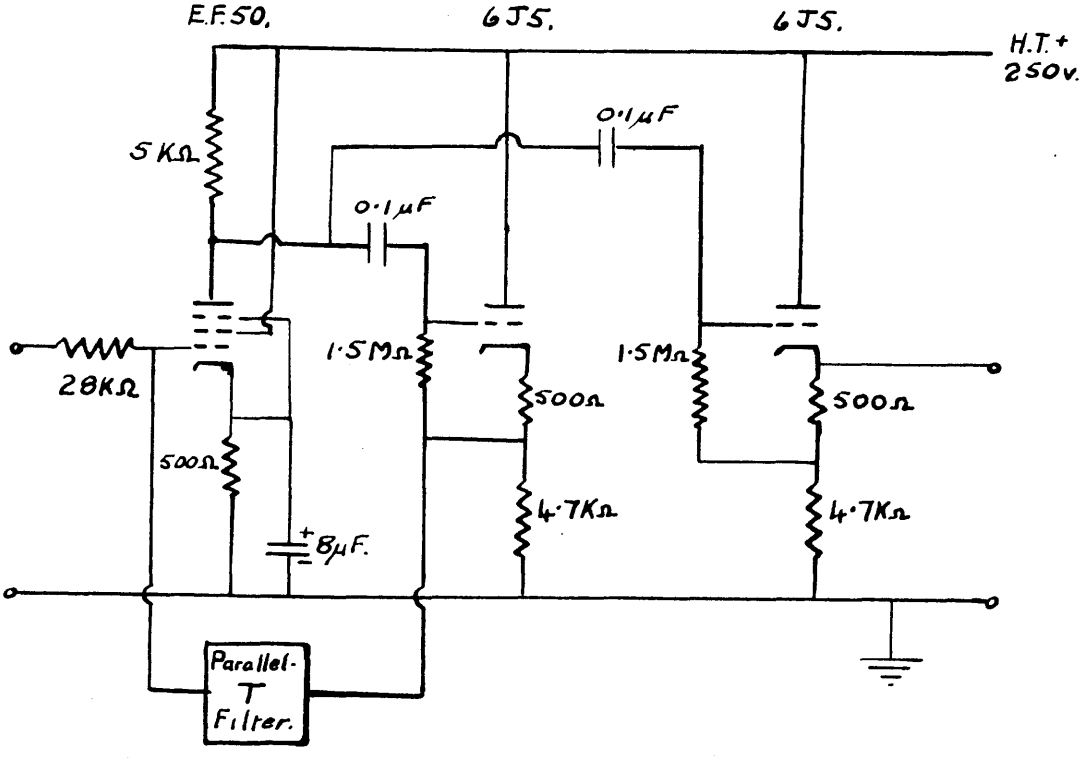
E.F.50.
6J5.
6J5.
H.T.+
250v.
0·1μF
5KΩ
0·1μF
28KΩ
1·5MΩ
1·5MΩ
500Ω
500Ω
500Ω
4·7KΩ
4·7KΩ
+
8μF.
Parallel-
T
Filter.

FIG. 2.6.

For $f_o = 500$ Kc/s and δf additive only, a balance frequency, f_o, of 700 Kc/s was chosen. To keep R (in the bridge) as high as possible, C was chosen as 51 pF, a standard value of a range of low-loss ceramic capacitors. Thus,

$$R = \frac{1}{\omega_o C} = 4{\cdot}46\,K\Omega.$$

The nearest standard resistor was 4.7 K.Ohms,

$\therefore$ the minimum filter input impedance $= \frac{4{\cdot}7}{\sqrt{2}} = 3{\cdot}3K\Omega.$

This low value required a cathode follower between the amplifier and the bridge, to prevent reduction of amplifier gain by the low bridge impedance at K = 1 shunting the anode load.

The filter alone is shown in Fig.2.5, where the variable elements in the earthed limbs were used to align the balance frequency on $f_o = 700\,Kc/s$. This was required because of the usual tolerances on components.

An EF.50 pentode was used as the amplifying valve, with a listed $R_a > 1M\Omega$ and a measured g_m of $6.6\ mA/V$.

Thus, for an anode load of 5 K.Ohms,

$$M \simeq g_m R_L = 33.$$

The parameter (a) must be chosen large enough to make the bridge load much greater than the output impedance of the signal source

For a = 6, the bridge load is,

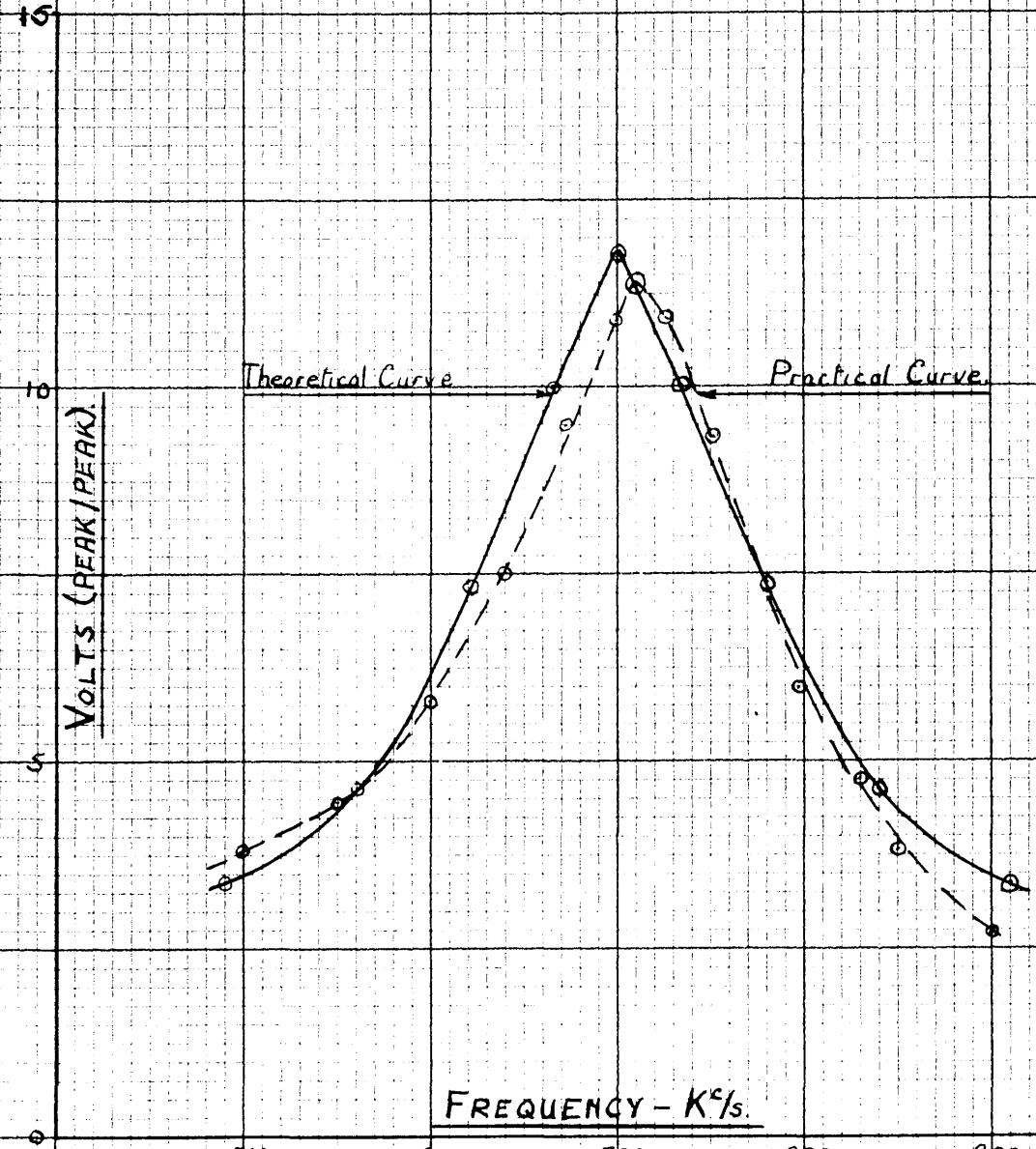
15
10
5
0
Theoretical Curve.
Practical Curve.
VOLTS (PEAK/PEAK).
FREQUENCY - K^c/s.
400
500
600
700
800
900

GRAPH 2.1.

$$aR = 28K\Omega, \quad \frac{C}{a} = 8pF,$$

the capacitance being supplied by interelectrode and stray capacities.

$$\therefore \quad G(\omega)_{\omega=\omega_0} = 4 \cdot 74 .$$

A cathode follower placed between the anode of the amplifier and the bridge does not decrease $G(\omega)_{\omega=\omega_0}$; it does decrease the sharpness of the selectivity curve, since at all other frequencies the voltage fed back is decreased by the fractional gain of the cathode follower, which, in this case, was 0.88. The complete circuit is shown in Fig.2.6. Using a Marconi Standard Signal Generator giving a 1v. R.M.S. output, the curve of Graph 2.1 was recorded on a Cossor Model 1035 Oscilloscope, with an external d.c. shift control on the second beam to measure amplitude of trace.

In the calculation of the theoretical curve, the gain of the feed-back amplifier G (ω), was modified by the inclusion of a cathode follower of gain g giving

$$G'(\omega) = 2M \left[\frac{(1 - \frac{1}{K^2}) + j\frac{4}{K}}{(1-\frac{1}{K^2})\{2 + a(1+gM)\} + j\frac{4}{K}(a+1)} \right]$$

This is the general equation for a Parallel-T amplifier.

An examination of Graph 2.1 shows that the practical curve is asymmetric about a frequency of 710 Kc/s., although the bridge circuit itself had been

set up to 700 Kc/s. From the theoretical curve, the maximum selectivity was found to be 17 Kc/s per volt - selectivity being defined as the change in frequency required to produce a change of 1 volt at the output. For the practical circuit, for frequencies below 710 Kc/s. the maximum selectivity was found to be 18.5 Kc/s per volt, but for frequencies above 710 Kc/s the selectivity rose to 13.3 Kc/s per volt. Thus, for K = 1, the theoretical and practical curves agree fairly well, but for K = 1 the sharper decrease in output voltage was attributed to the fall-off in available gain of the amplifier in the feed-back circuit with increasing frequency, together with some asymmetry in the bridge. At 850 Kc/s, the practical curve suggests that the available gain has fallen to 0.8 of its mid-band value, which gives a value of 25 pF. for the shunting capacitances, the anode load being 5 K.Ohms. A frequency response curve of the amplifier with the filter disconnected from the input grid was taken to check this, and showed that the actual gain was approximately 7.5% greater than was expected from graph 2.1 at 850 Kc/s; therefore there was asymmetry introduced by the bridge, probably due to the bridge 1 load values being other than the aR and c/a desired.

From the point of view of measuring a frequency variation with this circuit, the above work gave the

following information :-

(a) The accuracy of measurement would be low. A frequency variation of 5 Kc/s would produce, at the best, an output variation of only 0.3v. peak/peak, in the practical circuit. This represents a total increase in display magnitude of 0.1 cm. on a Cossor 1035 oscilloscope after amplification in an amplifier of 20db. gain.

(b) The amplitude of the input signal is limited, since the amplifying valve must not introduce non-linearity. For the valve used, the maximum grid drive for linear working is approximately 1.1v. R.M.S., and the choice of valve is governed by the requirements of low output capacity and high mutual conductance, to allow of a flat frequency response curve over the range considered.

(c) A variation in amplitude of input signal would have little effect upon the accuracy of frequency measurement. At 660 Kc/s. the gain of the selective amplifier is 3 and the output voltage 8.5v; if the input signal now decreases to 0.9v. R.M.S. from 1.0v. R.M.S. the output voltage becomes 7.6v. giving the apparent frequency of the input signal as 640 Kc/s - an error of -3%.

(d) The gain of a single-stage selective amplifier is reduced by the parameter (a). Greater selectivity could be obtained by a reduction of this parameter

but the filter load must not be affected by the output impedance of the signal source. A cathode follower input to the bridge circuit would allow (a) to be reduced considerably, but the bridge load must always be high enough to prevent instability.

Any odd number of stages may be used between input and output for greater selectivity, but the stability of such an arrangement is poor, since there is a closed loop between input and output terminals which passes high and low frequencies freely.

A third method of increasing selectivity is to use two or more frequency-selective amplifiers in series, each of moderate gain. This requires each component amplifier to be accurately aligned on the balance frequency, otherwise humping of the response curve appears, and the arrangement has a definite bandwidth.

It was considered that this circuit be used to measure a frequency variation, but the inherently low output sensitivity was a major disadvantage. The introduction of amplifiers to counteract this produces yet another potential source of spurious transient voltages, which must be avoided.

An attempt to measure the response of this circuit to a rapidly changing frequency will be described later.

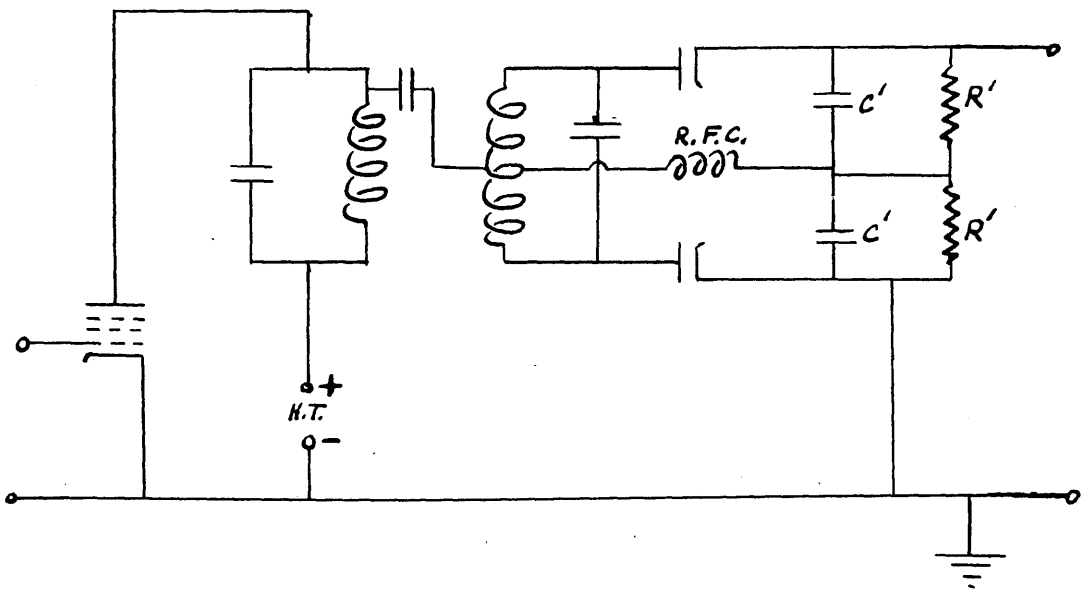

FIG. 2.7.

2.5 Foster-Seeley Phase Discriminator.

This type of frequency, or phase, measuring equipment was introduced by Foster & Seeley[28] in 1937 as a modification to the original discriminator of Travis.[29]

The circuit is shown in Fig. 2.7

Since this circuit is well-known[30] and normally used in F.M. systems as a demodulator in the receiver, and as the frequency measuring device in automatic frequency control circuits in the transmitter[8], it was thought to be a possible means of measuring a rapid frequency change. From the latter point of view, however, the circuit has two disadvantages.

Firstly, the circuit is phase sensitive. The frequency, or phase, discriminating elements are the primary and secondary tuned circuits, each resonating at the same frequency f_o. It was seen in section 2.2 (b) that a transient term existed when a pulse containing R.F. was applied to such a resonant circuit, the transient term depending upon the time constants of the circuits, the initial phase angle, and the ratio of the frequency of the impressed signal to the resonant frequency of the tuned circuit. Thus, if the input signal to the

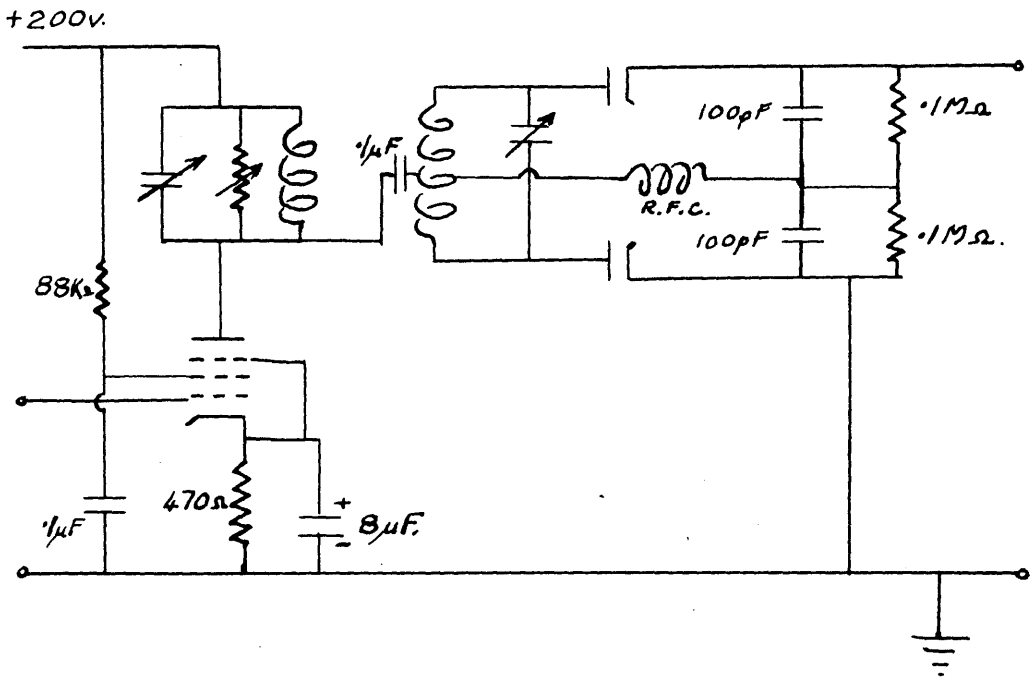

FIG. 2.8.

discriminator wassuddenly changed from the resonant frequency, say, to some new value, the output voltage of the discriminator would contain a term due to the transient modulation. This spurious output would make impossible the measurement of a fluctuating input frequency.

The second disadvantage is concerned with the diode loads, C - R, in Fig. 2.7. Under normal operation, these serve the two-fold purpose of acting as reservoirs at the audio-frequency with which the carrier is modulated, and short-circuits to the r.f. carrier frequency, thereby dynamically coupling the cathodes of the two diodes. Thus the output voltage could not follow any abrupt change of frequency of the input signal, since the capacitors cannot charge or discharge instantly; if the time constant of the R.C. network is small compared with the period of one cycle of the audio frequency, they will discharge rapidly during the portion of the cycle when their respective diodes are non-conducting, and the average output will be small. The R.F. Choke will further prevent a rapid change in output, but this component may be replaced by a resistance, at the cost of reduction of output voltage.

However, an existing discriminator was modified to the circuit of Fig. 2.8 and produced the static

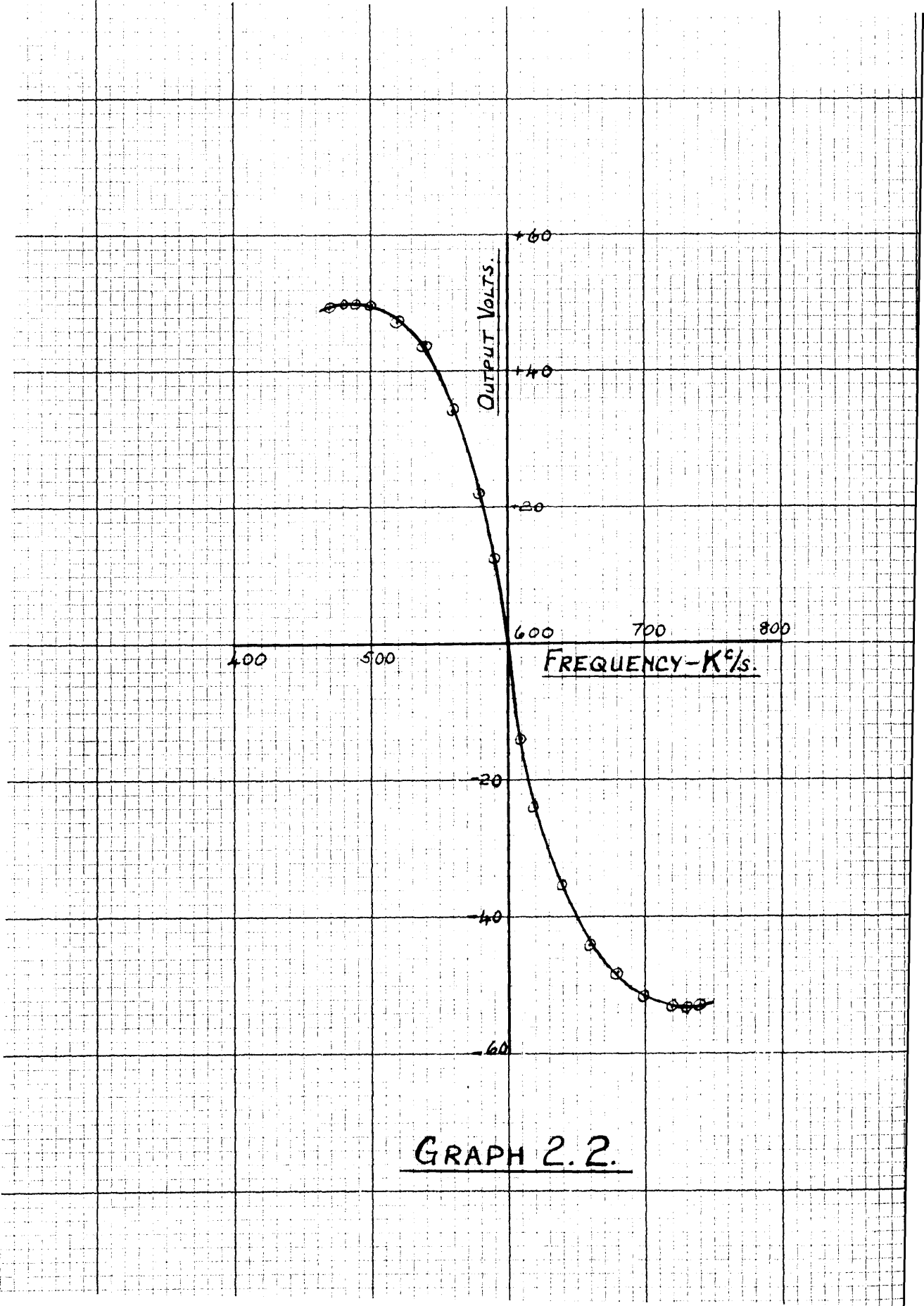
+60
+40
+20
OUTPUT VOLTS.
600
700
800
400
500
FREQUENCY-Kc/s.
-20
-40
-60

GRAPH 2.2.

characteristic of Graph 2.2. From this graph, it was evident that the discriminator was an excellent means of measuring slow rates of change of frequency, (normally about 3 Kc/s per sec. as pointed out in chapter 1.2) since it gave a fairly large output voltage, whose linearity with frequency did not depend on valve linearity, and produced a much more linear characteristic over the working portion than the Parallel-T Amplifier. Sensitivity to amplitude modulation in the input was reduced by injecting the input signal through a limiter pentode.

An attempt was made to measure the response of the discriminator to a rapidly changing frequency, as will be described later.

2.6 The Ratio Detector.

This circuit was given attention here since the output is insensitive to amplitude variations in the input signal and the overall sensitivity is higher than that of a Foster-Seeley Discriminator, although otherwise it still contains all the disadvantages of the Foster-Seeley Discriminator.

The Ratio Detector is also due to Seeley, and is shown in simplified form in Fig. 2.9. The action of this device is the same as that of the discriminator up to the diodes but here the diodes are in series aiding. It can be shown[31,32] that the output

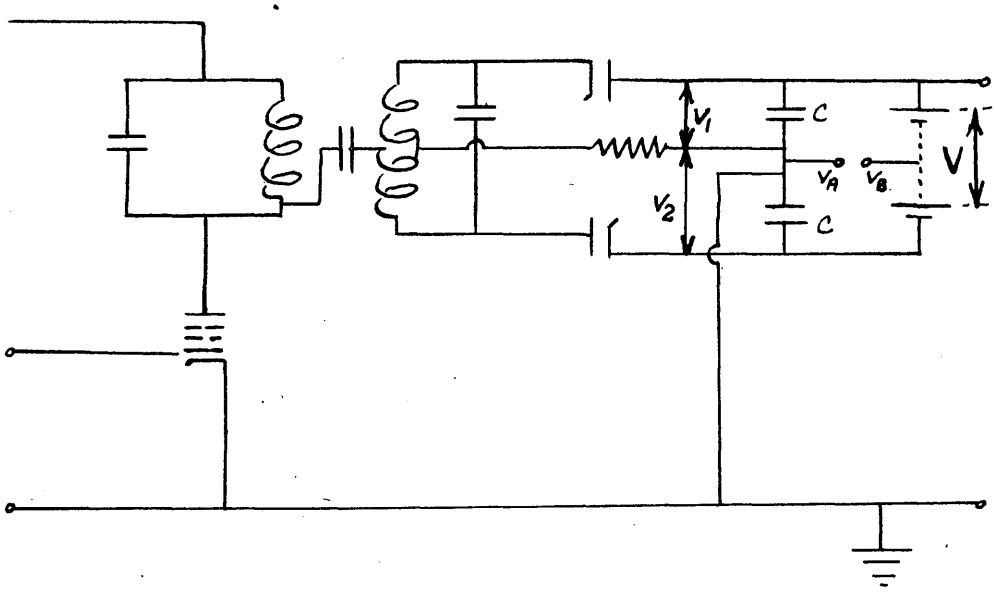

FIG. 2.9.

voltage is a function of the frequency deviation from the resonant frequency, and is independent of the amplitude modulation components at the input. For this reason, the pentode feeding the primary of the detector may be used under normal operating conditions, so that, although the ratio detector is itself less sensitive than the discriminator circuit, the overall sensitivity of the detector is much greater than that of the discriminator.

A practical circuit is shown in Fig.2.10. From the literature on the ratio detector it was found that for this type of circuit the alignment and balancing problems were much more acute than in the discriminator case, and so, for these and previous reasons, no experimental work was done on the ratio detector.

2.7 Arrangement for Testing.

For the sake of chronological order and clarity in the following sections, a description of an attempt to test the response of the above methods to a fast variation in frequency is included here.

The principle of the test procedure was to use two oscillators running at frequencies separated from each other by a desired amount, with an electronic switch which periodically switched the input terminals

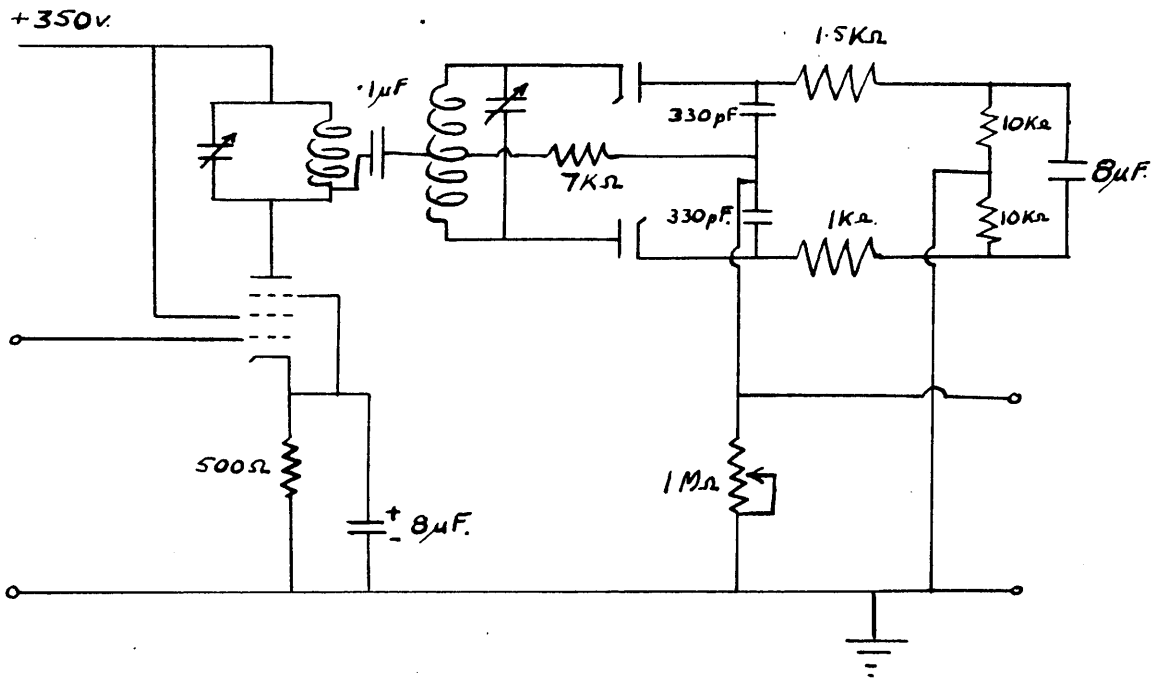

FIG. 2.10.

of the circuit under test from one oscillator to the other. The block diagram is shown in fig.2.11. Provided the switch could be 'thrown' in a time comparable to the rise-time of 0.2μsec. quoted in chapter 1.2., it was considered that this form of test would give a fair indication of the response of the circuits under test if they were used as the frequency measuring devices in the main investigation.

The design considerations of a suitable switch can be summarised as :-

(a) A change-over time of approximately 0.2μsec.

(b) Equal amplitude of output from the switch when closed on either oscillator.

(c) No over-shoot at either beginning or end of the change-over period.

(d) Both outputs to have the same d.c. level, i.e. the pulses used for switching must not appear in the output waveform from the switch.

(e) The switch must produce minimum distortion on the two oscillator waveforms.

Such a switching circuit is shown in Fig.2.12. In this type of switch, the two oscillator signals are applied to the control grids of two pentodes with a common anode load. The suppressor grid of each valve is so biassed that one valve is normally

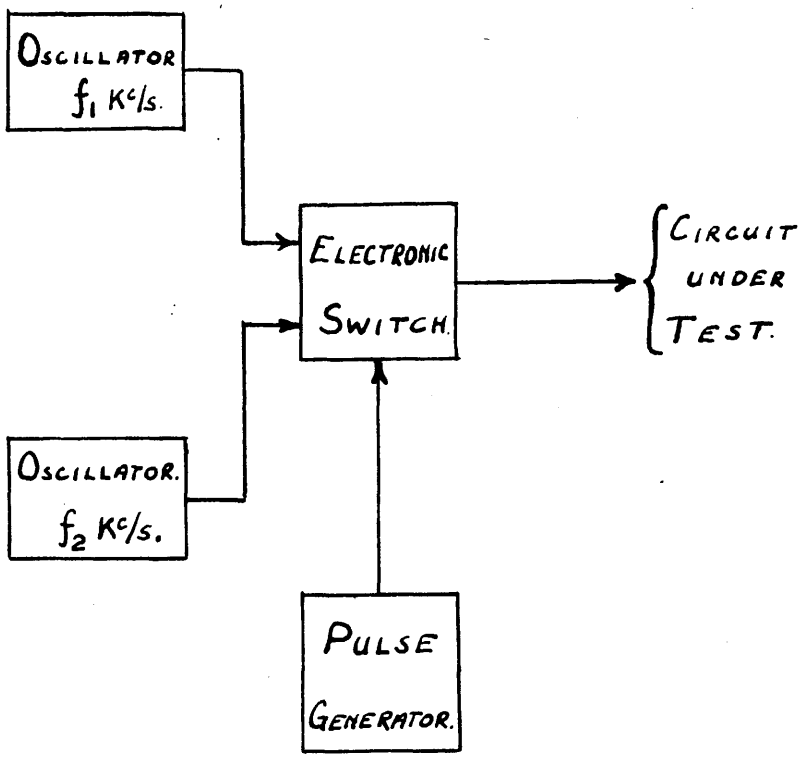
Oscillator
f_1 K^c/s.
Electronic
Switch.
Circuit
under
Test.
Oscillator.
f_2 K^c/s.
Pulse
Generator.

Fig. 2.11.

conducting, the other normally cut-off. On application of a positive switching pulse to V1 and a negative pulse to V2, a rapid switching action can be obtained.

In this form of switch, however, the control pulses must be fairly large in amplitude, about 60v. to 100v. being required in the case of an EF.50 with a suppressor grid base of -60v. Further, the two control pulses must be in accurate antiphase; the slope at any point on the rise of the pulses must be identical, and the magnitude of the pulses equal, if overshoot is to be avoided, for one valve should be cut off at the same rate as the other is turned on. This method of switching tends to give differentiated pulse edges in the output at change-over, due to the feed-through of the large amplitude, fast rising, control pulse edges via the suppressor/anode capacitance. Finally, since the control pulse amplitude is large, for a given change-over time, the requirements of the pulse generators are more stringent in terms of output volts per microsecond at the leading and trailing edges.

It was considered that a much better switch could be obtained if the control grid characteristics of a short grid-base pentode could be used for both switching and signal channels. Since grid mixing is bad practice in pulse techniques, the cathode is

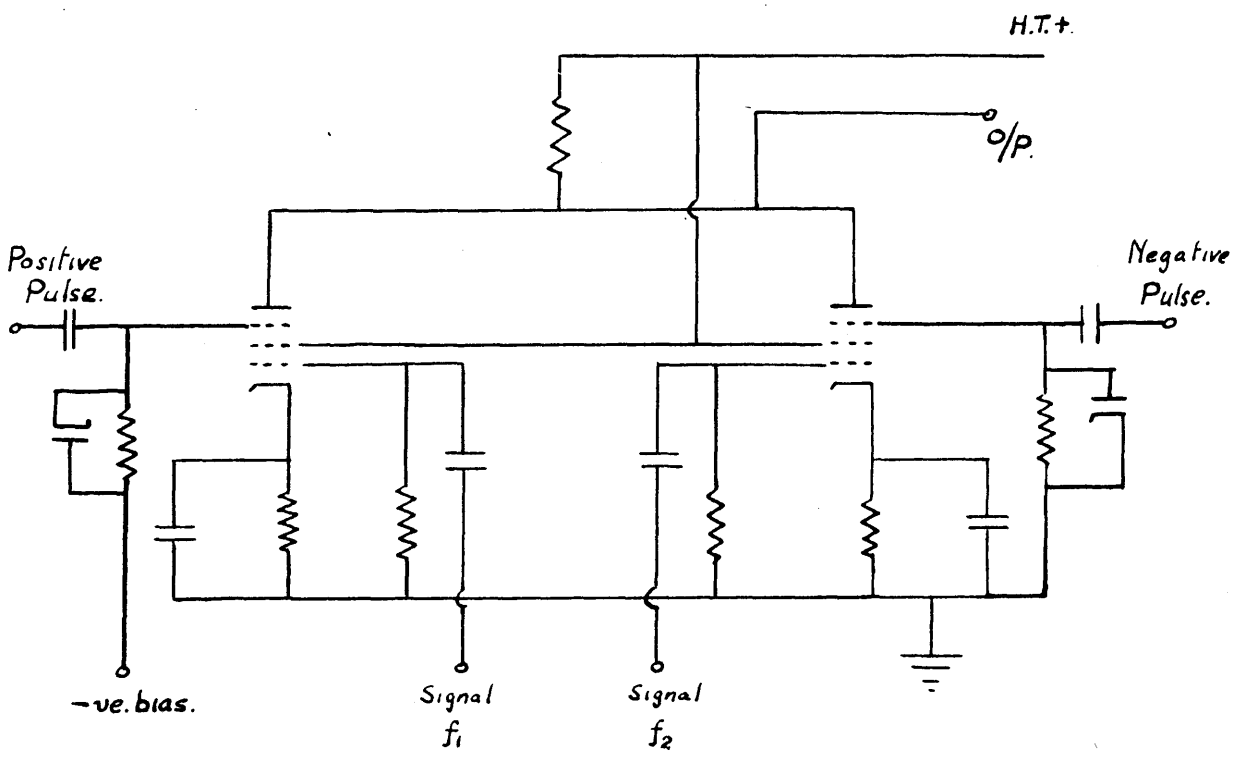
H.T.+
O/P.
Positive Pulse.
Negative Pulse.
-ve. bias.
Signal f_1
Signal f_2

FIG. 2.12.

the only other available injection point for the control pulses. Due to magnetising inductance, transformers are not suitable for the injection of fast edged, flat topped pulses, and so resistance injection to the cathode was used. The resistance in the cathode circuit of the switch valves must be in the order of a few hundred ohms, so that the generator supplying the pulses must either have an extremely low output impedance (less than 100 ohms) or some form of buffer must be used. Such a buffer was supplied by taking each control pulse to the grid of a triode whose cathode was commoned with that of one of the switching valves.

This circuit is shown in Fig.2.13. The diodes act as d.c. restorers on the grids of V3 and V4 respectively. The output of this switch was taken to a straightforward amplifier, and the resulting signal applied through an attenuator to the circuit under test. The switch gave a leading edge change over of 0.5 μsec. and the signals applied to the apparatus under test were constant in amplitude, and devoid of peaks. The trailing edge change-over time was about 1.5 μsec. due to the poor trailing edge of the contrd pulses, and this edge could be easily recognised and ignored.

The pulse generator supplying the control pulses

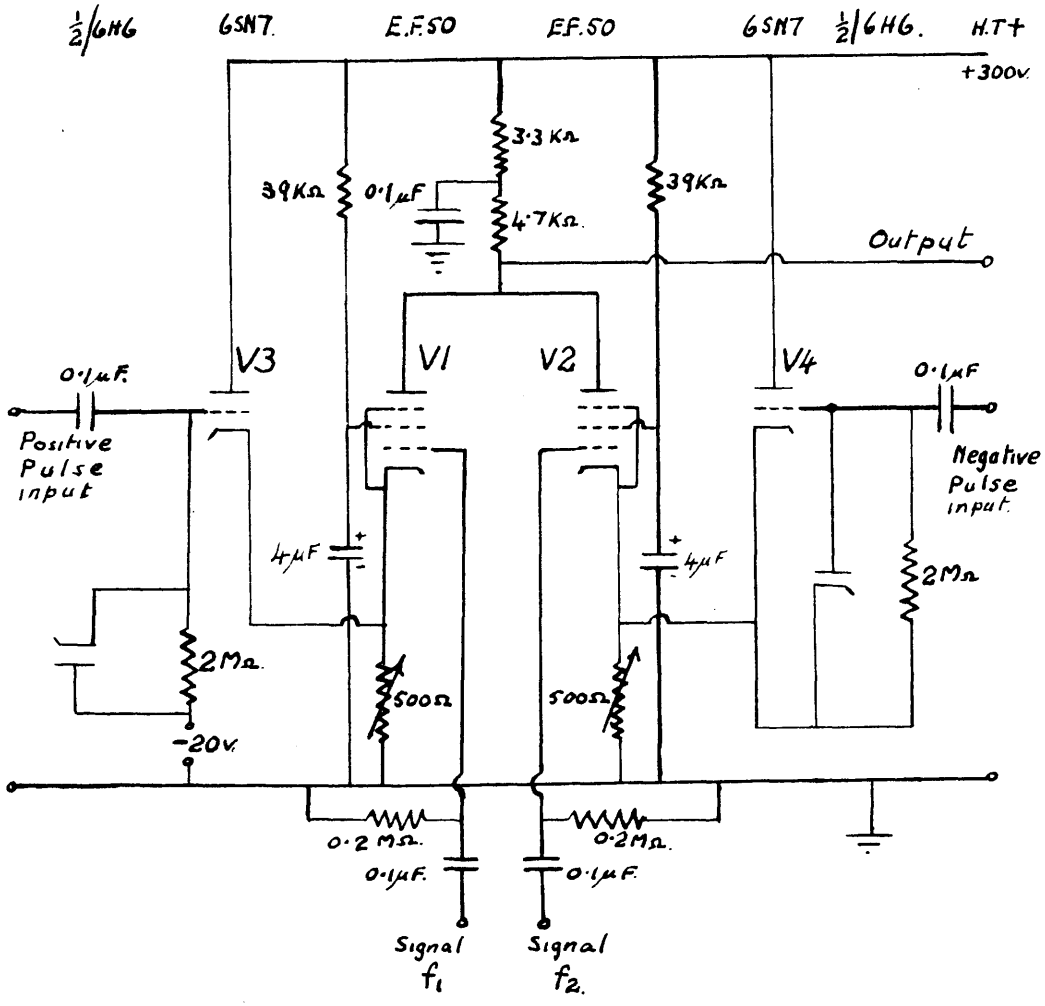
½/6H6
6SN7.
E.F.50
EF.50
6SN7
½/6H6.
H.T+
+300v.
3·3 KΩ
39KΩ
0·1μF
4·7KΩ.
39KΩ
Output
V3
V1
V2
V4
0·1μF.
0·1μF
Positive
Pulse
input
Negative
Pulse
input.
4μF
4μF
2MΩ.
2MΩ
500Ω
500Ω
-20v.
0·2 MΩ.
0·2MΩ.
0·1μF.
0·1μF.
Signal
f1
Signal
f2.

FIG. 2.13.

was a standard Dawe Instruments model, supplying positive and negative going pulses of variable width and repetition frequency. The p.r.f. used was 5 Kc/s the pulses being 100 μsec. wide, and approximately 30v. to 40v. in amplitude, although only the original 10v. to 15v. of this amplitude was required. The two oscillators supplying the signals were set at f_1 Kc/s and f_2 Kc/s, these frequencies depending on the frequency characteristics of the circuit under test, a Marconi Standard Signal Generator being used as the reference oscillator on account of its frequency stability and vernier tuning. The frequency of the second oscillator was set by comparison with the Marconi generator, using a Lissajou display.

During the testing of the switch circuit it was noticed that at the instant of change-over, the trace on the oscilloscope screen seemed to 'run', as though there was intermodulation over the last cycle of the outgoing signal and first two cycles of the incoming signal. Varying either oscillator varied the pattern, but again only affected the last and first two cycles; the pattern became static for certain values of oscillator frequency. This latter effect disproved the hypothesis of intermodulation, as was verified by obtaining the original effect with

one oscillator switched off. This led to the following explanation.

As stated above the pulse width was 100 μsec. so that each valve conducted for this period, or a little less if change-over time is taken into account. If T_1 μsecs. is the period of one cycle of frequency f_1, then

$$\frac{100}{T_1} = \text{no. of cycles of } f_1 \text{ in one switch period,}$$

$$= n_1 + \frac{\alpha}{\beta} \text{ in general, where } n_1, \alpha, \beta \text{ are integers, and } \beta > \alpha.$$

Suppose f_1 is appearing at the switch output, and for simplicity assume that at the instant that f_1 appears at the output the sine wave has value zero, but is increasing positively. At the end of the switch period, signal f_1 has completed $(n_1 + \frac{\alpha}{\beta})$ cycles, provided 100 is not a multiple of T_1. During the time that f_2 is appearing at the output, f_1 completes another $(n_1 + \frac{\alpha}{\beta})$ cycles, so that at the next appearance of f_1 at the output this signal has completed,

$$\left(2n_1 + 2\frac{\alpha}{\beta}\right) \text{ cycles.}$$

Thus, f_1 now appears with a phase angle corresponding to $2\frac{\alpha}{\beta}$: successive appearances of f_1 will therefore be made at differing phase angles. A similar argument applied to the end of the f_2

signal shows that at the instant of disappearing f_2 has a different phase angle for successive periods. On a repetitive time-base, this will produce the 'running' effect observed. If now f_1 is changed in value to f_1' such that $\frac{\alpha}{\beta}$ becomes unity, f_1' appears with zero phase angle always, and on a repetitive time-base, the pattern will appear static, again as observed.

Since this effect cannot be eliminated (locking the p.r.f. to a count down from one oscillator would not eliminate the effect for the other oscillator) and since the only solution of single-stroking the complete system is an unfair test due to time-constants etc., this method could not be used for accurate determination of the response of the circuits described in preceding sections; although this switch circuit was used to test the Parallel-T feedback amplifier and the Phase Discriminator, the results obtained could only be used as guides. Further, photography of the display was impossible, a blur being invariably recorded at the change over period, since the pattern could be made static by varying the oscillator frequencies but could not be maintained in this state due to overall drift. The type of result obtained for the Parallel-T amplifier is shown in Graph 2.3 as closely to scale

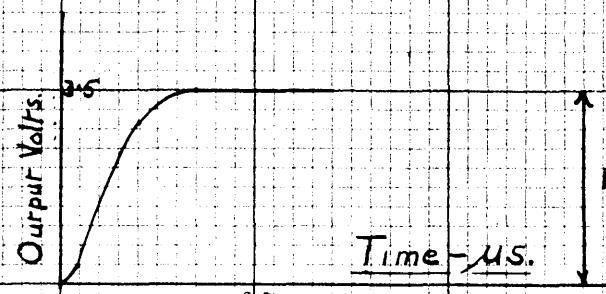

GRAPH 2.3.

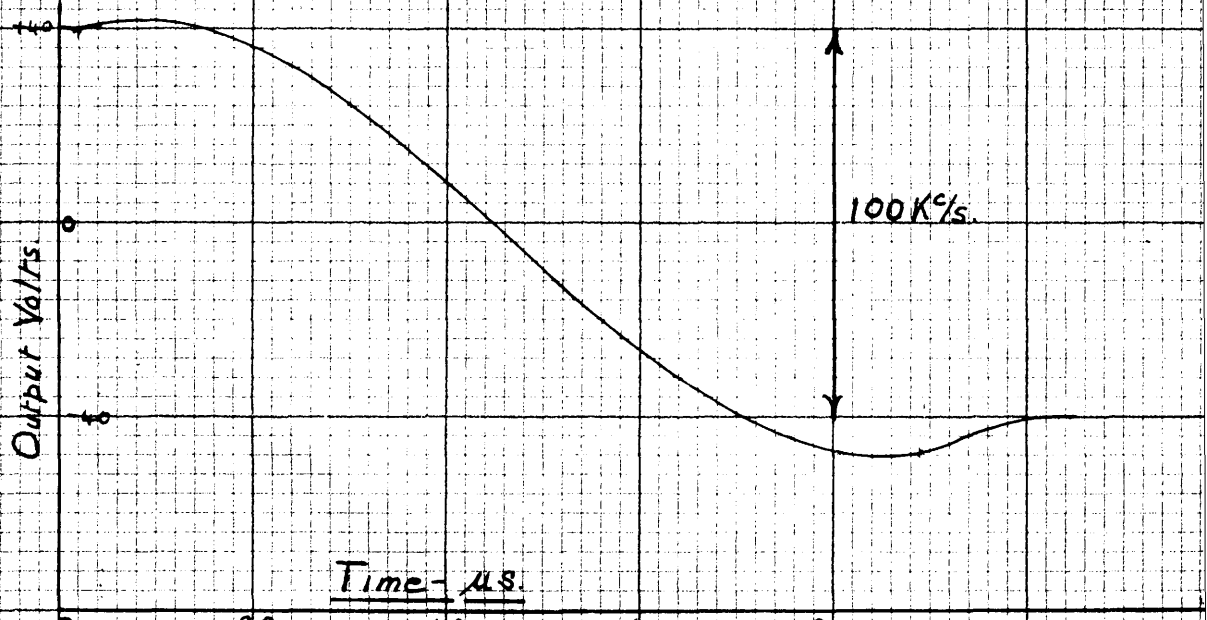

GRAPH 2.4.

as possible, a similar graph being drawn for the discriminator in Graph 2.4. A comparison of these two graphs shows that the Parallel-T amplifier gave a much better response to a rapid change of frequency than did the discriminator. Thus it would appear that the discriminator is the better circuit for measuring a relatively low rate of change of frequency, whereas the Parallel-T system is very much better than the discriminator at high rates of change of frequency.

Although this switch method was of little value in determining accurately the frequency response of the circuits tested, it brought out most clearly the need for accurate synchronisation of the system proposed in 1.2 and shown in Fig.1.1. The synchronisation would have to be such that each pulse in the pulse train from the pulse generator arrives with exactly the same time-phase in the cycle of the test oscillator. The simplest method of achieving this is to generate a train of master pulses which control the complete system. The master pulse would gate the oscillator 'on' over the duration of the pulse, and trigger the pulse generator at a predetermined but constant time after the oscillator had commenced duty, due time being allowed for the oscillator to become stable.

Such a pulsed synchronous system was therefore used from this time onwards, the design of the final system being discussed in chapter 4.

2.9 Radar Techniques as applied to Frequency Modulation.

Since all the techniques already considered relied on the voltage response of a circuit proportional to the change in frequency, a search was made to find a more direct method of measuring frequency. In most radar systems one of the three fundamental measurements is that of slant range, i.e. the straight line distance between the transmitter and the reflecting object. To obtain the slant range, all pulsed-type radar systems measure the time interval between a pulse of energy being transmitted and the reflected echo being received. A few of the methods used to measure the time interval were considered relevant to this work. In general, an auxiliary waveform is generated by an accurately calibrated source, the period of this waveform being used in some manner as a comparison with the time interval under measurement. Two such methods were considered, and their merits found.

(a) Calibrating Pulses.

The auxiliary waveform in this method takes the

form of a train of narrow pulses of voltage, the root width of each pulse being of the order of a few microseconds. These could be used as time markers since the time interval between each pulse is accurately known. The utilisation of this type of circuit was obvious in the field of frequency measurement, as was also its main disadvantage. Since the crests of a sine wave are very difficult to locate, the only feasible points at which the periodicity may be checked are at the intersection of the sine wave under test and the base line. To do this accurately requires a variable phase-shift control in the auxiliary circuits producing the pulses, and the exact coincidence of the pulses with the base line intersection is usually difficult to see on an oscilloscope screen, due to the relative width of the tips of the pulses. Also, pulses tend to distort the test signal due to capacity coupling between the two beams of the oscilloscope.

(b) Beam Modulation, Calibration Dots.

The calibration pulses of the previous method are injected to the grid of the oscilloscope in this case, the pulses having such a polarity that the electron beam of the oscilloscope is cut off for the duration of each pulse. When the frequency of the beam suppression pulses coincides with that of the

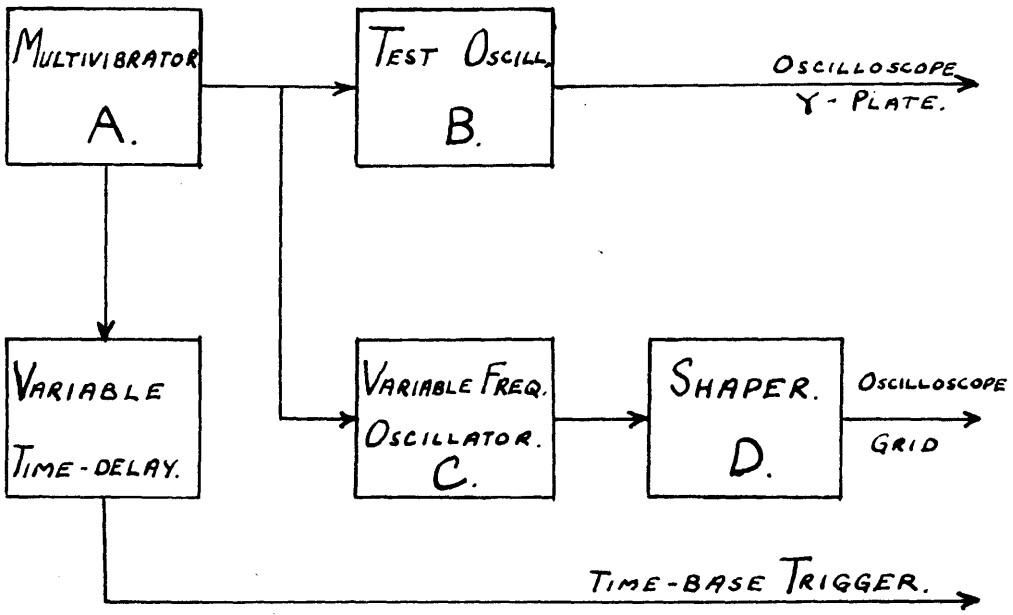
MULTIVIBRATOR
A.
TEST OSCILL.
B.
OSCILLOSCOPE
Y - PLATE.
VARIABLE
TIME - DELAY.
VARIABLE FREQ.
OSCILLATOR.
C.
SHAPER.
D.
OSCILLOSCOPE
GRID
TIME-BASE TRIGGER.

FIG. 2.14.

signal under test, the black spots, or dots, form a straight line horizontally across the screen.

For greater accuracy, the beam suppression pulses can be applied, say, at twice the signal frequency, and now frequency would have to be defined as twice the reciprocal of the time interval between successive crossings by the test waveform of any equi-area line parallel to the X-axis. If the test signal is distorted from a sinusoidal form, the frequency as found by this method for each half-cycle will be different (by half-cycle, here, is meant successive crossings of the axis, and not half the time required for a complete cycle). If the calibrating frequency is made many times the frequency of the test waveform, then an approach is being made to instantaneous frequency, where the instantaneous frequency may vary within one cycle of the test signal.

To test this method, the equipment of Fig.2.14 was developed. The whole equipment was pulse controlled by the master multivibrator 'A' in conformance with the findings of 2.8; the sinusoidal output of oscillator 'C' was squared, differentiated and shaped in 'D' to produce narrow, negative going, pulses which were applied to the grid of an oscilloscope. Since the oscillator

requires some microseconds to build up to its stable amplitude, a delay circuit was interposed between the control unit 'A' and the trigger circuit of the time-base.

The design of the circuits, A, B, C, and the delay line will be discussed in chapter 4. The shaping amplifier, D, comprised a conventional three-stage amplifier with output to input feedback, over-driven by the output of the oscillator 'C'. The waveform at the output of this squaring amplifier consisted of relatively square pulses at the frequency of oscillator 'C'. These pulses were differentiated, amplified and shaped, giving an output of negative-going pulses, 0.2 μsec. broad at the base, and 120v. in amplitude. Since this waveform was applied to the grid of an oscilloscope through a 0.1 μF. capacitor with a 1 M.Ohm leak to ground, the base-line of the spikes rose to approximately 30v. above ground (for a repetition frequency of 1 Mc/s). Since the oscilloscope used required -60v. for beam cut-off from full brilliance, at the black-out level of -60v, the pulse width was approximately only 0.1 μsec., corresponding to 90v. below the base-line of the original pulse train. The frequency of the test oscillator was fixed at 500 Kc/s, and the frequency of the auxiliary

oscillator was variable around 1 Mc/s.

When used with the test oscillator 'B', this system produced the desired effect when a large number of cycles of the test waveform were viewed on the Cossor Oscilloscope using a 50 μsec. time-base. But when a few cycles were examined closely with a 15 μsec. time base, the trace on the screen of the oscilloscope was found to fall off gradually from full-brilliance to all-black, instead of giving a distinct break in the trace; the break in the trace was found to be 0.6 cm. long, instead of being very narrow. The length of the black-out period on the 500 Kc/s. sinusoidal trace was the projection on to that trace of the width of the suppression pulse on a horizontal axis. In this specific case, the usable screen diameter was 10 cm; therefore, with the 15 μsec. time-base the scan speed was 0.66 cm. per μsec. For a pulse of 0.1 μsec. duration (the pulse width corresponding to black-out) the pulse width would be 0.06 cm. long on a horizontal axis. For a peak-to-peak amplitude of 7 cm. for the 500 Kc/s oscillation, as the trace swung from one peak to the next, it covered a distance of 7 cm. approximately, and did so in less than 1 μsec. Suppose the beam actually covered 7 cm. in 1 μsec. in a linear manner, then, a suppressing pulse 0.1 μsec. long, would give a blacked-out distance of 0.7 cm.

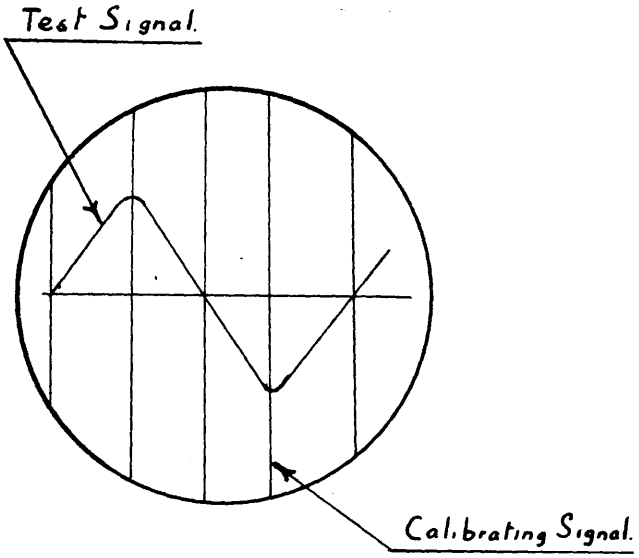

FIG. 2.15.

on the 500 Kc/s waveform, and the rise and fall times of the suppressing pulse would be clearly visible.

The conclusions drawn from this were that the method was no more accurate than the calibrating pulse method, and that the difficulties involved in producing a pulse shorter than 0.1μsec. at a repetition frequency of 1 Mc/s. or over, would introduce unwarranted complexity in the equipment.

This work was not completely valueless, however, for during the experimentation another idea had been suggested. If the auxiliary oscillator output is squared in the squaring amplifier, and if the amplitude of the squared output is great enough to sweep the electron beam of the oscilloscope over the full screen of the tube, then the sides of each half-cycle of the squared waveform would appear approximately vertical (Fig. 2.15) As before, the time interval per half-cycle of the test signal could be measured. Carrying this principle one step forward, let the auxiliary oscillator frequency be increased until it is several times that of the test signal. The sides of the auxiliary pulses would then break the test waveform into several segments, all these segments being of equal and known time duration.

If these segments could be used to measure frequency, then a very close approach is being made to instantaneous frequency. Thus, the next chapter deals with the usage of one such segment in the determination of the frequency associated with that segment.

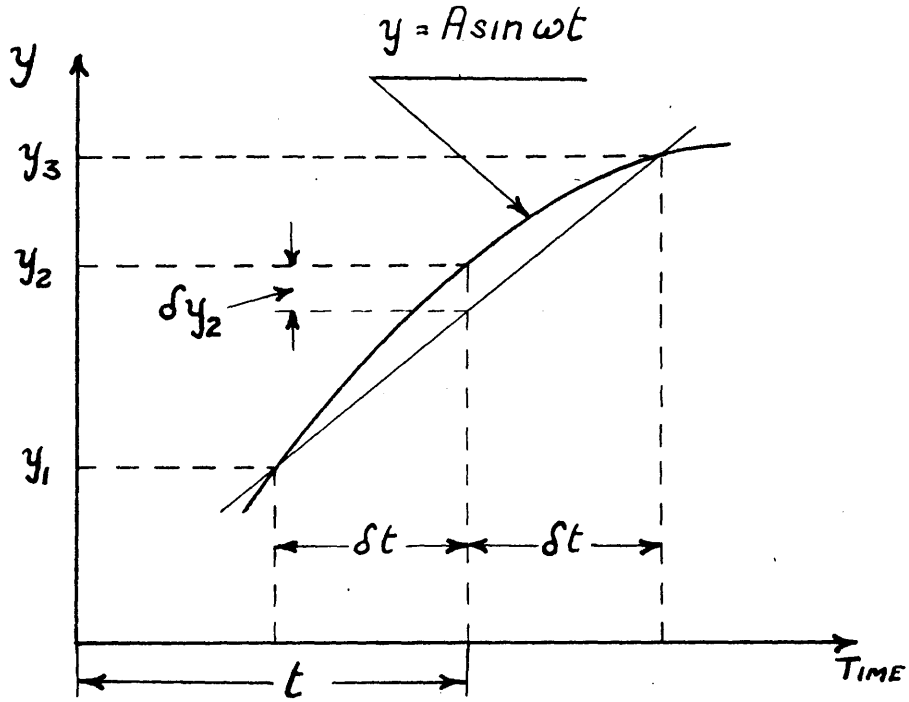

FIG. 3.1.

CHAPTER 3.

SEGMENTAL METHOD OF FREQUENCY ANALYSIS.

From the preceding work, if the term 'instantaneous frequency' as applied to the measured quantity is to have any meaning at all, then the method of measuring frequency must be such that a much smaller portion than half a cycle of the waveform to be analysed is considered. In terms of the angle swept out by the generating vector, it is required to consider a segment of the waveform corresponding to some angular displacement less than 180°. Fundamentally, instantaneous angular frequency is the angular velocity of the generating vector at any instant of time; segmental frequency may be defined as the average angular velocity of the vector over the segment.

Consider any segment δt of a curve and assume that an ordinate at any instant t is given by

$$y = A \sin \omega t \qquad (A \text{ constant within } \delta t).$$

where ω is the average angular velocity, during the time δt of the generating vector of length A; assume that both the time interval required by the vector to generate the segment, and the ordinates of the segment, are known. Then, the segmental frequency ω may be found from any one of several sets of measurements upon the segment as is demonstrated, assuming ω is constant during δt; ω is the value of angular frequency associated only with the given segment.

3.1. Mid-Segment Divergence Method.

With reference to Fig. 3.1

$$y_2 = A \sin \omega t.$$

$$y_1 = A \sin \omega(t - \delta t) = A \sin \omega t \cos \omega \delta t - A \cos \omega t . \sin \omega \delta t$$

$$y_3 = A \sin \omega(t + \delta t) = A \sin \omega t \cos \omega \delta t + A \cos \omega t . \sin \omega \delta t.$$

$$\therefore \quad y_1 + y_3 = 2A \sin \omega t . \cos \omega \delta t$$

$$= 2 y_2 . \cos \omega \delta t \quad \ldots\ldots 3.1.$$

To a first approximation,

$$\cos \omega . \delta t = 1 - \tfrac{1}{2} (\omega \delta t)^2 \quad \ldots\ldots 3.2.$$

Therefore,

$$y_1 + y_3 = 2 y_2 \left[1 - \tfrac{1}{2} (\omega . \delta t)^2 \right]$$

$$(\omega . \delta t)^2 = 2 - \frac{y_1 + y_3}{y_2} \quad \ldots\ldots 3.3.$$

But,

$$\delta y_2 = y_2 - \frac{y_1 + y_3}{2} \quad \ldots\ldots 3.4$$

$$\therefore \quad \frac{2 \delta y_2}{y_2} = 2 - \frac{y_1 + y_3}{y_2}$$

Hence,

$$(\omega . \delta t)^2 = \frac{2 \delta y_2}{y_2}$$

$$\omega = \frac{1}{\delta t} \sqrt{\frac{2 \delta y_2}{y_2}} \text{ rad./sec.} \quad \ldots\ldots 3.5$$

and,

$$f = \frac{1}{\sqrt{2} . \pi . \delta t} \sqrt{\frac{\delta y_2}{y_2}} \text{ c/sec.}$$

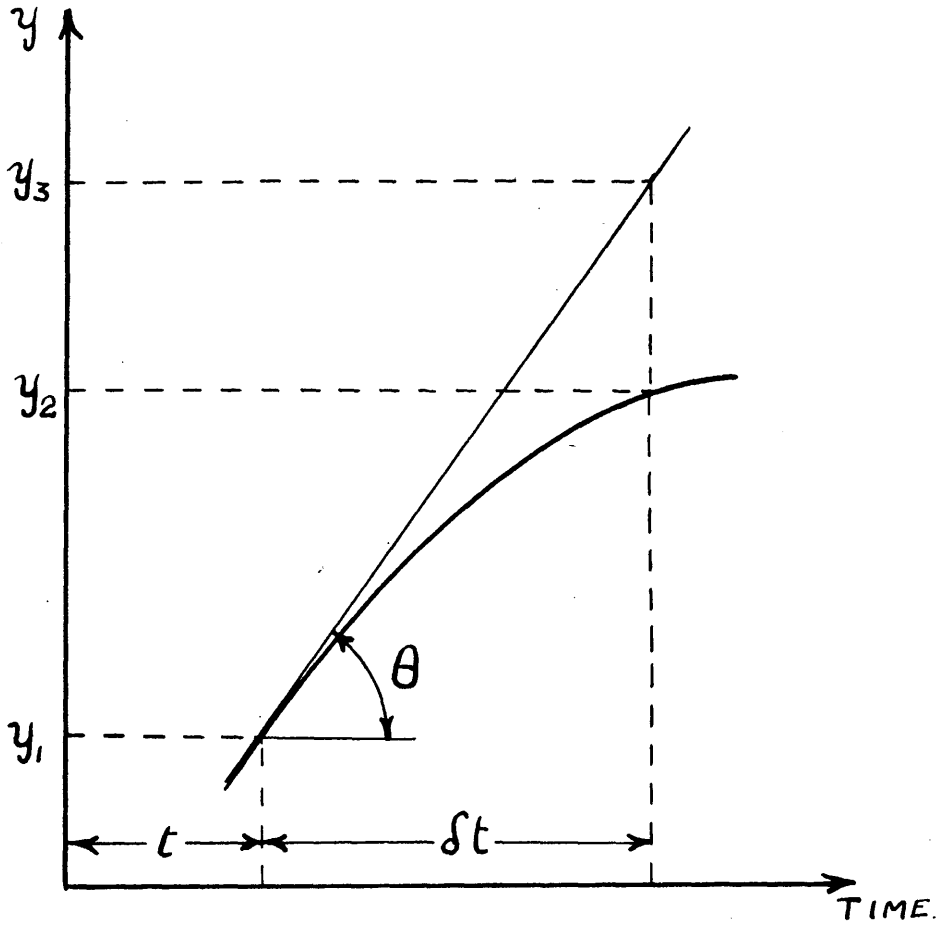

FIG. 3.2.

From the point of view of accuracy, this is a very poor method, measuring, in fact, the difference between the curve and its chord through y_1 and y_3.

Even if this method is stopped at equation 3.1, giving

$$\cos \omega \delta t = \frac{y_1 + y_3}{2 y_2} ,$$

and evaluating $\cos \omega . \delta t$ a very small error in the measurement of Y_2 would produce a greater error in ω.

3.2 Tangential Method.

Now referring to Fig. 3.2 dealing in terms of the tangent to the segment,

$$y_1 = A \sin \omega t \quad \ldots\ldots 3.6.$$

$$y_2 = A \sin \omega (t + \delta t)$$

$$= A \sin \omega t \cos \omega \delta t + A \cos \omega t \sin \omega \delta t \quad \ldots\ldots 3.7.$$

$$\left(\frac{\delta y}{\delta t}\right)_{y_1} = \tan \phi = \omega A \cos \omega t \quad \ldots\ldots 3.8.$$

$$\therefore \quad A \cos \omega t = \frac{\tan \phi}{\omega} \quad \ldots\ldots 3.9.$$

Hence,

$$y_2 = y_1 \cos \omega \delta t + \frac{\tan \phi}{\omega} \sin \omega \delta t \quad \ldots\ldots 3.10.$$

$$\therefore \quad y_1 \left[1 - \tfrac{1}{2} (\omega \delta t)^2\right] + \frac{\tan \phi}{\omega} \left[\omega \delta t - \tfrac{1}{6} (\omega \delta t)^3\right] \quad \ldots\ldots 3.11.$$

Ignoring terms of δt of higher than 2nd. order,

$$y_2 = y_1 - \frac{y_1}{2} (\omega \delta t)^2 + \delta t . \tan \phi . \quad \ldots\ldots 3.12.$$

$$\therefore \quad (\omega \delta t)^2 = 2 - \frac{2 y_2}{y_1} + \frac{2 \delta t}{y_1} \tan \phi$$

giving,

$$\omega = \frac{\sqrt{2}}{\delta t} \sqrt{1 - \frac{y_2}{y_1} + \frac{\delta t}{y_1} \tan \phi} \quad \text{rad./sec.} \quad \ldots\ldots 3.13.$$

In this expression for ω, the angle ϕ has to be determined, as well as the ordinates. The measurement of θ is, to any degree of accuracy, a difficult task, although the effect of any error in the value of tan θ is made relatively smaller if $\delta t/y_1$ is much less than unity.

3.3 Tangental Divergence Method.

In order to remove the necessity of measuring the slope of the tangent, the ordinate Y_3 in Fig. 3.2 may be measured.

Then, as before,

$$y_2 = y_1 \cos \omega \delta t + \frac{\tan \phi}{\omega} \sin \omega . \delta t \quad \ldots\ldots\ldots 3.10.$$

But, now, $\tan \phi = \dfrac{y_3 - y_1}{\delta t} \quad \ldots\ldots\ldots 3.14.$

$$\therefore \quad y_2 = y_1 \left[1 - \tfrac{1}{2} (\omega \delta t)^2 \right]$$

$$+ \frac{y_3 - y_1}{\omega \delta t} \left[\omega \delta t - \tfrac{1}{6} (\omega \delta t)^3 \right] \quad \ldots\ldots 3.15.$$

$$= y_3 - (\omega \delta t)^2 \left[\frac{y_1}{3} + \frac{y_3}{6} \right] \quad \ldots$$

$$\therefore \quad (\omega \delta t)^2 = \frac{6 (y_3 - y_2)}{2 y_1 + y_3}$$

giving,

$$\omega = \frac{\sqrt{6}}{\delta t} \sqrt{\frac{y_3 - y_2}{2 y_1 + y_3}} \quad \text{rad./sec.} \quad \ldots\ldots 3.16.$$

This is a better expression for ω than those derived previously, since the cube term is not ignored. However, then general accuracy is not very good, being dependent on the

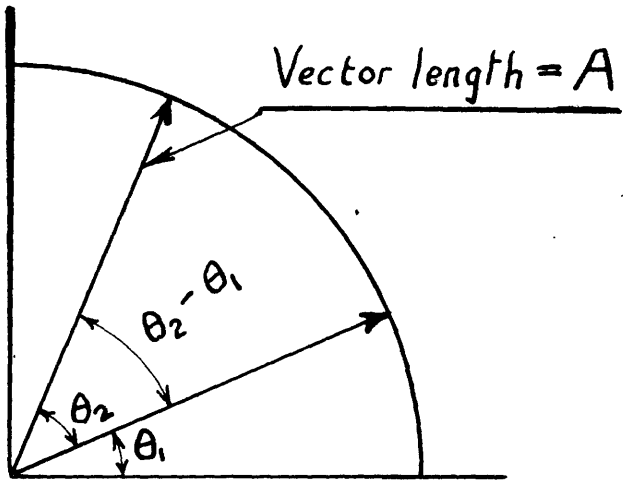

FIG. 3.3.

sum and difference of quantities which may differ by only a small amount, depending on the position of the segment on the waveform.

3.4 Equivalent Amplitude Method.

The generating vector, A, is now considered, as in Fig. 3.3. Let the vector sweep through the angle $(\theta_2 - \theta_1)$ rads in time δt, and let the length A be known. Then,

$$y_1 = A \sin \omega t = A \sin \theta_1 \quad \ldots \quad 3.17$$

$$y_2 = A \sin \omega (t + \delta t) = A \sin \theta_2 \quad \ldots \quad 3.18$$

$$\therefore \quad \theta_1 = \sin^{-1} (y_1/A) \quad \ldots \quad 3.19$$

$$\theta_2 = \sin^{-1} (y_2/A) \quad \ldots \quad 3.20$$

Hence,

$$\omega \delta t = \theta_2 - \theta_1 \quad \ldots \quad 3.21$$

and,

$$\omega = \frac{\theta_2 - \theta_1}{\delta t} \quad \ldots \quad 3.22$$

Here, θ_2, θ_1, are determined by measuring the ordinates Y_1, Y_2, and the peak value A. The latter is assumed constant over the period

3.5 Criticism and Extension of Segmental Analysis.

In methods 3.1 to 3.3 above, the frequency of an equivalent sine wave was found from any segment of the given waveform, without any knowledge of the peak value, A. To do so entailed the determination of a) linear distances, b) a time interval, and, for method 3.2, c) an angle. None of these methods can be accurate, for, apart from measurement considerations, a series expansion was used for a

trigonometric ratio in all of them, and only the first two or three terms were taken for the sake of simplicity in the final equations for the angular frequency. Also, the drawing of an exact tangent to a segment is very difficult. Thus these three methods were included, not as practical approaches to the problem, but merely to show that if the peak value, A, is either unknown, or cannot be found, then the frequency can only be found in an approximate manner.

This finding is important. As has already been stated in Chapter 1.2, to obtain the required frequency change for this investigation a reactor stage is placed in parallel with an oscillator; the reactor stage produces a change in amplitude, as well as in frequency, of the oscillator waveform. If Segmental methods are to be used to determine the 'instantaneous' frequency of the oscillator output, then only an approximate result can be obtained if the amplitude is unknown. Further, the amplitude will be some function of time, varying continuously throughout the period during which the oscillator is changing to its new conditions. Thus, it appears that the frequency can only be found approximately by these methods, since quite apart from the objections already raised, the amplitude was assumed constant over the time δt in which the segment was generated, although its absolute value was not required to be known.

Now consider method 3.4. Here the amplitude has to be known, but the accuracy of this method is better than

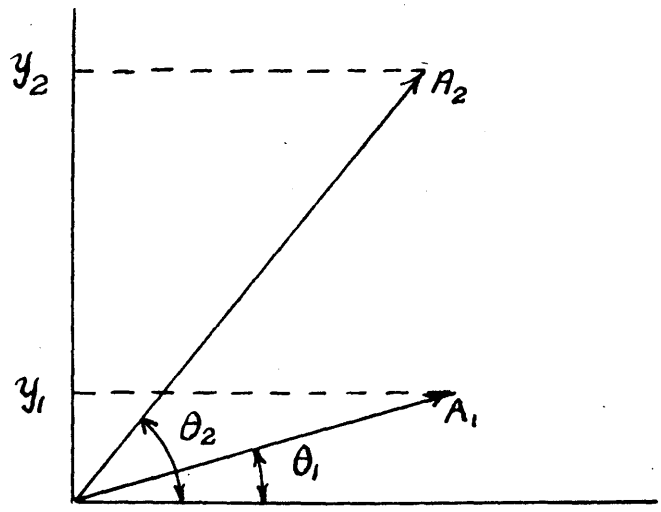

FIG. 3.4.

in any of the previous methods, for no series expansions are required, no direct angular measurements are made, and provided Y and A are not alike in value, error in measuring Y and/or A has comparatively little effect on ω. In addition, if the vector length A (Fig. 3.3) changes during the time interval δt, then the equation for ω is still true if the relevant values of A at Y_1 and Y_2 are used in calculating θ_1 and θ_2.

Thus,

$$\theta_1 = \sin^{-1}(y_1/A_1),$$

$$\theta_2 = \sin^{-1}(y_2/A_2),$$

and if ω is assumed constant over the time δt, then,

$$\omega = \frac{\theta_2 - \theta_1}{\delta t} \quad rad./sec.$$

Therefore, in any waveform in which the frequency and amplitude are functions of time, it is considered possible to divide the waveform into a large number of small segments, each segment having a particular frequency assigned to it, as calculated by the above method. In other words, one such segment is a portion of an equivalent sine wave of frequency ω which exists over that one segment only. The segmental angular frequency is the average angular velocity, over any one segment, of the vector which generates the actual frequency - modulated wave. In normal F.M. terms, this vector is the resultant of the constant amplitude carrier - frequency vector and the modulating signal vector.

To utilise method 3.4 in evaluating the segmental frequency, the value of the amplitudes A_1, A_2, of Fig.3.4

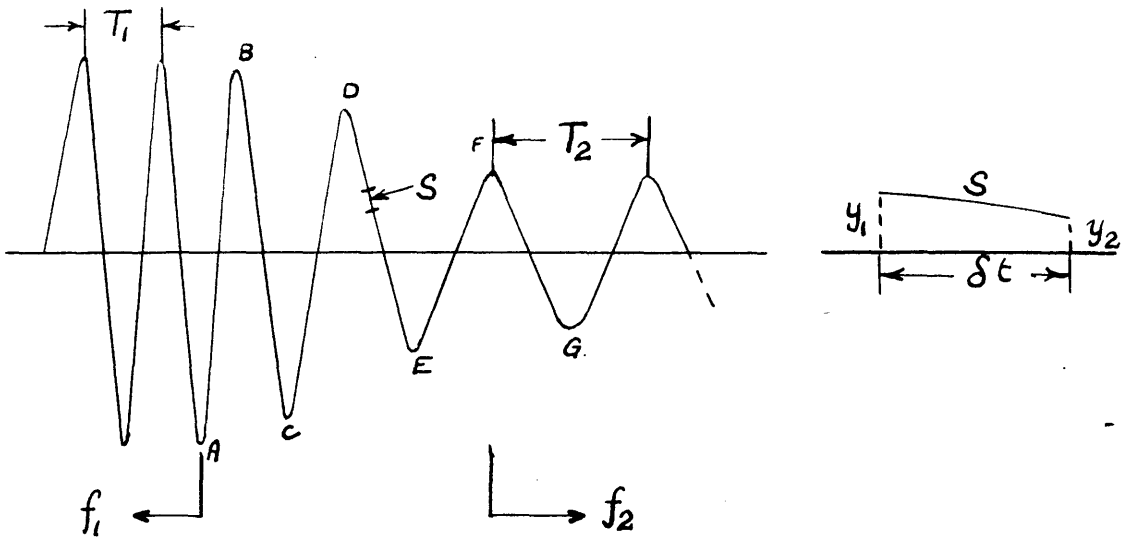

a). b).

FIG. 3.5.

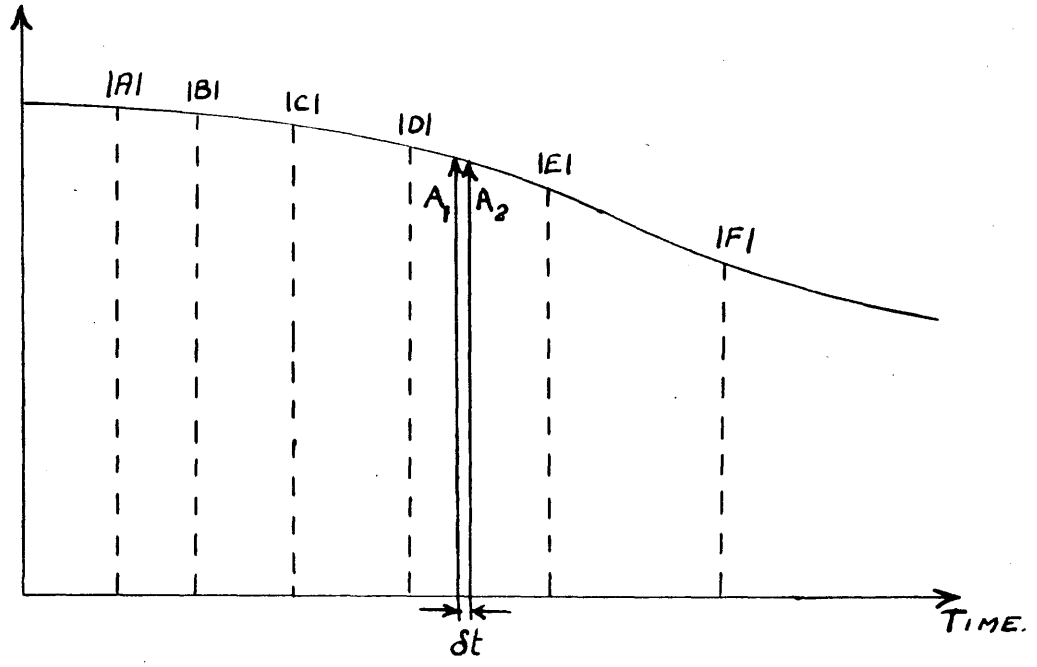

FIG. 3.6.

must be ascertained. Consider a wave-form as shown in Fig. 3.5(a)., the original steady frequency f_1 C/S being given by $1/T_1$ c/s and the new steady value of frequency f_2 C/S being given by $1/T_2$ c/s. During the time that the frequency changes from f_1 to f_2, the amplitude also decreases to its new value. Assuming some segment S of known time-length has been isolated as shown in Fig. 3.5(b), on an expanded time scale, then the equivalent amplitudes associated with Y_1, Y_2, may be found to a good degree of accuracy by the following method.

The true length of the generating vector can only be found at the peaks of the waveform. If the successive positive and negative peaks such as A, B, C, D, are measured and their magnitudes $|A|, |B|, |C|, |D|$, are plotted on the correct time abscissa, an envelope shape of the form of Fig. 3.6., is obtained. The equivalent amplitudes A_1, A_2, associated with S may be taken from this curve, by correctly positioning the time-interval δt of the segment S on the time axis. This procedure does assume that the length of the generating vector varies smoothly with time between successive peaks, but it is thought that this is a reasonable assumption if all the peak values lie on a smooth curve, as in Fig. 3.6 with no sudden, non-repetitive, crests or hollows.

The problem is now that of isolating and examining a series of small segments of the waveform to be analysed, in this case the output of the frequency modulated oscillator,

and the determination of their relative positions on the time axis. The equipment required to do this is described in the following chapter.

CHAPTER 4.

TEST EQUIPMENT, ITS DESIGN AND CALIBRATION.

The design considerations of the test equipment can now be discussed in detail.

It was found in Chapter 2 that the whole equipment must be pulse operated. Thus the apparatus may be sectionalised to some extent, although the various sections are naturally interdependent. In general the three sections into which the equipment is divided are :-

(a) Control circuits.

(b) The Oscillator and reactor stages, and

(c) The measuring devices.

Logically, the control circuits had to be built first, and then these were modified as the development of the oscillator and reactor stages proceded and the requirements of the control circuits altered. Finally, the measuring circuits were designed to suit the finalised control equipment.

4.1 General Considerations.

To use the principle of frequency measurement developed in chapter 3, it was required to view small segments of the waveform on an oscilloscope in such a manner that the various measurements may be made upon the segment. Thus, the equipment must select any portion of the waveform under analysis, the time

duration of the selected portion being short with respect to the period of one complete cycle of the waveform; this selected portion must be displayed on an oscilloscope screen in an expanded form, such that the ordinates of two points on the segment can be measured. The time interval between these two ordinates must be known. If the selected segment is to be displayed in an expanded form, once the time length of the segment is decided, then the speed of scan of the time-base required can be fixed. In accordance with chapter 1.2., the frequency of the test oscillator is approximately 500 Kc/s, giving a period of 2 μsec. If the time-base scan is made 0.2 μsec. (effective) the segment will correspond approximately to a 36^{o} rotation of the generating vector. This was deemed too great, and a figure of 18^{o} was aimed at.

Since the time-base speed is so high, and the system is pulse-operated, the pulse repetition frequency must be made fairly high for clarity of trace. But this cannot be increased indefinitely, for during the period that the oscillator is running the reactor valve must be operated and the consequent transient allowed enough time to decay to zero (mensurably). Also, any pulsed oscillator will have some build-up time[33], and the reactor valve must not operate until the amplitude of the oscillation is stable; the oscillator will also have a decay time depending on the time-

constant of the tuned circuit. Hence, the pulse length must be long enough to accommodate the build-up time and frequency-transient time, the space long enough to allow the complete decay of the oscillator output otherwise the oscillator may not always commence operation in the correct phase. The highest permissible repetition frequency can thus only be found by experiment as the development of the equipment proceeds.

Since the oscillator must be allowed time to stabilise, there must be a time delay inserted between the control pulse being applied to the oscillator and to the reactor stage; it must not introduce random time-variation or the phase of switching-in the reactor stage will vary. Similarly, the high-speed time-base must commence operation at intervals of 18^{o} along the waveform for many microseconds, and again, the delay system must be completely free from random variations for if the time-base speed is .2μsec. and sweeps over only 5 cm. of the oscilloscope screen, the traverse time is 1 cm. in .04μsec. Since a 1 m.m. movement of the trace horizontally is observable when projected on to a trace at some angle to the horizontal scan axis, then the delay must be free from time variation to better than 4 milli-micro-secs. This figure also applies to the oscillator,

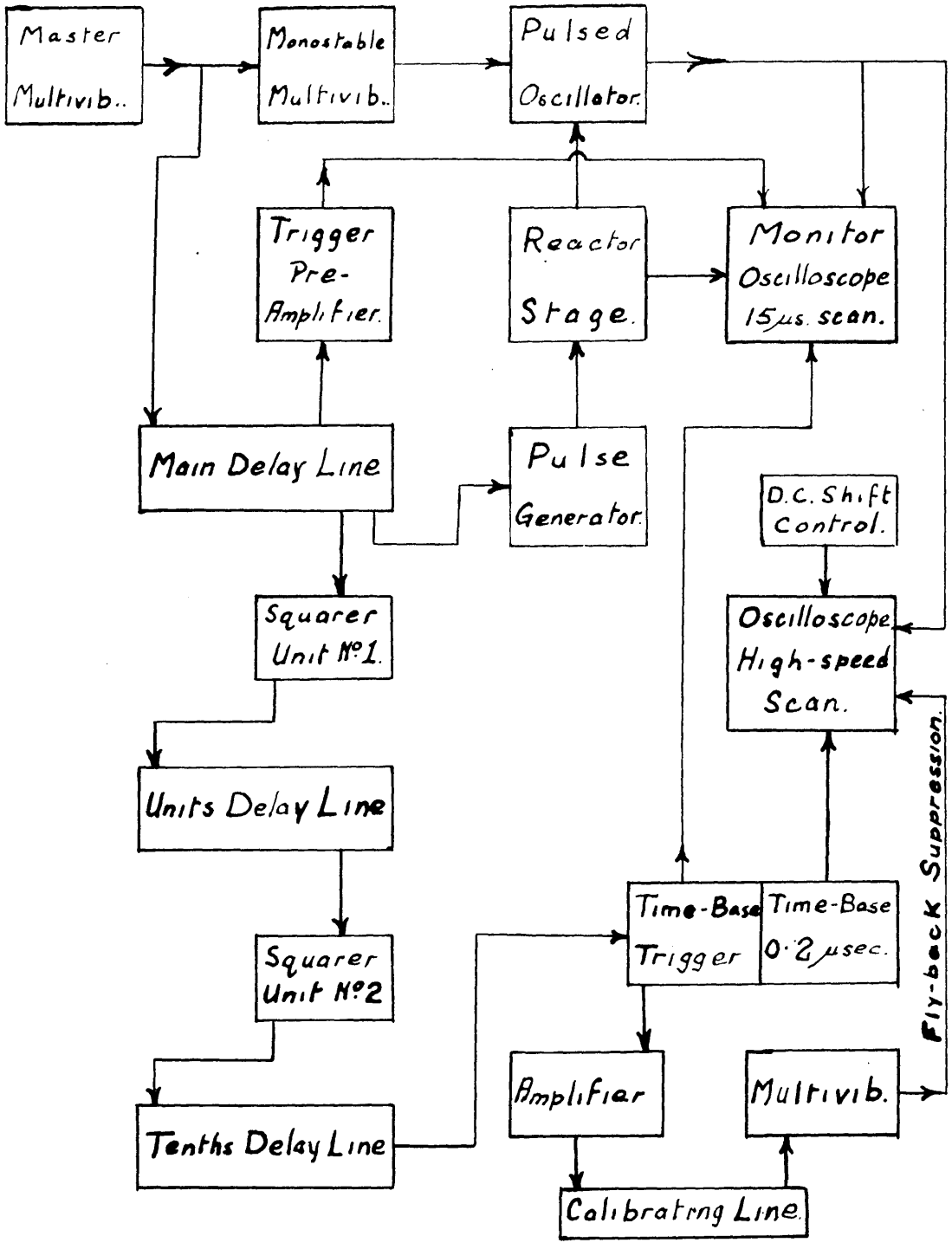
Master Multivib..
Monostable Multivib..
Pulsed Oscillator.
Trigger Pre-Amplifier.
Reactor Stage.
Monitor Oscilloscope 15μs. scan.
Main Delay Line
Pulse Generator.
D.C. Shift Control.
Squarer Unit No.1.
Oscilloscope High-speed Scan.
Units Delay Line
Time-Base Trigger
Time-Base 0·2μsec.
Squarer Unit No.2
Amplifier
Multivib.
Tenths Delay Line
Calibrating Line.
Fly-back Suppression.

FIG. 4.1.

whose instant of commencing duty with respect to its control pulse must not vary by more than the given amount. Only delay lines (i.e. artificial transmission lines) can produce this quality of delay; any system depending for its delay on, say, the grid base of a valve, must introduce some random amount of time variation due to random temperature fluctuations within the valve. The delay lines must introduce a delay of many microseconds, but with a variability of 0.1 microsec. or less (to move the time-base along the waveform at 18° intervals).

Finally, a time-base of the required scan speed with an amplitude of at least 150v. must be obtained, together with a method of measuring as accurately as possible both the actual scan-time and linearity.

To fulfil these requirements the system, drawn in block diagram form in Fig.4.1 was used; the details of the sequence are as follows with reference to the time-phase diagram of fig. 4.2. The master multivibrator produces a control pulse which is used directly to trigger a monostable multivibrator of mark period some 20 μsec. less than the control pulse. Thus the oscillator runs for a shorter time than the control pulse, otherwise the large control pulse trailing edge produced distortion of the oscillator waveform due to feed-through. After the leading edge

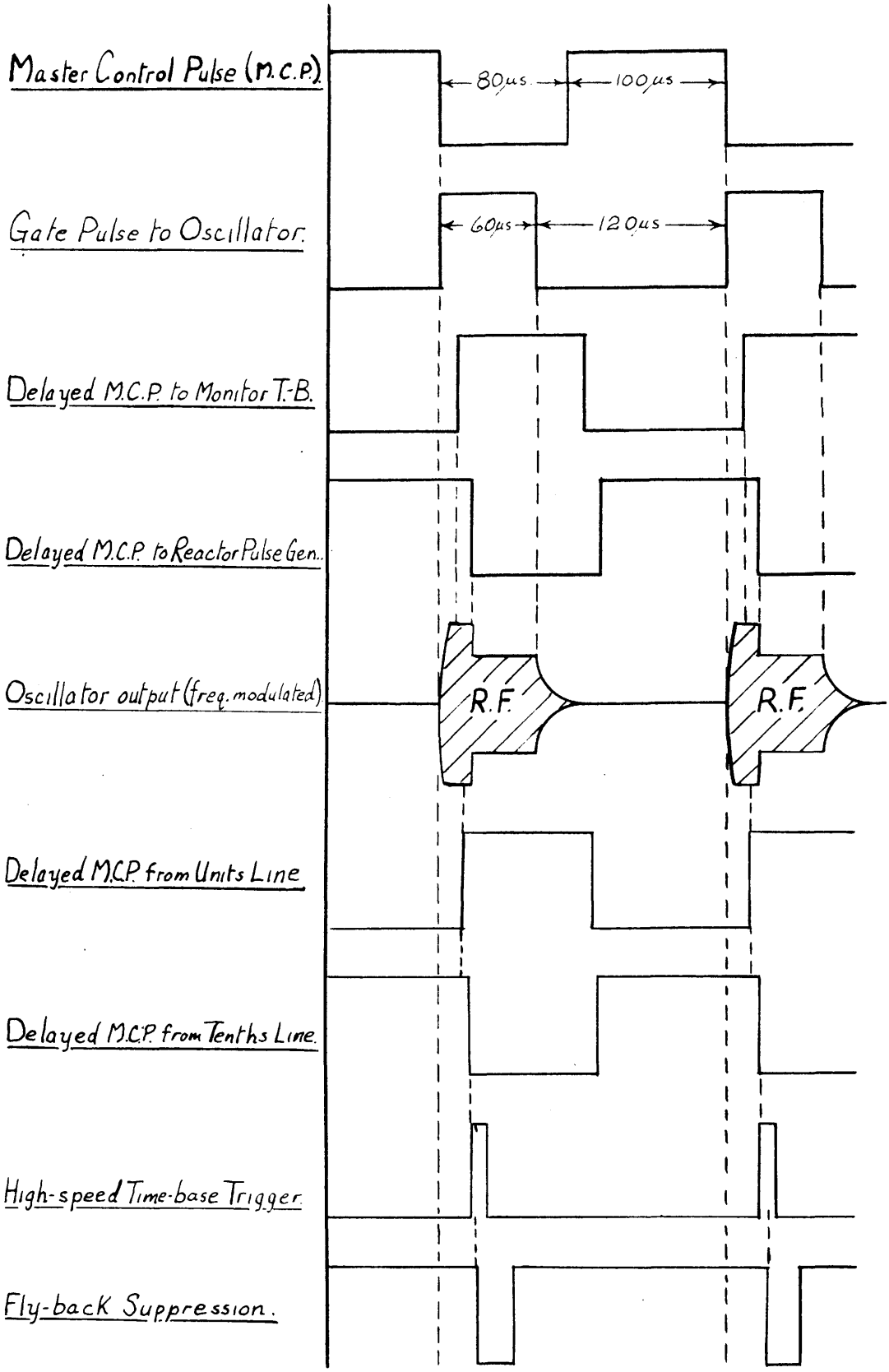
Master Control Pulse (M.C.P.)
80μs.
100μs.
Gate Pulse to Oscillator.
60μs.
120μs.
Delayed M.C.P. to Monitor T.-B.
Delayed M.C.P. to Reactor Pulse Gen..
Oscillator output (freq. modulated)
R.F.
R.F.
Delayed M.C.P. from Units Line
Delayed M.C.P. from Tenths Line.
High-speed Time-base Trigger.
Fly-back Suppression.

FIG. 4.2.

of the control pulse had started the oscillator, there is a delay of some 20μsec. (maximum) before the 15μsec. time-base is triggered, thus blanking out the build up of the oscillator. About 5μsec. after this time-base is triggered the reactor valve is operated, the resultant change in the oscillator waveform being viewed conveniently in the middle of the 15μsec. sweep on the monitor oscilloscope. Before the reactor valve was operated, an output from the main delay line had gone through a decade delay-chain to trigger the high speed time-base. Thus the high speed time-base could be triggered from any time before the reactor valve had operated, in 0.1μsec. steps, until some 30μsec. thereafter. Any segment of the oscillator waveform could thus be viewed on the measuring oscilloscope. Finally, the trigger pulse to the high-speed time-base was fed back through a buffer stage to the monitor oscilloscope to show which portion of the oscillator waveform was displayed on the msasuring oscilloscope. This is the operation of the basic scheme, although waveforms other than those mentioned above were monitored as required.

4.2 Control Circuits.

Under this general heading will be considered the design of the master and monostable multivibrators,

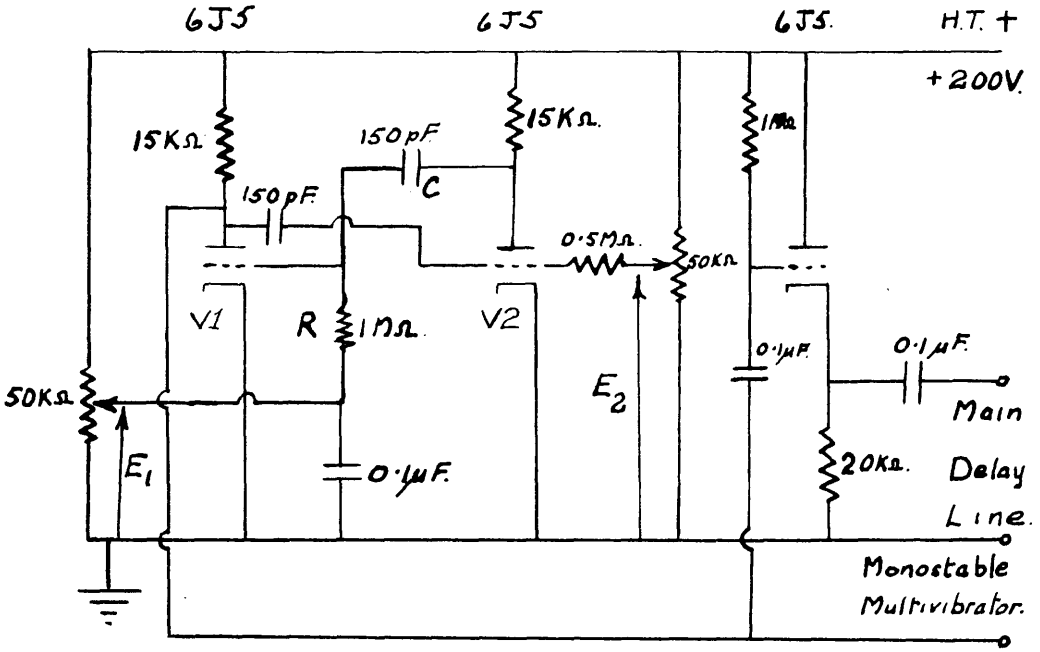
6J5
6J5
6J5.
H.T. +
+200V.
15KΩ.
150pF.
C
150pF
15KΩ.
1MΩ.
0·5MΩ.
50KΩ.
V1
R
1MΩ.
V2
50KΩ.
E1
0·1μF.
E2
0·1μF.
0·1μF.
Main
Delay
Line.
20KΩ.
Monostable
Multivibrator.

FIG. 4.3.

the main and decade delay-lines, and the inter-line squaring amplifiers and cathode follower units.

(a) Master Multivibrator.[34] The specification for this circuit is simple. Since all other circuits will be synchronised from the Master, its frequency stability does not matter, but from an experimental viewpoint the mark/space ratio and repetition frequency must be variable. A reasonable amplitude of output, say 100v., is required with a good leading edge; the trailing edge does not matter.

For simplicity, two 6J5 triodes were used in the anode-coupled circuit of fig. 4.3. Since the anode-loads and coupling capacitors are symmetrical, but the grid-leaks are 1 M.Ohm and 500 K.Ohms, there is an inherent asymmetry introduced in the output waveform when E_1 and E_2 are zero. Thus, for the circuit condition V1 cut-off, V2 conducting, from characteristics for the 6J5 it is found that V2 anode potential will be + 80v. when its grid-cathode potential is zero (i.e. ignoring the positive-going, short time-constant, transit of V2 grid). The corresponding drop inV1 grid potential is (200 - 80)V = 120v., and this potential will decay exponentially towards earth (E_1 = 0) with a time constant C R = 150 μsec. For a supply of 200v. the grid-base of a 6J5 is -12V., and hence the time t_1 during which V1 is cut-off is found

From - $$-12 = -120\, e^{-\frac{t_1}{CR}}$$

$$\text{i.e.,} \quad t_1 = 350\,\mu\text{sec.}$$

Similarly, the time t_2 during which V2 is cut-off will be approximately, $t_2 = 175\mu$sec. If E_1 and E_2 have any positive values these times will be reduced, for now, in the case of t_1

$$E_1 + 12 = (E_1 + 120)\, e^{-\frac{t_1}{CR}}$$

$$\text{i.e.,} \quad t_1 = CR \log_e \frac{E_1 + 120}{E_1 + 12}$$

From Fig. 4.2 the actual value of t_1 was given as 100μsec. This required E_1 to be about +100V., which was considered good design practice, since the slope of the exponential recovery of V1 grid-potential at the cut-off value of V1 was made steep; in this way, any small variations in grid-swing, H.T. supply etc., have less effect on t_1 than if E_1 was zero. The same applied to t_2 where E_2 was adjusted to make t_2 = 80μsecs. The resultant 120v. negative going pulse, 80μsec. wide, at V1 anode was fed direct to the monostable multivibrator, and also via the cathode follower to the main delay-line. The waveform was d.c. restored at the grid of the cathode follower, this stage being required to isolate the Master multivibrator from the low input impedance of the main delay line. Since the effective cathode load was the iterative impedance of this line the output from

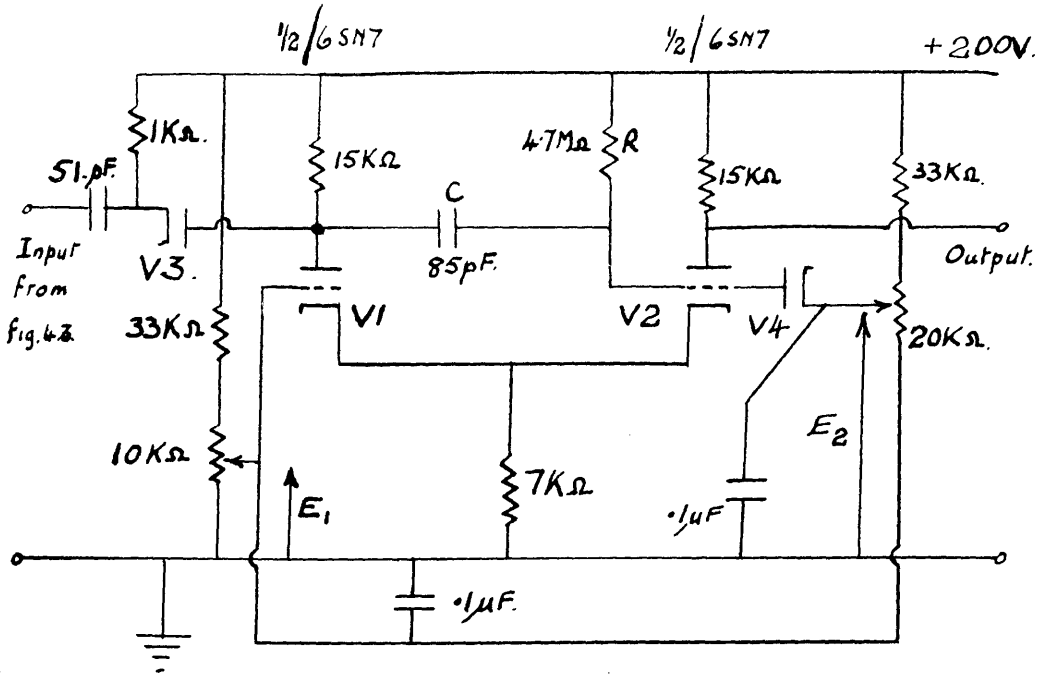

FIG. 4.4.

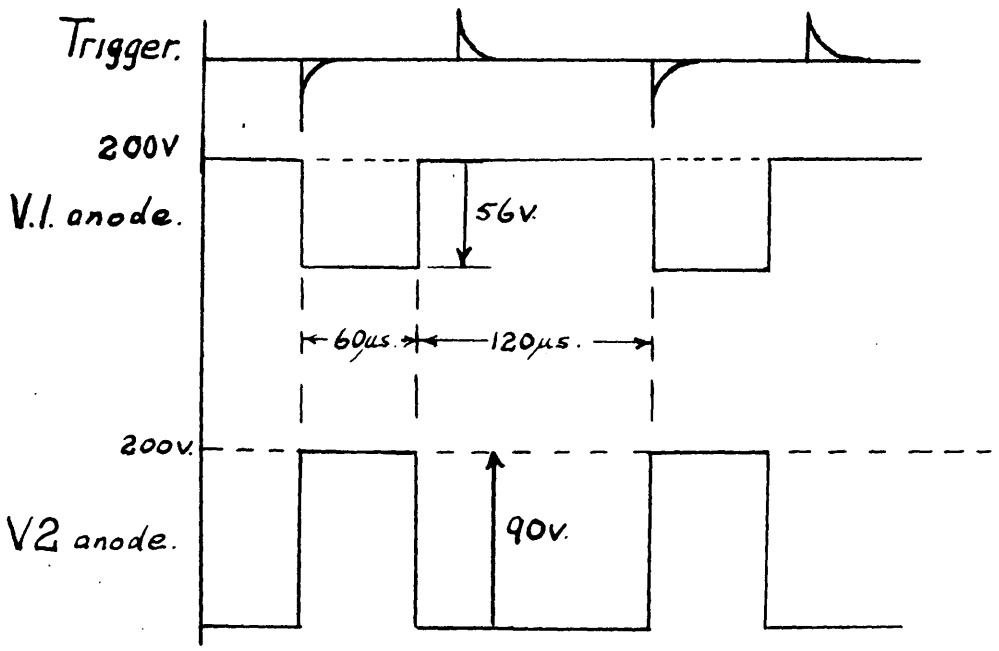

FIG. 4.4.(a).

the C.F. was only 38V.

(b) Monostable Multivibrator.

The monostable multivibrator circuit is shown in fig. 4.4. Since the output of this circuit was used to gate the oscillator on and off, a flat-topped pulse with good leading and trailing edges was required. The cathode coupled form of monostable multivibrator is capable of meeting these requirements, although the design[35] of the circuit is very much a case of trial and error; this is so because of the interdependence of the variables. Hence, from experience, certain values of circuit elements were tried in the first place, and then modified until the desired output waveform was obtained. Since the oscillator gating pulse was to be narrower than the master pulse, it was found that a 60μsec. oscillator gate was suitable.

The action of the circuit is best seen by considering the circuit of Fig. 4.4. together with its output waveforms of Fig. 4.4(a). Normally, V2 is conducting, and since its grid-leak, R, is returned to the H.T. supply rail, the diode V4 is conducting and the grid to ground potential of V2 is that of the diode cathode, i.e. + E_2volts. During this period, the anode to ground potential of V2 is 110V; hence the anode current is 6 mA. From characteristics of the

6J5 ($\frac{1}{2}$/6SN7), a load line corresponding to (anode load + cathode load) of 22 K.Ohms, gives the required grid-cathode potential of -.5V for this current. Since the anode current of V2 flows through the 7 K.Ohm cathode resistor, the cathode-ground potential is +42V. Hence E_2 is + 41.5V, and V2 draws a very small value of grid current. On the application of a negative going pulse from the Master Multivibrator, which is differentiated by the 51 pF. and 1 K Ohm. input circuit, the resulting narrow negative-going spike carries the cathode of V3 negative. Thus the grid of V2 is carried negative, and cumulative regeneration takes place, the anode of V1 dropping by 56V. from +200 V. This drop also appears on V2 grid, taking it from +41.5V. down to - 14.5V. and cutting V2 off. The capacitor C now begins to charge exponentially towards +200V. with a time constant of RC (to a very good approximation since R $\gg$ 15 K.Ohms in parallel with the Ra of V1). Since V1 anode dropped by 56V., its anode current must be 3.73 mA., and hence the cathode ground potential must now be +26V. From characteristics for a 6J5, and a 22 K.Ohm load line, the grid-cathode potential is found to be -4V., giving E_1 = + 22V. Since V_4 ceased to conduct whenever V2 grid potential fell, the capacitor C will

charge towards the full supply voltage of +200V. The valve V2 will begin to conduct again when its grid potential is approximately 1½ V. below the cathode-ground potential of +26V., i.e., at +14V. Therefore, taking + 200V. as the base line for the exponential, the time that V2 is cut off is found from :-

$$(200 - 14) = (200 + 14{\cdot}5)\, e^{-\frac{t}{RC}},$$

i.e., $$186 = 214{\cdot}5\, e^{-\frac{t}{400}}$$

where t and RC are in microseconds;

whence $$t = 59{\cdot}5\ \mu sec.$$

After this time, V2 conducts and the original conditions obtain, with V1 cut off (the cathode potential is +42V., and V1 grid-ground potential is +22V.) The lower end of the V2 grid potential-divider chain is taken to V1 grid to permit a certain degree of fine control of pulse width. Since the anode load of V2 was only 15 K.Ohms, the rise time of the output pulse was good, having a measured value of about .4 μsec; this measurement was carried out on the time scale of a Cossor Model 1035 Oscilloscope, and was approximate. The diode V_4 served the dual purpose of setting the level of V2 grid potential, and also of preventing V2 drawing much grid-current at the transition period when V2 started to conduct

again. Due to the latter action, there was very little overshoot at the trailing edge of V2 anode pulse.

Thus a positive going 90V. pulse, 60μsecs. wide, was delivered to the Pulsed Oscillator, the leading edge of this pulse being synchronous with the leading edge of the Master pulse. The random time variation on the trailing edge of the former pulse was negligible since the slope of the exponential recovery of V2 grid potential was steep at the cut-off value of V2.

(c) Delay Lines. The design of the delay lines will now be discussed. Three in number, their design and method of calibration was essentially similar. All three were designed around stock values of inductance and capacitance, and hence do not represent the best design; since all were found satisfactory in practical performance, there was no need to improve upon them, by winding special coils etc.,

Dealing first with the Main Delay-Line, it was required to produce the longest delay of the three. It must provide a sufficient delay to permit the full growth of output of the pulsed oscillator before the oscilloscope time-base (15μsec. scan) is triggered, and a further delay before triggering the

the pulse generator supplying the reactor stage. Since the time-base speed was 15 μsec. the latter delay was fixed as 8μsec. i.e. an effective delay of 5μsec., since there was an inherent 3μsec. delay in the Cossor 1035 oscilloscope between the application of the trigger pulse and commencement of the visible trace. The delay required by the oscillator to build up was only finally obtained by experience of operating the equipment, but as long as the actual delay introduced by the line was greater than the build-up time, then it sufficed; this delay was taken as about 10μsec. Therefore the total required delay was about 20μsec. To obtain this delay without using an impractically long line inferred a large delay per section, and hence a low cut-off frequency. The delay per section used was 1μ sec. To obtain this, stock coils of value L = 3mH. were used in conjunction with 300 pF. mica capacitors. Therefore the delay per section was,

$$T = \sqrt{LC} = 0.94\mu sec.$$

To obtain a delay of not less than 20μsecs., 22 such sections were used, giving an approximate delay of 20.7μsec. (calculated). The iterative resistance was :-

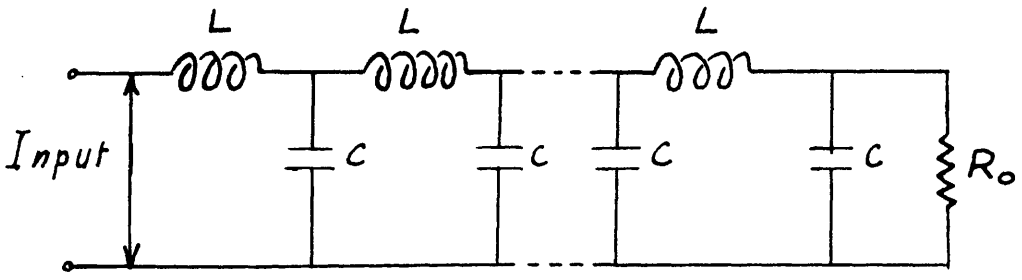

	L	C	R_o
A.	3 mH.	300pF.	3·3 KΩ
B.	3 mH.	100pF.	5·0 KΩ.
C.	0·7mH.	10 pF.	8·0 KΩ.

FIG. 4.5.

$$R_0 = \sqrt{\frac{L}{C}} \quad (\text{ignoring } \frac{\omega^2 L^2}{4})$$

$$= 3{\cdot}16 \text{ K}\Omega.,$$

i.e. the line could be matched very closely with a standard 3.3 K.Ohm resistor. Finally, the cut-off frequency of the line was

$$f_0 = \frac{1}{\pi\sqrt{L.C}} = \frac{1}{\pi T} = 340 \text{ K}^c/_s.$$

This was considered poor but since the amplitude of the output pulse of the matched line was 34V. a short grid-base valve could be used as a squaring amplifier without introducing random time variations in the delayed pulse.

The main delay line was constructed of sections as shown in Fig. 4.5 (A), the line being matched at its far end. Since it was supplied from a source resistance much less than its own iterative resistance, the matching at the far end had to be good. The coils used were selected from a large number by measurement of their inductances on a Marconi Q-meter, the capacitors being similarly selected. The absolute value of delay per section was not important on this line, and provided the sections were similar no reflection would occur.

The delay time of the line was checked experimentally as follows. The 15 μsec. and 50 μsec. time-

base ranges of a Cossor 1035 oscilloscope were calibrated in terms of microseconds per cm. of sweep, with a Marconi Standard Signal Generator (Model TF.144G) using suitable frequencies. Since the accuracy of the signal generator was much higher than the accuracy of visual measurements from the oscilloscope, the accuracy of calibration was the accuracy of the latter, i.e. about $\pm$ 2%. By taking a large number of such readings and averaging, this figure was considerably bettered (since the statistical possibility of taking high or low values is equal, for un-related readings). The line was opened 8 sections down from the input end, and the Master pulse applied to the remaining 14 sections. This pulse was also applied direct to the Trigger terminal of the oscilloscope. The output from the delay line, taken to the Al oscilloscope amplifier, was moved section by section away from the input. The leading edge of the output pulse from the delay line was not observed on the oscilloscope screen until three sections had been traversed. The inherent oscilloscope delay was thus just under the delay time of these three sections, the sections being noted. The line was now closed, and fed from its true input end. The position on the oscilloscope screen of the leading edge of the output from the third and fifth

sections was obtained, their displacement in cm. representing a time difference found from the relevant calibration. In this way the delay per pair of sections was found for all the line. Then the matched load and its parallel capacitor were put across the input end of the line, the line being now fed from its normal load end, and the delay per pair of sections was again taken. Plotting delay against section number for both cases showed the error due to measurement and that due to sectional inequalities in the line. The line was thus found to have a delay per section of 0.92 μsec. consistently, the overall delay being measured as 20 μsec. The slight discrepancy in these two figures is due to slight calibration error between the two different time-base ranges used. For the former figure, two sections were used to allow more accurate measurement of the spacing between their outputs. From these figures, the oscilloscope delay was found to be 2.76 μsec. The rise-time of the output pulse, taken between 10% and 90% of its amplitude, was 2 μsec.

The second delay-line in the chain was the first of the two decade lines, with a sectional delay of 1 μsec. (nominal). Since this line was required to produce an overall delay of 10 μsec., to obtain a better frequency characteristic, the 1 μsec. delay

was obtained over two sections and twenty such sections were used. Again using the stock inductor of value 3mH., a capacitance of 100 pF. was used, the components being selected as before. Hence the delay per section was theoretically 0.548 μsecs., giving an overall delay of 10.95 μsec; the cut-off frequency was 580 Kc/s., and the iterative resistance 5.48 K.Ohms. This line is shown diagramatically in Fig. 4.5(B). It was found that a load resistor of 5 K.Ohms produced minimum reflection. The delay per section was checked as before, for the main delay line, taking pairs of sections. It was found that there was apparently no loss of accuracy in using here a much shorter displacement on the oscilloscope screen between consecutive pulse fronts than was used previously. A consistent sectional delay of 0.54 μsec. was found, the overall figure of 10.7 μsec. agreeing well with this. Due to the higher cut-off frequency of this line and to a much improved input pulse from the Squaring Amplifier Unit No.1, the rise-time between 10% and 90% of the output pulse from this line was 0.9 μsec. This line will be referred to as the Units line of the two Decade delay lines.

For the last of the three lines, ideally ten of its sections should produce the same delay as one section of the Units line. Therefore, the total

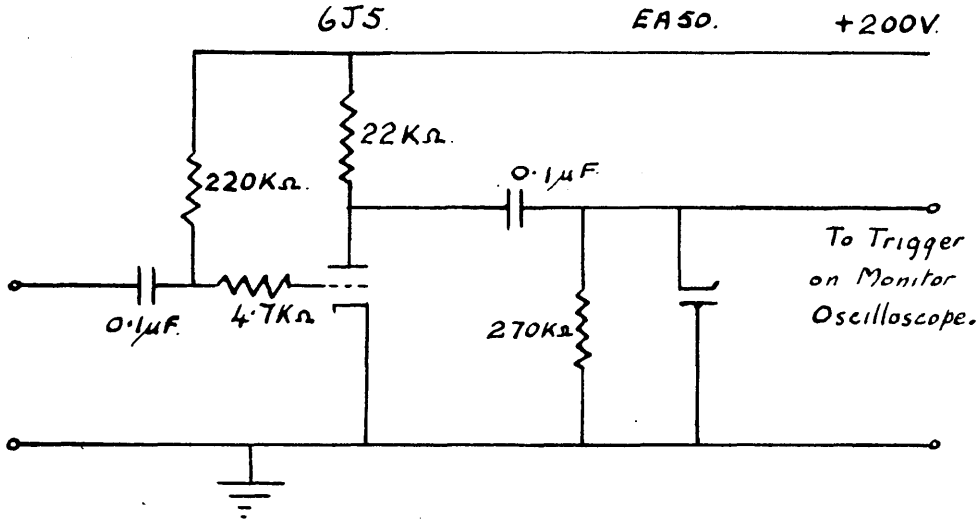
6J5.
EA50.
+200V.
22KΩ.
220KΩ.
0·1μF.
To Trigger
on Monitor
Oscilloscope.
0·1μF.
4·7KΩ
270KΩ

FIG. 4.6.

delay of this, the so-called Tenths line, should be 1.08 μsecs. Again using the only suitable stock coil available, of value 0.7mH., with a standard capacitor of 10 pF., the delay per section should be 0.0836μsecs., the cut-off frequency 3.8 Mc/s., and the iterative resistance 8.36 K.Ohms. The components were carefully selected as before. To give ample coverage of one section of the Units line, fourteen sections were used, giving a calculated overall delay of 1.17μsec. Since the sectional delay was so short, the previous methods of measurement could not be used, except to check the overall delay, which gave a figure of 1.15μsec. (average of ten readings). However, a comparative method of measurement was used, any 6 and 7 sections of the Tenths line straddling equally the delay of one section of the Units line. The Tenths line is shown in Fig. 4.5 (C), the output pulse rise-time being 0.2μsec. (approx.).

(d) Trigger Pre-Amplifier. Between the Main delay line and the Trigger terminal of the monitor oscilloscope (15μsec. scan), a pre-amplifier was inserted to provide a certain degree of pulse edge-squaring and amplification. Since the latter was not critical here, the 6J5 triode circuit of Fig.4.6 was used. The input, negative going, was d.c. restored at the grid of the valve, and the resultant positive going

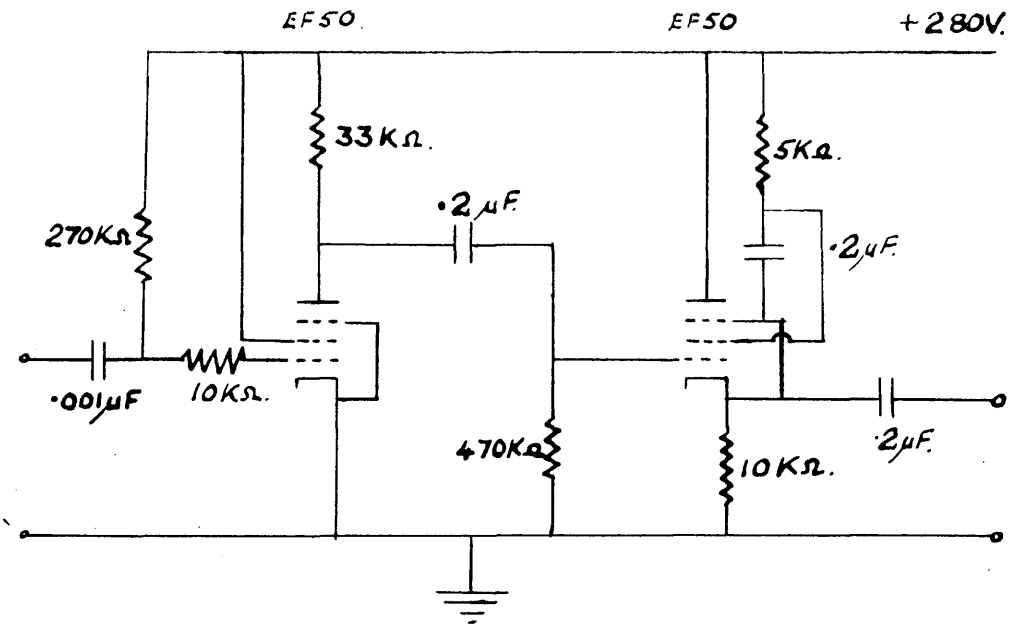
EF50
EF50
+280V.
33KΩ.
5KΩ.
·2μF.
270KΩ
·2μF.
·001μF
10KΩ.
·2μF.
470KΩ
10KΩ.

FIG. 4.7.

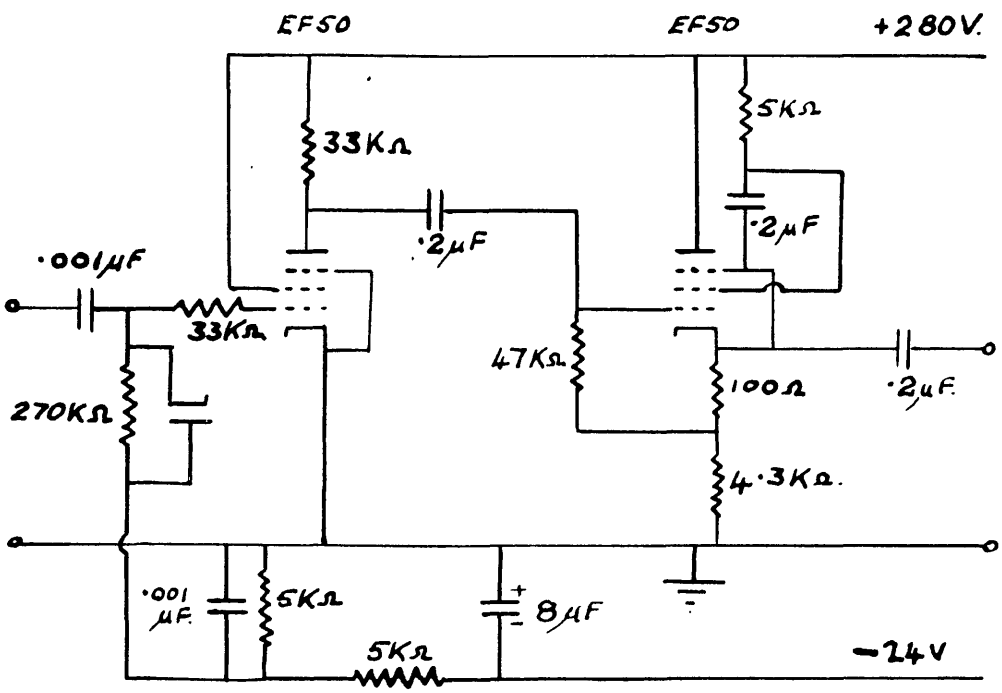
EF50
EF50
+280V.
33KΩ
5KΩ
·2μF
·2μF
·001μF
33KΩ
47KΩ
100Ω
·2μF
270KΩ
4·3KΩ
·001 μF
5KΩ
8μF
5KΩ
−24V

FIG 4.8.

output was clamped to earth by the diode. Due to the 4.7 K.Ohms grid stopper the maximum positive grid excursion was just over 1V., the negative going input pulse taking the valve down to cut-off, thereby giving an output pulse of approximately 170v. in amplitude. This amplitude ensured firm synchronisation of the oscilloscope time base.

(e) Squaring Units. The Squaring Amplifier and Cathode Follower (Unit No.1) had to meet more stringent requirements than the above. The input to this unit was a negative going pulse, 80 μsec. wide and of 34V. amplitude with a 2 μsec. rise time. Thus, over the linearly rising portion of the leading edge the rate of rise was 17V/μsec. If a short grid-base pentode, such as an EF.50, is used, the maximum rate of rise of the output pulse is G.17 volts/μsec. where G is the stage gain. The circuit used is shown in Fig.4.7. Since the grid leak was returned to the +280v. supply, the grid normally drew current, and hence the pulse train was d.c. restored, since the time constant of the grid path when grid current was flowing was in the order of 15 μsec. (the relevant space width being 100 μsec.). On the application of the negative going pulse, the valve was driven through its grid-base; also, for the given anode load of 33 K.Ohms, bottoming occurred at a grid-

cathode potential of -1.5v. Hence, effectively, a 4.5v. portion of the middle and not the beginning of the leading edge of the pulse was amplified giving an anode swing of 255v. This pulse was fed via the 0.2 μF. capacitor to the cathode follower, comprising an EF.50 triode strapped, with a 10 K.Ohm. cathode load. At the grid of the cathode follower the mean, or d.c., level of the 255v. pulse was +110v. approx. and since the cathode follower operating point was very close to cut-off, only the positive going portion was amplified; due to grid current flow, an output pulse amplitude of 80V. (positive going) was obtained with a rise time of 0.7 μ sec. This pulse formed the input to the Units delay line, the source impedance during the positive going pulse being less than 300 Ohms; during the space period it was roughly 10K.Ohms.

Thus for the Squarer and cathode follower unit No.2, the input pulse was positive going, about 80v. in amplitude, and with a rise time of 1.3 μ sec., i.e. the rise time worsened as the pulse progressed down the units delay line. Therefore, the only portion of the pulse which may be used for squaring was a small portion near the base, for if a portion near the top was used a progressive time-phase error would be introduced due to the increasing rise-time as the tap point was moved down the line. Thus in the circuit of Fig. 4.8, the base of

the input waveform was d.c. restored to -12v. such that any rounding at the lower corner was ignored, and a 4.5v. portion of the input between 6v. and 10.5v. was amplified. The amplifier valve was normally cut-off, and, with an 33 K.Ohm anode load, bottomed at a grid-cath. potential of -1.5v; the corresponding negative going anode waveform was some 250v. in amplitude. Due to the cathode load of the cathode follower being low, the output of this valve was very nearly only that portion of its input that lay below the mean d.c. value. The input to the Tenths line was therefore a negative going 60v. pulse, with a rise time of approximately 0.2μsec.

This completes the Control Circuits used. It should be noted that, with the exception of the Monostable Multivibrator, the main concern was with the leading edges of the pulses, for it was these edges that maintained the synchronism of the system; the tops and bases contributed nothing to this. In the case of the Monostable Multivibrator, the tops and bases were equally important, for a sloping top may alter the amplitude of the oscillator output. In the Squaring Units, close attention was paid to time-constants, and the component values were so chosen that the minimum rise-time and maximum gain was obtained.

4.3 Oscillator and Reactor Stages.

(a) The Oscillator.

The only limitation in choice of circuit was

that an L.C. circuit was to be used. Since a wide frequency variation was desired a tuned-anode tuned-grid circuit was eliminated; this still left great scope of choice, and the other criterion of ease of gating the circuit on and off was applied. If a triode valve was used, the gating pulse can either be applied to grid or cathode. In the former case, the gating circuit of necessity produced interference when the oscillator was running, while in the latter the necessary resistor reduced the output considerably (transformer coupling produced a slowly rising gate pulse). If a pentode was used, then either the screen or the suppressor was available for gating. For gating via the screen grid, the gating circuit must be capable of supplying normal screen current at normal screen potential when the oscillator is running; a valve in series with the screen grid supply is capable of doing this, provided its anode supply volts are high enough to counteract the d.c. drop in potential across the series valve. For gating by the suppressor, the gating pulse must be at least 100v. in amplitude to ensure a clean cut-off (the suppressor grid-base of an E.F.50 is approximately 60v.) This produces difficulties in obtaining a fast rise-time, and hence a rapid cut-off, or on, is more difficult to obtain. However, both these methods gave good results using a tuned anode

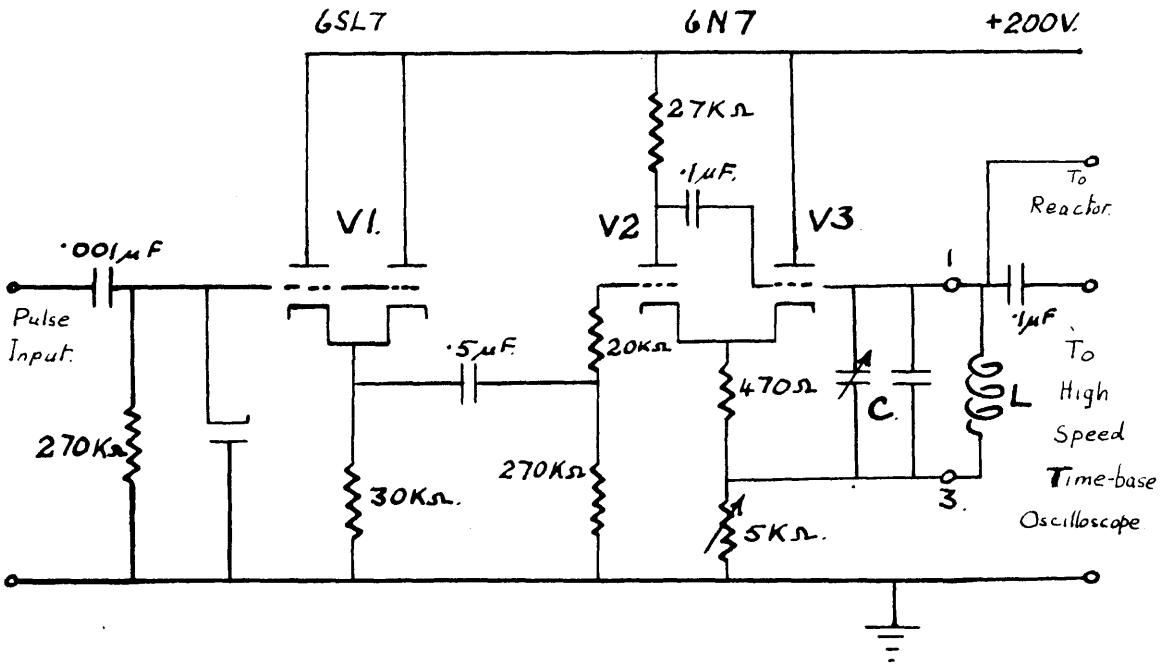

FIG. 4.9.

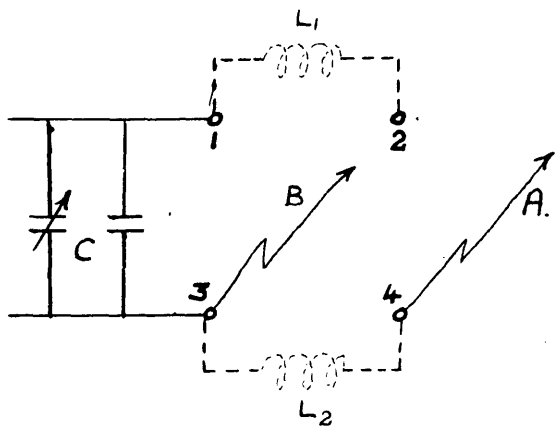

FIG. 4.10.

anode circuit with an EF.50 valve (a physical feed-back capacitor of 50 ρF. was used). But with both the triode and pentode circuits supply voltage variations produced output amplitude fluctuations, as also did heater-voltage variations. Also, the build-up times of the oscillations were rather long, particularly as the frequency was increased.

Finally, a cathode-coupled form of oscillator was found to give much superior results. The circuit is shown in Fig. 4.9. Here, the feed-back loop was via the cathode resistor from V3 grid to V2 anode, and thus the effect of supply voltage variations was greatly reduced. The build-up time was of the order of 4 μsecs. at 1 Mc/s. becoming worse as the frequency was increased; at 3.5 Mc/s. the build-up time was about 30 μsecs. and the amplitude about 10% of that at 1 Mc/s. This circuit also possessed the desirable feature of giving an output of some 80v. peak to peak; if the oscillator output is small an amplifier must be used for adequate display amplitude, and the bandwidth of such an amplifier must be great enough to accommodate all the side-bands of the frequency-modulated oscillator output. Thus if the output is great enough for direct display, the source of waveform distortion introduced by an amplifier is disposed of.

The positive going output from the Monostable Multi-

vibrator was used to gate the cathode-follower stage, V1. Since the positive going input to V1 was d.c. restored to earth, V1 was not completely cut-off during the 120μsec. space period, and hence during the 60μsec. mark (or gate) period the cathode to ground potential was 86v. The rather low value of coupling capacitor to the grid of V1 was so chosen to give a time-constant of about 5μsec. with the output impedance of the multivibrator and forward diode resistance for as good d.c. restoration as possible compatible with a long time constant (with the 270 K.Ohms leak) during the gate period. The grid leak cannot be increased without limit owing to grid-cathode capacity, which in this case was reduced by cathode follower action. Since no d.c. restoration was used at the grid of V2, this valve was completely cut-off during the space period of 120μsec. With the d.c. level of the pulse train at the grid of V2 being 28 volts (approx.) this grid was driven from -28v. to +59v; this gave an effective grid swing of just over 70v., since the grid base of V2 was about 12v. Thus when V2 was cut-off there was no feed-back path, and V3 was conducting, its current limited by the bias resistor.

On application of the gate pulse V2 was driven into conduction, and the feed-back loop closed, oscillation building up quickly due to the highly regenerative action.

Provided the cathode potential did not rise above +59v. on the positive peaks of the oscillation, the gain of V2 was approximately constant; on negative peaks, due to the large coupling capacitor of 0.5μF. V2 could draw grid current without producing noticeable sag on the top of the V2 gate pulse. Again, with V2 conducting, the increase in cathode current moved the operating point on the V3 dynamic characteristic farther down from the grid-current point to roughly the middle of the range (i.e. the range from cut-off to grid current). Thus the grid to ground potential of V3 grid could swing from +59v. down to a few volts below earth without introducing undue distortion. The observed output was 80v. peak to peak at the output terminal to the high-speed scan oscilloscope and the monitor oscilloscope; it was symmetrical about ground, and the amplitude given above applies to the circuit when loaded by the reactor stage, the latter in its quiescent state (see the following section). It was found by segmental analysis later that in fact the harmonic content of the output of this oscillator when unmodulated was small, as suggested by the above description of its action.

Since it was desired to use various known values of inductance and capacitance on the tank circuit of the oscillator, Fig. 4.10 shows the physical arrangement

used. The coils used were Standard Marconi Q-Meter plug-in coils, whose values were known to an accuracy of $\pm$ 2% and possessing inherent Q-values of greater than 150. To permit a wide range of total inductance-values across sockets 1 and 3, sockets 3 and 4 were provided with wander crocodile clips. Thus coils could be plugged in to sockets 1,3 and/or 3, 4; the values L_1 and L_2 could be arranged either in series or parallel. The fixed capacitor was soldered across the base of 1, 3, a ceramic low-loss type being used, and the variable capacitor in parallel was an air-dielectric ceramic-mounted trimmer, which was calibrated both by a Marconi Bridge (at 1000 c/s) and by a Marconi Q-Meter (at 1 Mc/s). The actual value of the fixed capacitor was measured by Q-Meter at 1 Mc/s, and for large values of capacitance each component capacitor was measured, if the total parallel capacitance was too great to be measured by the Q-meter at one frequency. (The useful range for substitution measurement of C on the standard Q-meter, at a given frequency, was 450ρ F; the frequency scale on the Q-meter was not so accurately calibrated as the capacitance vernier scale, and hence changing frequency invariably meant loss of measurement accuracy) Thus the ratio L/C was known to an accuracy of $\pm$4%

With the reactor valve quiescent, the measurement of

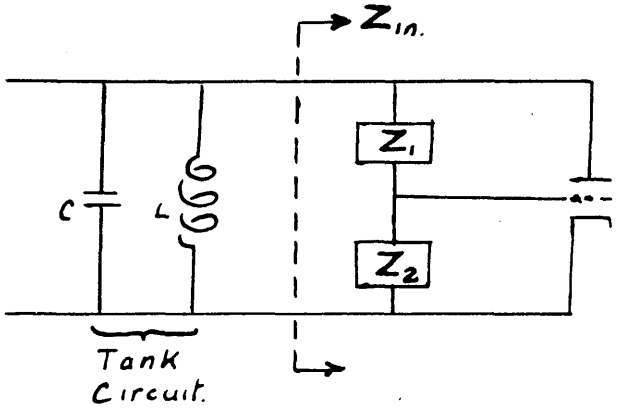

	$Z_{in.}$			
	Inductive		Capacitive.	
Z_1	R	L	C	R
Z_2	C	R	R	L

FIG. 4.11.

the unmodulated frequency of the oscillator was carried out on the 15 μ sec. scan monitor oscilloscope, whose X-shift had already been calibrated in terms of time, for frequencies up to 1 Mc/s. Above this figure, the period per cycle became too small, and the average period, taken over five or six cycles, was used to reduce the overall error by the number of cycles taken.

(b) The Reactor Stage.

In general a reactor stage draws from the tank circuit a current which either leads or lags in phase with respect to the voltage across the tank circuit; thus the input admittance to the reactor stage contains a capacitive or inductive susceptance term. This is accomplished by applying to the grid of a valve whose anode and cathode are connected in parallel with the tank circuit, a voltage which is in quadrature with the tank circuit voltage; the anode current is in phase with the grid voltage, and in quadrature with the anode voltage. Normally, the required grid voltage phase-shift is obtained by a simple two-element (R and C or R and L) phase-shift circuit. Hence this type of circuit is called the Phase-Shift reactor-stage. A typical skeleton circuit is shown in Fig. 4.11. It is analysed fully in the literature.[36,37,29] The input impedance to such a circuit comprises a resistance in parallel with a

reactance, both being functions of the valve parameters and frequency. Since the purpose of a reactor stage is to change the frequency, any change in valve parameters leads to a change both in the resistive and reactive components, the former producing amplitude modulation. By suitably designing the phase-shift circuit, the resistive term may be neutralised at a given frequency[37]; if the change in frequency is not too large, effective neutralisation may be obtained over the bandwidth. Normally, this type of neutralisation limits the frequency change inherently, and the four-element type of reactor stage can be used for wider frequency deviations.[37] In this type, the main disadvantage is complexity, and it is rarely used in practice. With both types the main objection to their use in this investigation was their small frequency swing, a swing of some 5% being about the limit. Since d.c. anode supply must be applied to the valve, either a choke or resistor is required to prevent the r.f. being earthed through the (low) d.c. supply impedance; a choke is normally used, but in this case a pulse modulation is to be applied to the reactor valve, and a choke would not permit the rapid change in anode current (and hence valve parameters) required. If a resistor is used, it must be large enough not to damp the tuned circuit seriously, i.e. the anode current is limited, and hence the change in valve parameters and frequency is limited.

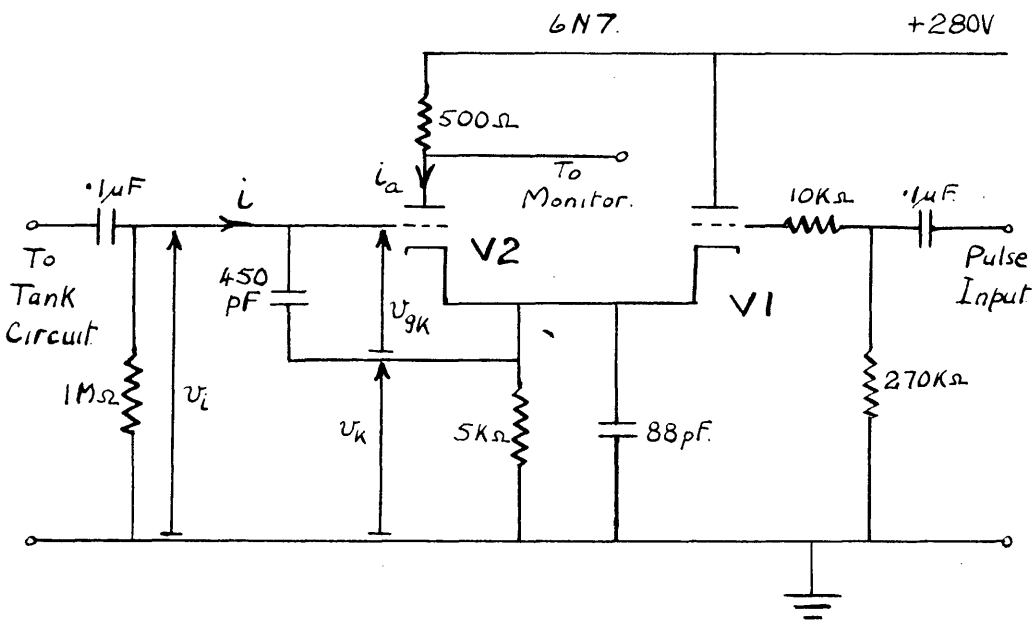
6N7
+280V
500Ω
To
Monitor.
·1μF
i
i_a
10KΩ
·1μF
To
Tank
Circuit
V2
V1
Pulse
Input
450
pF
v_{gk}
1MΩ
v_i
v_k
5KΩ
88pF.
270KΩ

FIG. 4.12.

also.

To obtain a large frequency swing, a novel type of reactor stage was developed. The circuit is shown in Fig. 4.12. In this circuit, V2 is switched off and on by V1 through the common cathode load. When V2 is conducting, and V1 off, due to cathode follower action the grid-cathode capacitance is reduced to C_{gk} (1 - G) approximately, where G is cathode follower gain.[38] When V2 is cut off, the full capacitance C_{gk} is presented, in series with the output impedance of V1 across the tuned circuit. If G is high, i.e. $G \rightarrow 1$, the change in capacitance in parallel with the tuned circuit is large, and a large frequency swing results. Normally, V1 is held cut-off, and the cathode follower condition of V2 obtains, but on application of the gate pulse, V1 conducts and V2 is cut off. Since a repetitive pulse train was used, the sinking of the base line of this train at the grid of V1 was sufficient to cut off this valve during the space period. The phase diagram of Fig. 4.2 shows the relative phasing and duration of the gate pulse used.

As applied herein, the input impedance of V2 may be found for the two conditions,

(a) V2 acting as a cathode follower, and

(b) V2 totally cut-off.

(a) From Fig. 4.12, it is seen that,

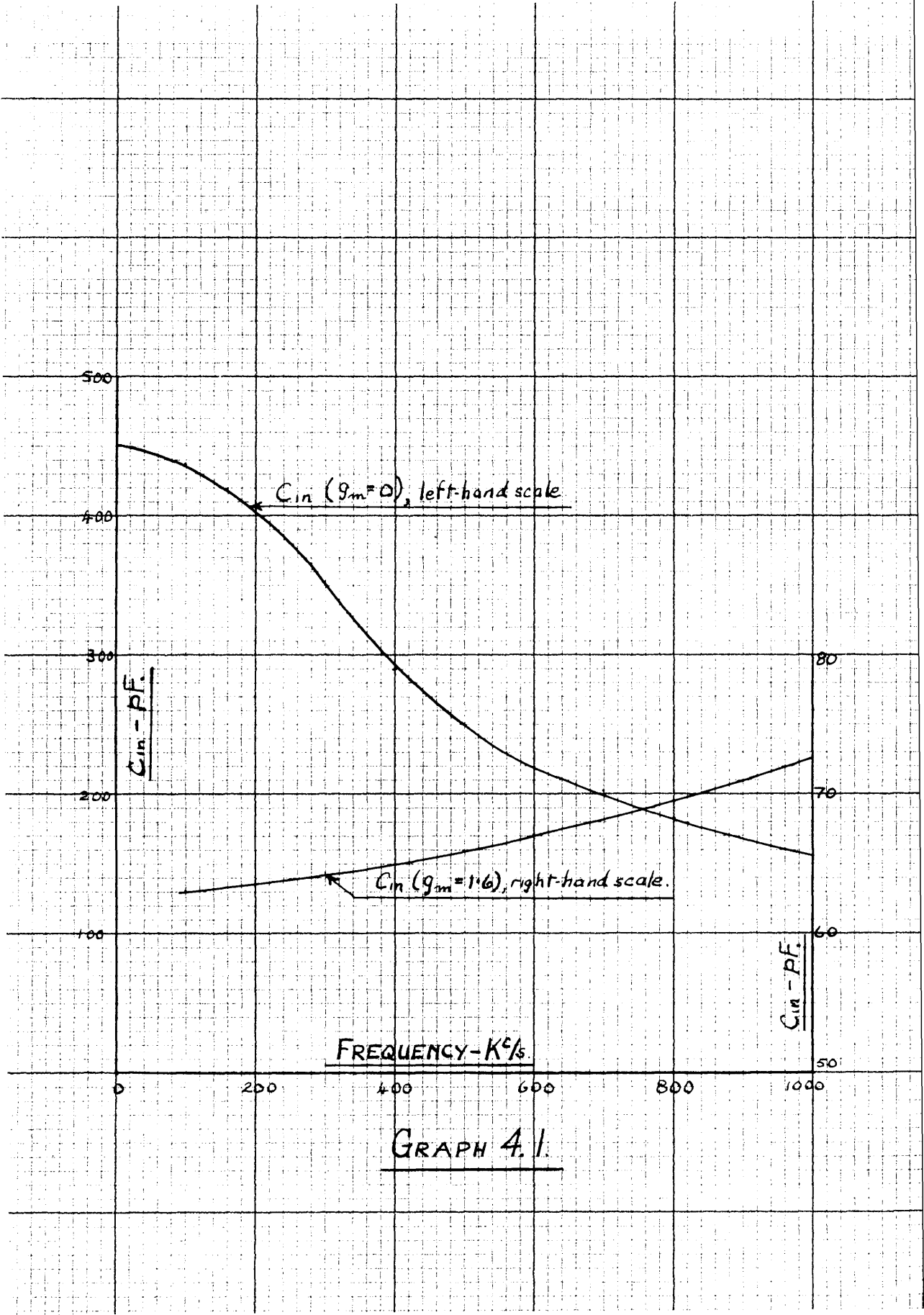
500
400
300
200
100
C_{in} - pF.
C_{in} (g_m = 0), left-hand scale
C_{in} (g_m = 1·6), right-hand scale.
80
70
60
50
C_{in} - pF.
FREQUENCY - Kc/s.
0
200
400
600
800
1000

GRAPH 4.1.

$v_K = (i_a + i)Z$ where Z = cathode impedance

$\mu v_{gK} = i_a R_a + v_K$

$\mu(v_i - v_K) = i_a R_a + v_K.$

These are the fundamental relationships, in which R_a is the valve plate resistance, the 500 Ohms. being ignored, and from which v_i and i can be isolated. Thus the input admittance i/v_i is found, and hence the values of the equivalent parallel resistance and capacitance. Writing G + jB for $1/Z$, and restricting μ to be always much greater than unity ($\mu > 10$ in practice), the parallel components are given by :-

$$R_{in} = \frac{(G + g_m)^2 + (B + \omega C_g)^2}{\omega C_g [B(g_m + 1/R_a) + \omega C_g (G + 1/R_a)]},$$

$$C_{in} = \frac{C_g [G(g_m + 1/R_a) + (G^2 + B^2) + (g_m/R_a + \omega C_g B)]}{(G + g_m)^2 + (B + \omega C_g)^2}.$$

(b). When V2 is cut off then the actual input circuit is C_g in series with the parallel combination of Z and the output impedance of V1 (conducting) at its cathode, i.e.

$$Z_{in} = \frac{1}{j\omega C_g} + \frac{Z/g_m}{Z + \frac{1}{g_m}}$$

Thus, from $Y_{in} = 1/Z_{in}$, the equivalent parallel resistance and capacitance values are found.

Curves of parallel input capacitance for each of the two conditions are plotted against frequency in graph 4.1. In obtaining this graph, the valve parameters used in the

formulae were taken from data sheets, and the circuit elements had the values shown in Fig. 4.12. From the graph the considerable change in input capacitance is obvious, and, with the tank circuit constants used, produced frequency changes of between 10% and 20%; the amplitude modulation produced was large, but apart from this application it could easily be removed by a limiter. The linearity of this type of reactor stage cannot be caluclated due to tube characteristic non-linearity, but calibration at constant frequency of the change in input capacitance of V2 per volt change on the grid of V1 was linear over approximately 75% of the working range; due to the large overall change in capacitance the sensitivity in pF/volt on V1 grid was of the same order as that obtained with Phase-shift Reactor stages. The 88pF. capacitor across the cathode resistor, although bad from all design view-points, was found necessary in practice to stop the tank circuit and reactor stage oscillating under certain conditions during the space period.

To ensure that V1 grid was driven from well below cut-off to near the grid-current point, a pulse generator was built for this specific purpose. Its output must be positive going on the reception of a trigger from the Master multivibrator, and the rise time must be good. Since the trigger must be derived from the main delay line, a pulse shaper was used to form the trigger to the pulse

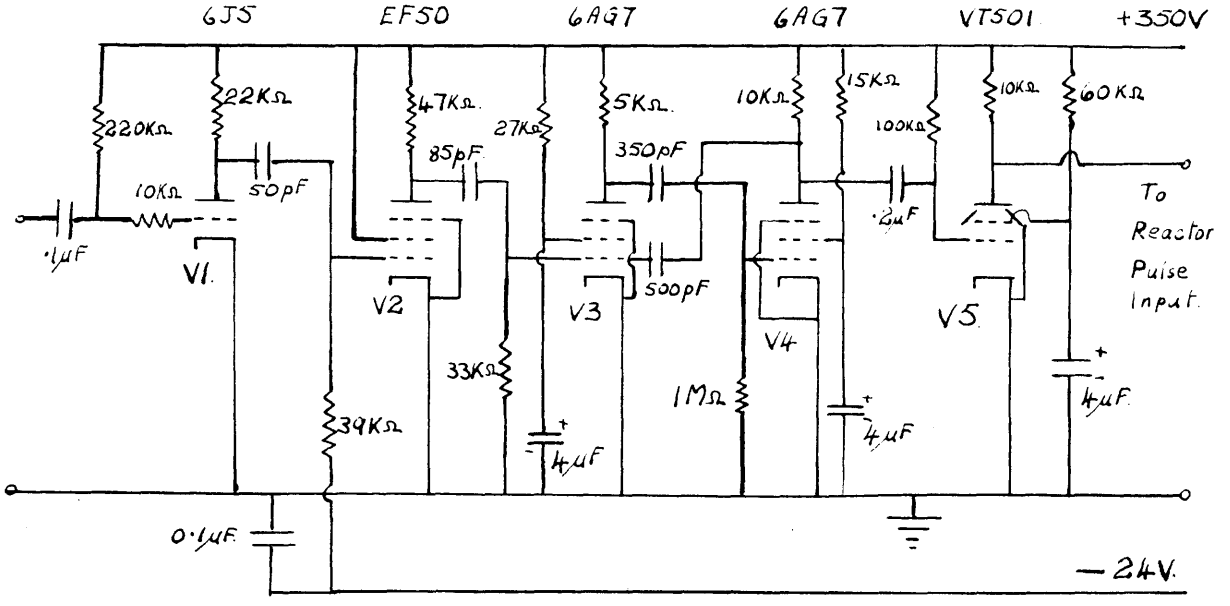
6J5
EF50
6AG7
6AG7
VT501
+350V
220KΩ
22KΩ
10KΩ
50pF
·1μF
V1
47KΩ
85pF
27KΩ
5KΩ
350pF
V2
V3
500pF
33KΩ
39KΩ
4μF
10KΩ
15KΩ
100KΩ
·2μF
V4
1MΩ
4μF
10KΩ
60KΩ
V5
To
Reactor
Pulse
Input
4μF
0·1μF
—24V.

FIG. 4.13.

generator; the complete circuit is shown in Fig. 4.13. The pulse from the main line was first amplified to obtain a certain amount of edge squaring, differentiated, and a portion of the differentiated pulse amplified in the shaping pentode circuit. At the anode of this pentode, a fast-rising narrow pulse appeared. This trigger pulse was again differentiated by the coupling network to the grid of V3 the first valve of the triggered astable multivibrator. Due to the long time-constant coupling from this valve's anode to the grid of the second multivibrator valve, V4, and the repetition frequency used, V4 was normally cut-off, and V3 conducting. On the application of the negative trigger pulse to V3 grid, V4 conducted as long as the grid potential of V3 was below the cut-off level. The resultant negative going pulse from V4 anode was inverted in V5, and the positive going pulse of some 220v. amplitude and rise time of 0.2 μsec. fed to the reactor stage. The pulse width was 80 μsec. and the space period was 100 μsec. Thus the base-line of the pulse train sank to -100v. at the grid of V1 of the reactor stage, that grid being driven from -100v. to + 120v; this drive ensured the proper switching-off of the reactor stage.

By the circuits described above, a stable oscillator was gated on and off, and during its running time the

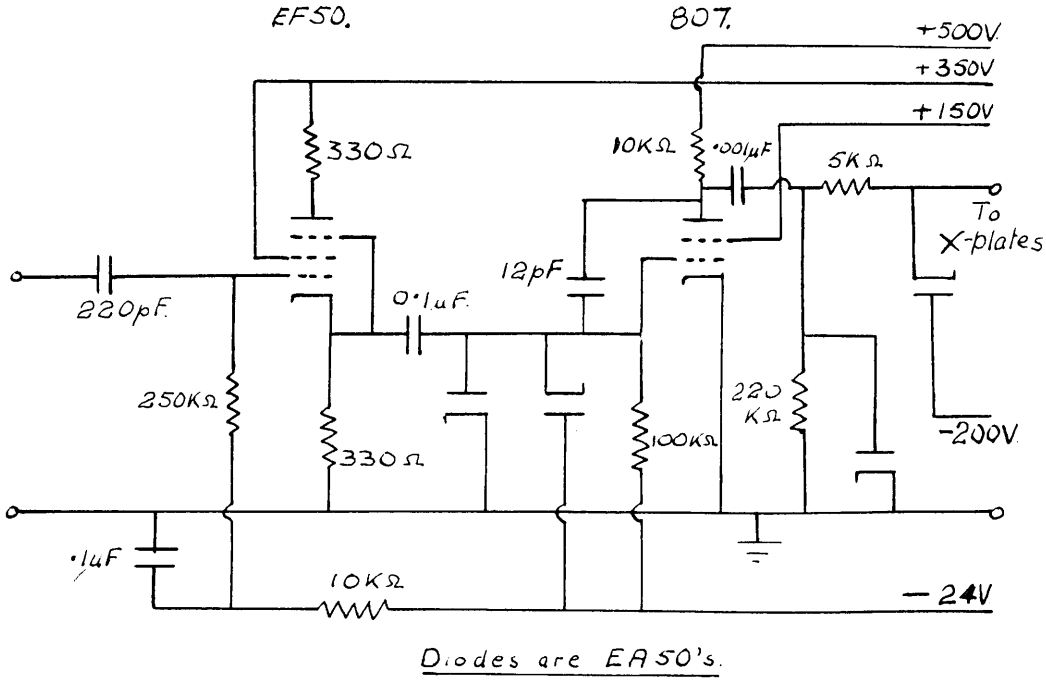

Diodes are EA50's.

FIG. 4.14.

frequency was changed by up to 20% of the original frequency by a pulse of rise time 0.2 μsec. applied to the reactor stage; the whole being maintained in perfect synchronism by the master control pulse. For constancy of performance, as far as possible all H.T. and heater supplies were stabilised but the oscilloscope supplies were not. Thus if the E.H.T. voltage to the oscilloscope dropped, the deflection sensitivity increased, and this had to be allowed for in obtaining the speed of scan of the high-speed time-base described below.

4.4 Measuring Circuits.

The principal measuring circuit was the high speed time-base; auxiliary circuits had to be developed both to control it and calibrate it. Finally, the very simple d.c. shift circuit was designed for measuring ordinates on the segment under examination. Taking things out of chronological order for ease of description, the high-speed time base circuit is described first.

The full circuit including the trigger valve is shown in Fig. 4.14. Basically, the time-base generator is a simple exponential type formed by the 807 valve, its anode load, and, total shunting capacitances. With no trigger applied, the input valve and the 807 are held cut-off, the grid of the 807 clamped to the bias voltage, the X-plate of the oscilloscope clamped to earth. On application of a trigger pulse of some 2 μsec. duration, the cathode potential of the input

807 VALVE.

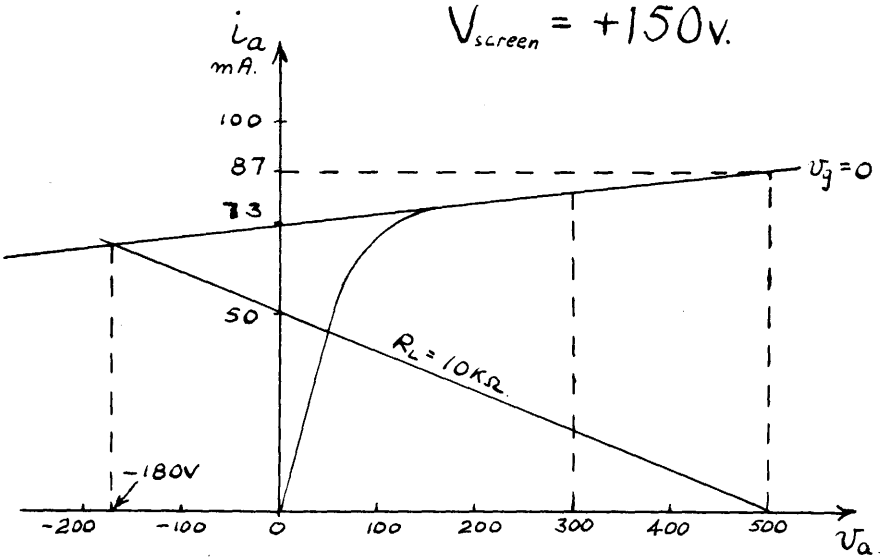

FIG. 4.15.

valve jumps positive, taking the grid of the 807 from -24v. up to earth level, the grid staying at earth due to the clamping diode. The 807 then conducts fully, and its anode potential drops. However, due to the low impedance source provided by the cathode-follower the grid of the 807 stays fixed at earth as the anode potential runs down exponentially with a time-constant formed by the 10 K.Ohm anode load and its parallel capacitances. When the resultant negative going waveform at the X-plate goes more negative than -200v. the final diode conducts, and the X-plate excursion is halted at this level. When the trigger pulse ceases, the circuit reverts to its original condition.

The time of the anode run-down from 500v. to 300v. may be calculated with the aid of the 807 measured characteristic reproduced in Fig. 4.15. From this characteristic, over the range of anode voltage considered the plate resistance is found to be R_a = 35.7 K.Ohms. Therefore, during conduction the output resistance is,

$$\frac{R_L R_a}{R_L + R_a} = 7.8 K\Omega.$$

For the total shunting capacitances, the output capacitance of the valve is 10pF, the total input capacitance of the oscilloscope and diode plates is about 20 pF., and allowing 8 pF. wiring capacitance,

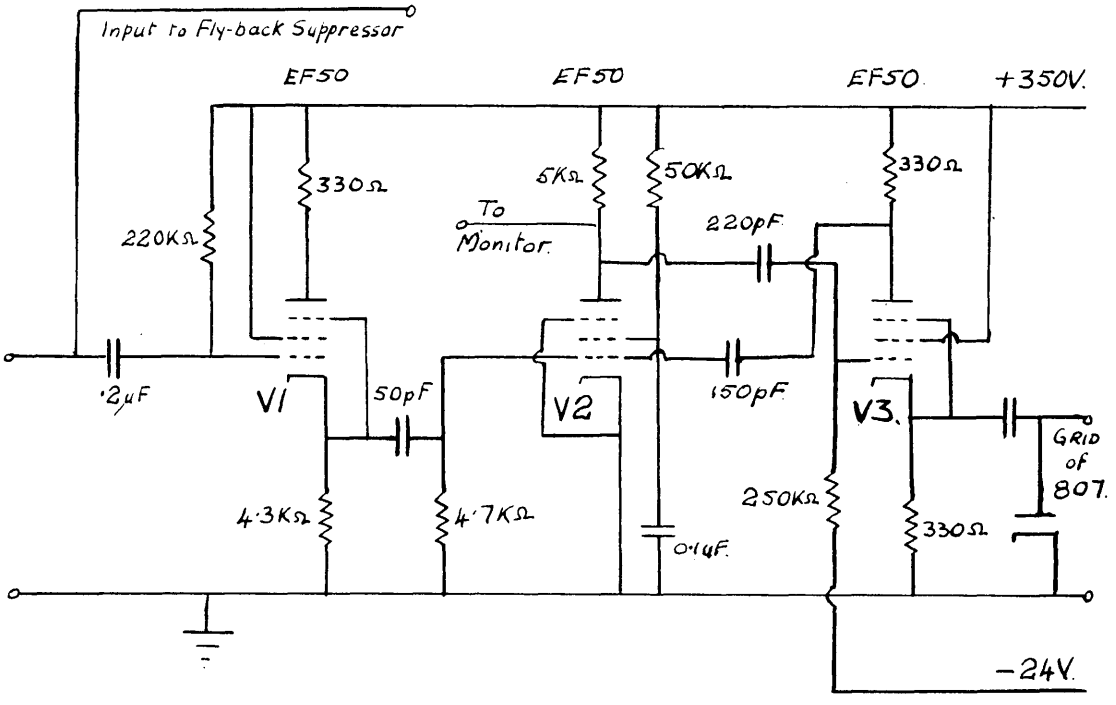
Input to Fly-back Suppressor
EF50
EF50
EF50
+350V.
330Ω
5KΩ
50KΩ
330Ω
220KΩ
To
Monitor.
220pF
·2μF
V1
50pF
V2
150pF
V3.
GRID
of
807.
4·3KΩ
4·7KΩ
250KΩ
330Ω
0·1μF.
-24V.

FIG. 4. 16.

etc., the total is (12 + 10 + 20 + 8) = 50pF.

Hence, the anode time constant is

$$T = 0.39\,\mu\text{sec.}$$

Therefore, the anode potential will start from +500v and fall exponentially towards an aiming potential of -180v. as shown in Fig. 4.17; this is true since the working portion is above the knee of the characteristic. For an anode potential drop of 200v. the corresponding value of potential measured from the -180v. baseline is (500 - 200 + 180)v = 480v. Thus,

$$480 = (500 + 180)\,e^{-\frac{t}{0.39}},$$

$$\text{i.e., } t = 0.13\,\mu\text{sec.}$$

Therefore the scan time is 0.13μsec. by calculation; the observed scan time was 0.2μsec. The agreement is close enough to substantiate the design.

The full control circuit is shown in Fig. 4.16. The input is a negative going pulse from the Tenths line, which is d.c. restored on the grid of the input valve V1. The resulting negative pulse at the cathode is differentiated by the 0.25μsec. time-constant formed by the coupling network to the grid of the second valve V2. Valves V2 and V3 form a monostable multivibrator, with V3 normally biassed beyond cut-off, and V2 conducting. On the application of the negative

trigger pulse at the V2 grid, this valve is cut off and the subsequent rise in its anode potential lifts the grid potential of V3 such that V3 conducts, Due to regenerative action, the grid potential of V2 is carried as far negative as the cathode potential of V3 goes positive; when this grid potential recovers to the conduction level for V2, the reverse action takes place and V3 is once more cut off. The coupling from V3 anode to V2 grid is such that the time of recovery of V2 grid is roughly 2 μsec. The resultant pulse at V3 cathode has extremely sharp leading and trailing edges, since a very large current is available to charge thestray capacitance during the former edge, and a low resistance discharge path is presented during the latter. V3 is, of course, the input valve of Fig.4.14. Since the time-base valve acts as an exponential generator, the pulse on its grid must have a rise-time much less than the trace sweep, and therefore the essential quality of the pulse generated by the circuit of Fig. 4.16 was the rapid rise-time, which was considerably less than the sweep duration. A marker pulse (See Fig. 4.1) was taken from V2 anode back to the 15 μsec. sweep monitor.

For its application here, the high-speed oscilloscope time-base need not be linear, but from a general utility point of view the time-base was calibrated to

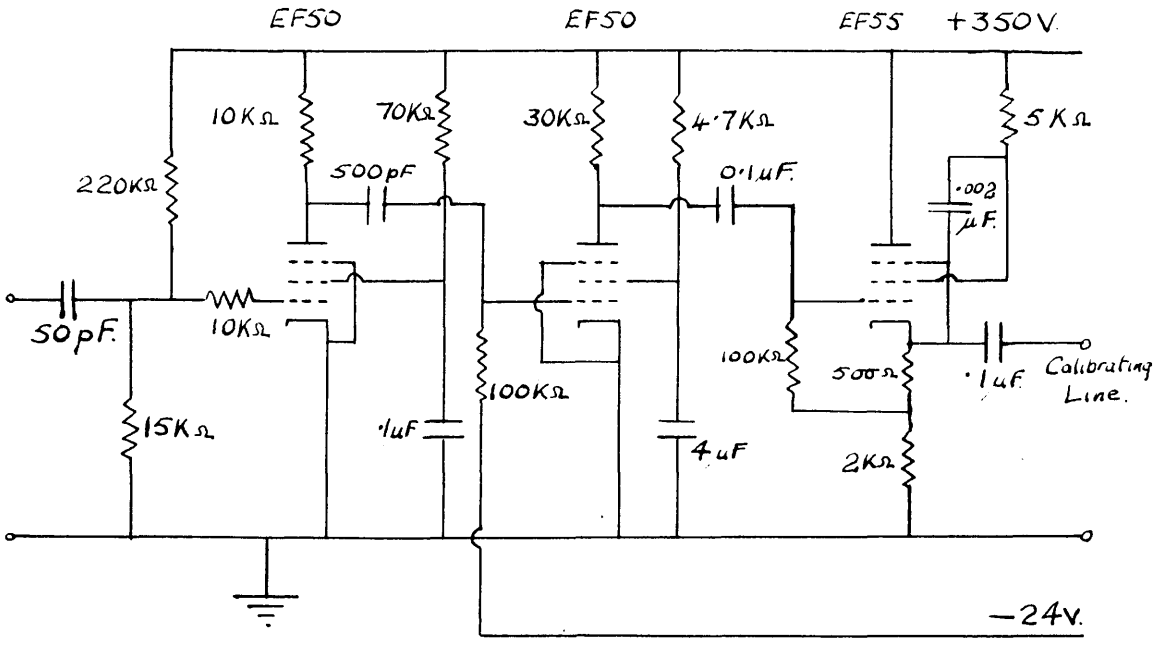
EF50
EF50
EF55
+350V.
10KΩ
70KΩ
30KΩ
4·7KΩ
5KΩ
220KΩ
500pF
0·1μF.
·002 μF.
50pF.
10KΩ
100KΩ
500Ω
·1μF.
Calibrating Line.
15KΩ
·1μF
4μF
2KΩ
—24V.

FIG. 4.17.

check its linearity. A ringing circuit at a frequency of 40 Mc/s or over could have been used, but it in turn requires its frequency measured. Hence a delay line was constructed, using hand-wound coils and carefully selected capacitors, with a delay per section of 0.024 μsec. Twenty-four such sections were used, giving an overall delay of 0.576 μsec., at an impedance of 462 Ohms and cut-off frequency of 13.3 Mc/s. In measuring coil and capacitor values, the inductance and/or capacitance of connecting leads was measured and allowed for in obtaining the true value of the component. The amplifier and impedance matching unit of Fig.4.17 was built to feed this Calibrating line from the Tenths line. This amplifier shortened the pulse from the Tenths line to a more convenient width for use on a 15 μsec. scan oscilloscope. The high-speed time-base was applied to the X-plates of the oscilloscope, and the position of the pulse from each section of the calibrating line was measured on the screen of the oscilloscope, the pulses being applied to the Y-plates. The calibrating line was then reversed, the former input end being correctly terminated; the procedure was repeated. Thus any error in the calibrating line could be ascertained and the true time-base linearity obtained. As was expected, the non-linearity was high, being

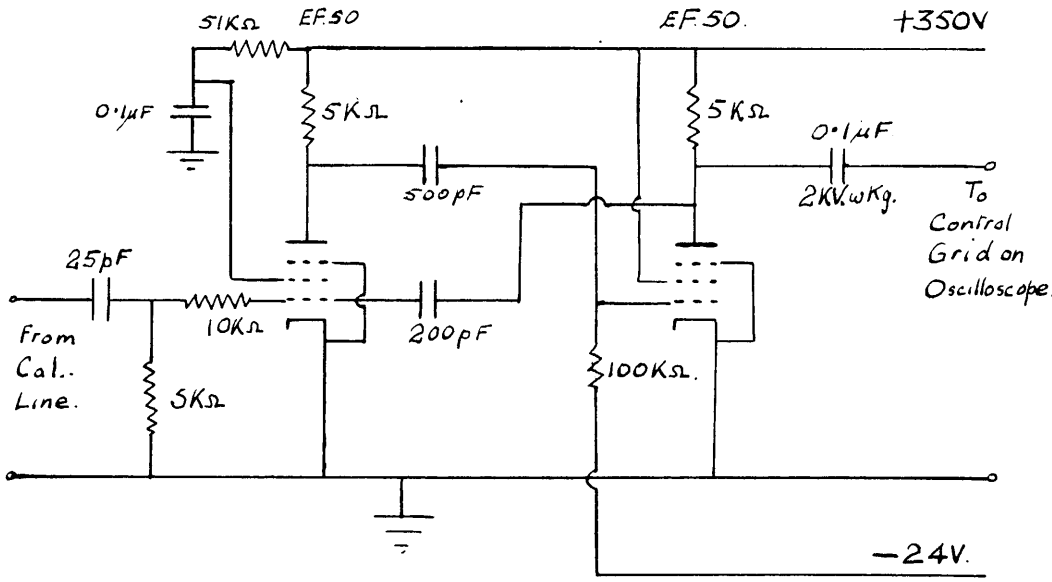
51KΩ
EF.50
EF.50.
+350V
0·1μF
5KΩ
5KΩ
0·1μF
500pF
2KV.wKg.
To
Control
Grid on
Oscilloscope.
25pF
From
Cal..
Line.
10KΩ
200pF
100KΩ.
5KΩ
−24V.

FIG. 4. 18.

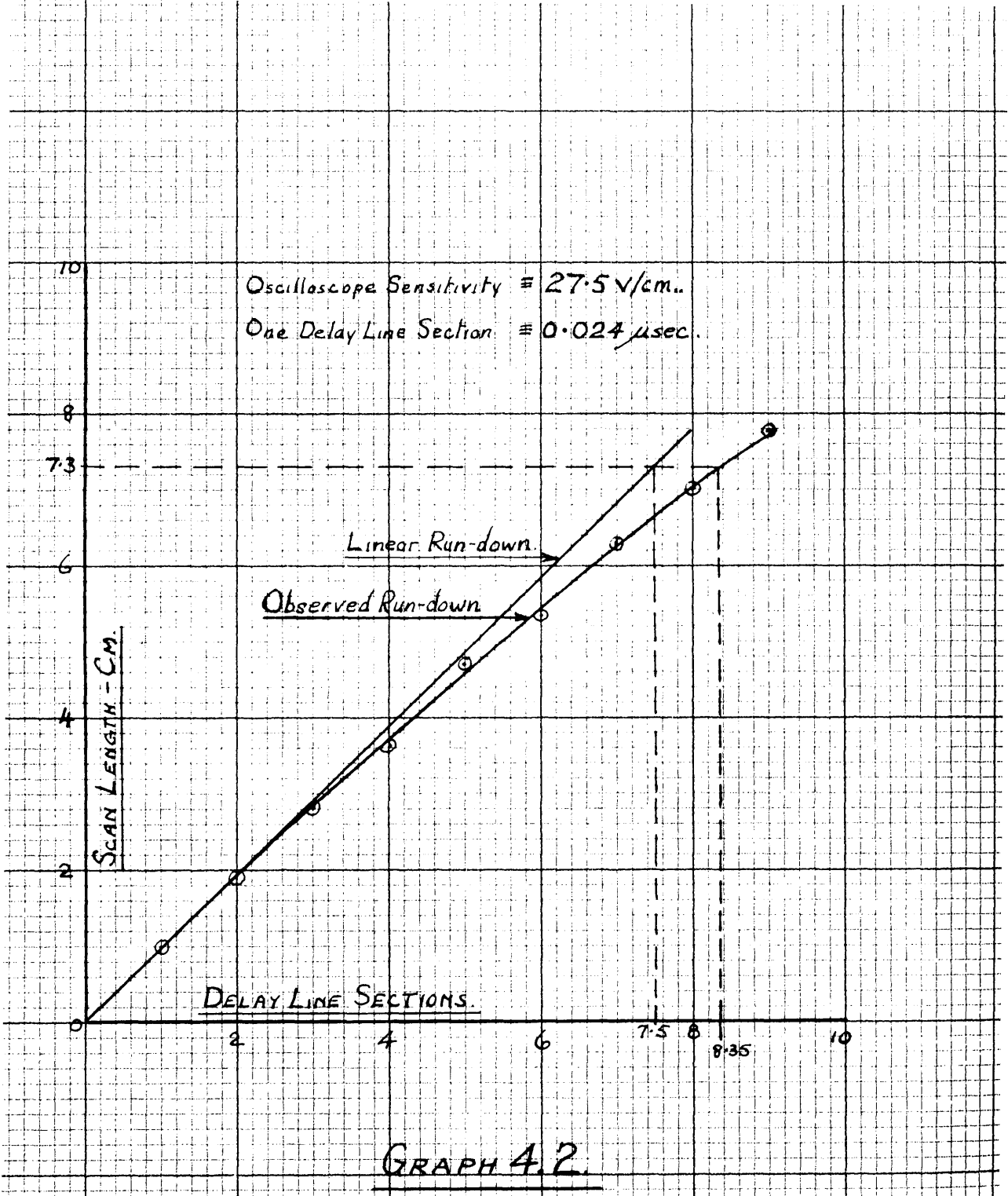
Oscilloscope Sensitivity = 27·5 V/cm.
One Delay Line Section = 0·024 μsec.
10
8
7·3
6
4
2
0
Linear Run-down
Observed Run-down
SCAN LENGTH - CM.
DELAY LINE SECTIONS.
2
4
6
7·5
8
8·35
10

GRAPH 4.2.

measured at 10%; this was obtained from the curve of graph 4.2 . Thus both the speed and linearity of this time-base were known.

To complete the time-base circuits, a beam modulation circuit was required for fly-back suppression. The gate pulse to the time-base was about 2 μsec. long, and therefore the time-base valve (the 807) conducted for that period, its anode potential climbing back to the supply potential in a few microseconds thereafter. Therefore, beam suppression need only commence sometime between the completion of the 200v. sweep and the end of the gate pulse, and continue until just after the anode has regained its maximum potential. Thus the input to the time-base unit of Fig. 4.16 was also fed to the amplifier of Fig. 4.17, delayed by the full calibrating line's delay of about 0.5 μsec., and used to trigger the multivibrator (monostable) shown in Fig. 4.18. In this manner the required delay was obtained in applying the negative-going 10 μsec. wide beam suppression pulse to the control grid of the cathode-ray tube.

Finally, to permit the measurement of ordinates at a known time separation, a double-beam oscilloscope was used, the second (or idle) beam being utilised for this purpose. The d.c. shift potential was supplied by back-to-back connection of two 120v. batteries,

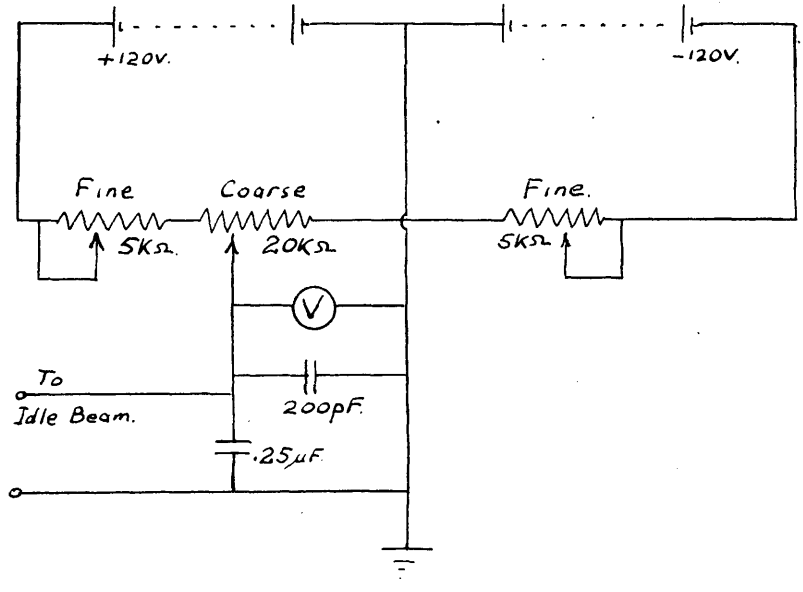
+120V.
-120V.
Fine
Coarse
Fine.
5KΩ.
20KΩ
5KΩ
V
To
Idle Beam.
200pF.
.25μF.

FIG. 4.19.

with coarse and fine control as shown in Fig. 4.19. The voltmeter used was a standard Model 7 AVO-meter, which was calibrated on its d.c. ranges specially for this purpose. Thus, the values of ordinates could be found to an accuracy determined by the observation error. To obtain the zero axis, or base-line, with no signal applied to the 'work' beam, the idle beam was set to coincide with the former, and the reading on the voltmeter noted. This initial reading was then used to correct the observed values of ordinates obtained in the immediately subsequent test run.

This completes the description of the equipment used in, and built specially for, this investigation. The power-packs used were standard un-stabilised un-regulated laboratory models, but in all suitable cases 280/80 Stabilivolt units were added for stabilisation. In all cases, de-coupling was used between units, but not necessarily within them. Each of the figures attached to this chapter utilising valves is to be considered one unit. The oscillator and reactor, and the time-base generator and fly-back suppression circuits were the only exceptions, de-coupling being provided for each supply source to each circuit in these cases. Heaters were supplied from batteries if the a.c. supply mains voltage

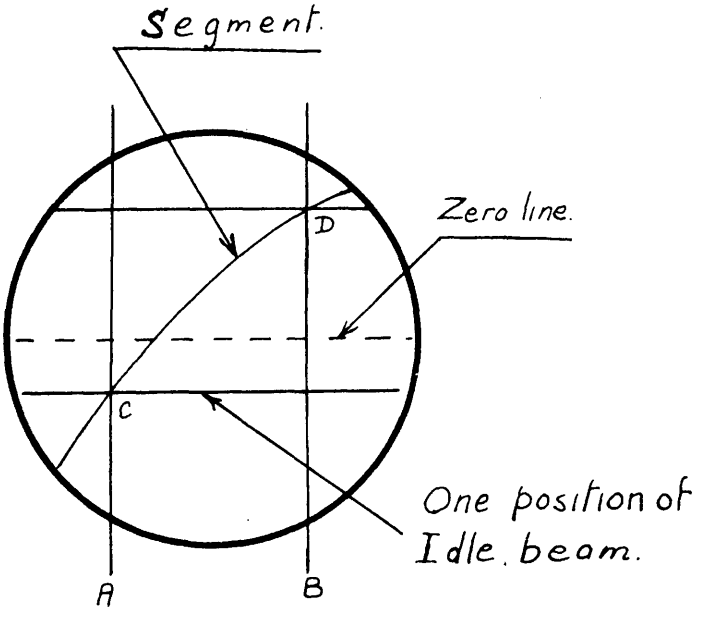

A, B :- Anti-parallax Cursor lines.

FIG. 4.20.

dropped too low, and were normally monitored, as were all supply voltages.

For every test carried out all supply voltages were checked, and the zero error obtained for the 'work' beam of the high-speed time-base oscilloscope. The oscillator and reactor stages which had been heated previously were then switched on and allowed time to stabilise (about 2 minutes). The marker from the reactor stage (Fig. 4.12) was then phased coincident with a peak of the waveform from the oscillator on the monitor; the time-base marker was phased roughly two cycles in advance of the reactor marker. Thus, segmental analysis was commenced some two cycles before any frequency modulation took place. The type of display which was obtained on the high-speed oscilloscope screen is portrayed in Fig. 4.20. The lines A and B were engraved on a double-sided anti-parallex transparent plate close to the screen; from the data obtained by the Calibrating line, their linear spacing was transformed to a time displacement. The ordinates, in volts, of the points of intersection of the segment of the curve with these two lines at C and D were found by moving the idle beam by the shift control up from the base-line (dotted) to C and D respectively. Thus the ordinates of two points of known time separation were obtained. The

amplitude, or peak values, were obtained by tangentiality of the idle and work beams, and could be read off accurately. To obviate drift, at the end of each test run, peak values and zero set were checked. In this manner, the overall oscillator waveform was broken into segments of known length and position, such that the segmental frequency as defined in chapter 3 could be found for each segment, and the result plotted against time. Thus the transient behaviour of the frequency of the oscillator could be studied.

CHAPTER 5.

RESULTS OF WAVEFORM ANALYSIS.

5.1 Parameter Control

The conditions imposed on the circuit parameters gave four distinct groups of tests. They were :-

(1) the original frequency maintained constant and the L/C ratio varied,

(2) the original L/C ratio maintained constant and the frequency varied,

(3) the original value of inductance maintained constant and the capacitance varied, and

(4) the original value of capacitance held constant and the inductance varied.

In all cases the original values refer to intial conditions before operation of the reactor stage. Further, since it is difficult to measure accurately the phase of the r.f. cycle at which the additional capacitance is switched into circuit, the point on the switching pulse at which V2 of the reactor stage commenced conduction was phased coincident with a positive peak on the waveform in each case.
An arbitrary value of the ratio (inductance to capacitance) was chosen as the basic L/C ratio, and all other values of L/C ratio were referred to the basic value by a numeric, a^2. The basic ratio chosen was

$$R_o = \frac{L_o}{C_o} = \frac{200 \times 10^{-6}}{355 \times 10^{-12}} = \frac{200}{355} \times 10^6 \ \Omega/F.$$

at an initial frequency of 597 Kc/s. If, for case (1) the frequency has to remain constant, then for any value of inductance $L = aL_o$, the corresponding capacitance must be made $C = C_o/a$, where $0 \leq a \leq \infty$. Thus,

$$R = \frac{L}{C} = a^2 \frac{L_o}{C_o} = a^2 R_o.$$

Similarly, in case (2) for constant R but variable frequency, for any value of inductance $L = b.aL_o$ the corresponding capacitance must be $C = bC_o/a$, such that $R = a^2R_o$ always, but $f = f_o/b$ where f_o is 597 Kc/s, and $0 \leq b \leq \infty$. In tests (3) and (4) both a^2 and b were variables. Finally, one other parameter found to be of importance, and measured, but not controlled, was the ratio $e = \delta f/f$, where f was the initial frequency and δf was the frequency swing, i.e. the difference between the initial and final steady-state frequencies. Thus, a, b and e become the dimensionless circuit parameters.

Since the rise-time T_i of the input switching pulse was constant in all tests, the rate of change of frequency, $\delta f/T_i$ was directly proportional to δf, and the ratio T_i/T was directly proportional to $1/T$ or f, where T is the period of the frequency f.

Test Details.

The specific details of the tests carried out are now listed.

(1) Constant frequency, variable a^2 group. For each of the three values of b

$b = 0.75, \quad b = 1, \quad b = 1.5,$

eight values of a^2 were used, within the range

$$0.25 \leq a^2 \leq 4.$$

The lower limit of a^2 was set more by unsatisfactory circuit performance than by choice. For small a^2 the value of capacitance required is large, and the injected capacitance produces a small change in frequency. The upper limit was set less rigidly, but the capacitance cannot be reduced too far or the error in estimating strays becomes significant.

For each value of a^2, segmental analysis was commenced two cycles before the switch pulse was applied, and thereafter for 20 microseconds. The latter figure was found by experience always to be adequate for the ranges covered. Thus, some 200 or more pairs of successive ordinates were required for each value of a^2, and peak amplitudes were measured during each test not only as they appeared in the sequence of ordinates, but also were checked at the end of each test to ensure that drift, either in the equipment or in the mains supply, had not been present during the test. Peak amplitude variation was plotted against time, and the angles θ_1 and θ_2 computed for each pair of ordinates in conjunction with the amplitude-time graph, the difference of these angles, when divided by the time interval between the

corresponding ordinates giving the segmental frequency. In this way, curves of segmental frequency to time were drawn for each value of a^2.

(2) Constant a^2, variable frequency group. For each of the three values of a^2

$$a^2 = 0.5, \quad a^2 = 1, \quad a^2 = 1.25$$

eight values of b were used within the range

$$0.6 \leq b \leq 3$$

In this casethe range of b was limited at the lower end by slight random time variation in the oscillator, which was only apparent on the high-speed time-base, and at the upper end by increasing harmonic content in the original waveshape. The procedure was as for group*I*.

(3) Constant L, variable capacitance. In this case, the inductance was maintained at $L_o = 200\mu H$. and six values of the ratio C/C_o were used within the range

$$0.75 \leq C/C_o \leq 1.375.$$

For this range of C/C_o, the corresponding range of a^2 was

$$1.33 \leq a^2 \leq 0.725$$

and that of b was

$$0.865 \leq b \leq 1.17.$$

The latter two ranges are purely incidental, the controlled range being that of C/C_o. The procedure

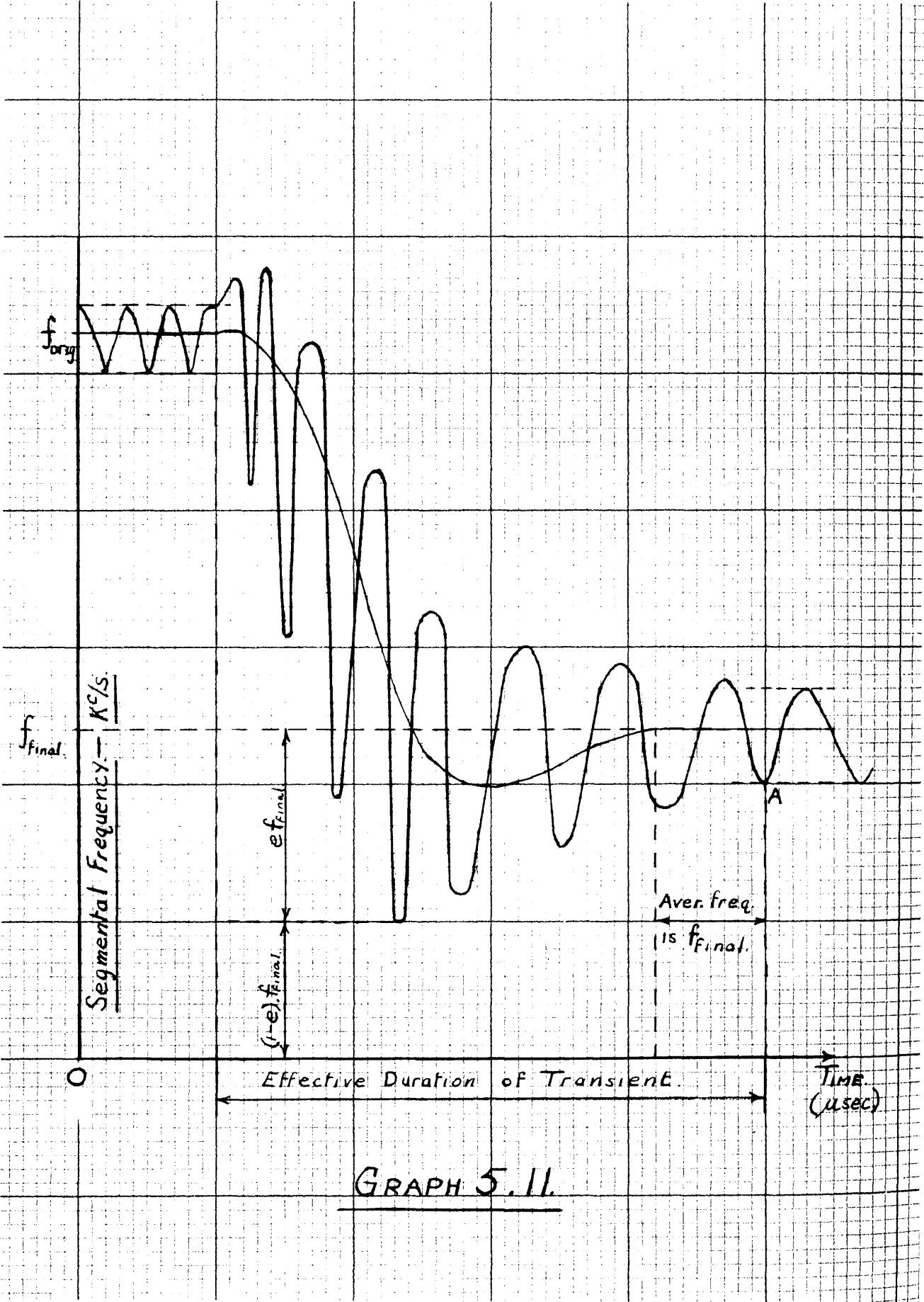
$f_{orig.}$
$f_{final.}$
Segmental Frequency — K^c/S.
$ef_{final.}$
$(1-e).f_{final.}$
A
Aver. freq. is $f_{final.}$
O
Effective Duration of Transient.
TIME. (μsec)

GRAPH 5.11.

was as in (1) for each C/Co value.

(4) Constant C, variable inductance. The value of capacitance chosen was C_o = 355 pF. Eight values of the ratio L/L_o were used within the range,

$$0.5 \leq L/L_o \leq 1.375.$$

The correspnding ranges of a^2 and b were

$$0.5 \leq a^2 \leq 1.375$$

$$0.702 \leq b \leq 1.17$$

The procedure was as in (1) for each value of the ratio L/L_o.

Thus, from these four groups of tests there resulted some 62 graphs of segmental frequency to time, all of the general form depicted in Graph 5.11 and it is the results of analysing these primary graphs that are now considered.

5.2 Analysis of Results.

The results of this experimental investigation may be considered in two ways. They may be analysed mathematically, or they may be treated from the view-point of their utility in the design of F.M. equipment. The latter view will be taken here, empirical design formulae and graphs being derived rather than the mathematical function of time represented by each frequency curve of the primary results. No correlation between such a mathematical function and that derived from theoretical analysis of the circuit

is possible. In this case, the oscillator output varies both in frequency and magnitude during the transient period; the capacitance and resistance in the resonant circuit are both, therefore, functions of time. If the resonant circuit alone be considered, a second-order differential equation with variable coefficients may be formed,[4,5] defining capacitor charge in terms of time. Since a general solution of this type of equation is unknown, the variation of the circuit parameters is normally assumed[17,11,6] (cisoidal) and the resulting Mathieu's or Hill's equation solved with the restrictions (a) that the magnitude of the variation is small with respect to its mean value, and (b) that the percentage change in the value of any parameter in one cycle of the carrier frequency is very small. Neither of these restrictions is true in this case, and such a theoretical solution cannot apply. Further, to obtain any solution of the differential equation at all, the variations in capacitance and resistance must be known as functions of time.[4,7] In this case a known pulse waveform was applied to the input of the reactor stage, but the variation in resistance and capacitance across the resonant circuit was indeterminate, depending on the non-linear characteristics of two valves. Since the author knew of no method, experimental or theoretical, of determining this

variation, no theoretical solution could be attempted. An empirical approach was therefore resorted to.

The important factors for design purposes are the duration of the transient and the maximum overshoot in frequency for any given a^2 and b values. The latter factor is relatively unimportant, in telemetry in particular, for that portion of the channel signal containing any frequency transient is useless for data transmission; but the maximum frequency overshoot may produce receiver paralysis. If this overshoot is great enough to drive the frequency discriminating element far beyond its normal range, the recovery time of the element may be longer than the remaining frequency transient, thereby reducing the available data carrying period and the power in the sample. In present systems this is avoided by suitably gating the receiver in advance of the frequency discriminator. Again, in all F.M. systems, the amplitude variation is quite immaterial, as the amplitude is invariably severely limited to eliminate amplitude modulation both from the source, as in this case, from impulsive noise, and also, in telemetry, from selective fading as the missile rolls or precesses in flight. Therefore, the most important results of this investigation from the design point of view are those concerning the duration of the frequency transient and its dependence

on circuit parameters.

Since the primary graphs of segmental frequency versus time are all oscillatory in character, the method of estimating the duration of the transient used throughout the work is, of necessity, not absolute. It is illustrated in graph 5.11 which is typical of all the primary graphs. With reference to this graph, since any oscillator produces a certain amount of harmonic content, the segmental frequency in the original and final steady states is oscillatory, of period equal to the reciprocal of the relevant steady state frequencies. Since the point in the oscillator cycle at which the reactor commenced operation is known, together with the rise-time of the switching pulse, the beginning of the transient is fixed (if the resultant frequency variation faithfully follows the switching pulse, the transient duration is to be considered zero). For the end of the transient, two horizontal lines were drawn to give the limits of the peak to peak swing of the segmental frequency for the final steady state condition, and the transient was here deemed to end at the first peak of the segmental frequency waveform which lay on one of these limiting lines, i.e. at point A on the graph. The original and final steady state frequencies were taken as the mean value of the waveform between the limiting lines.

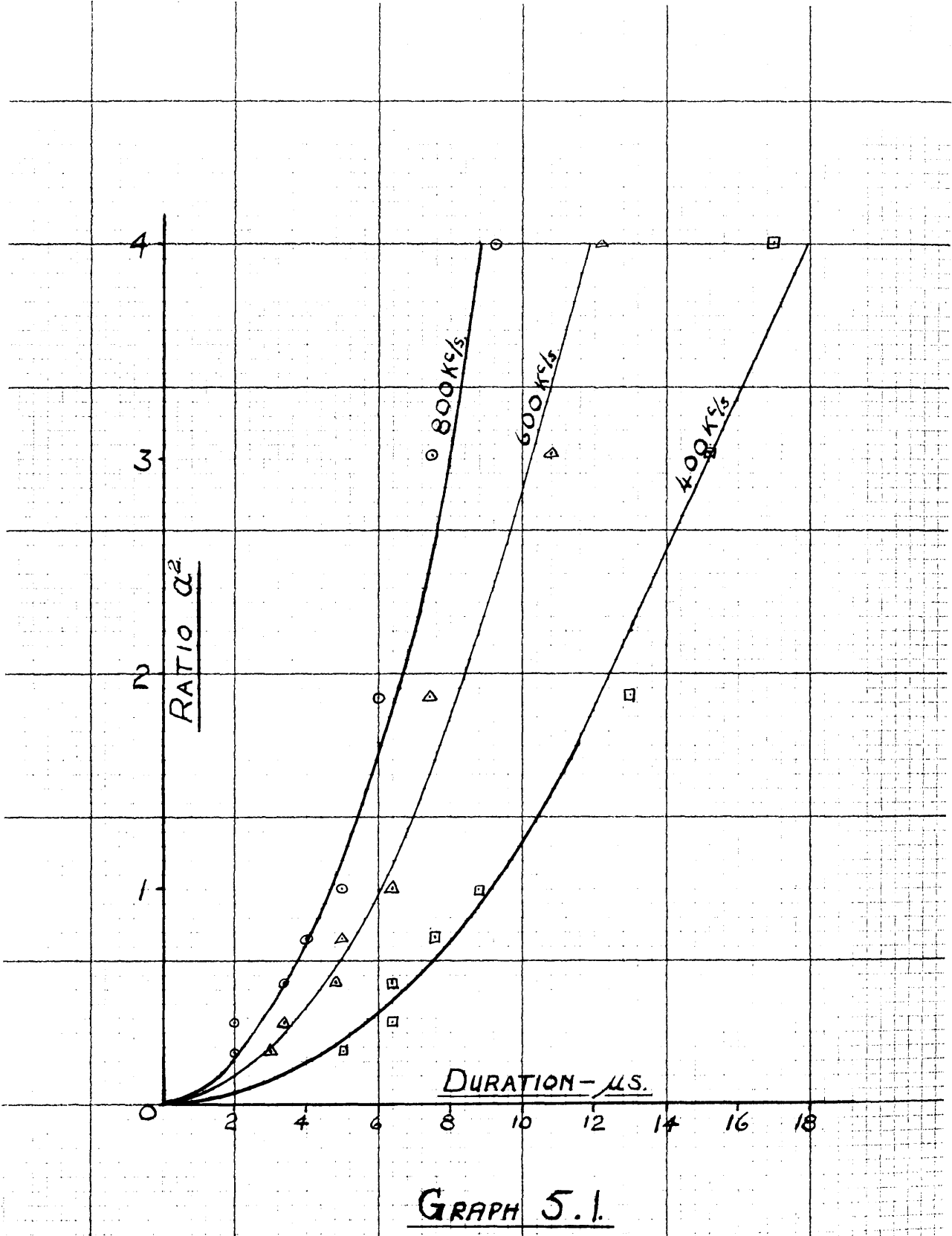
4
3
2
1
0
RATIO a^2
800 Kc/s
600 Kc/s
400 Kc/s
2
4
6
8
10
12
14
16
18
DURATION – μs.

GRAPH 5.1.

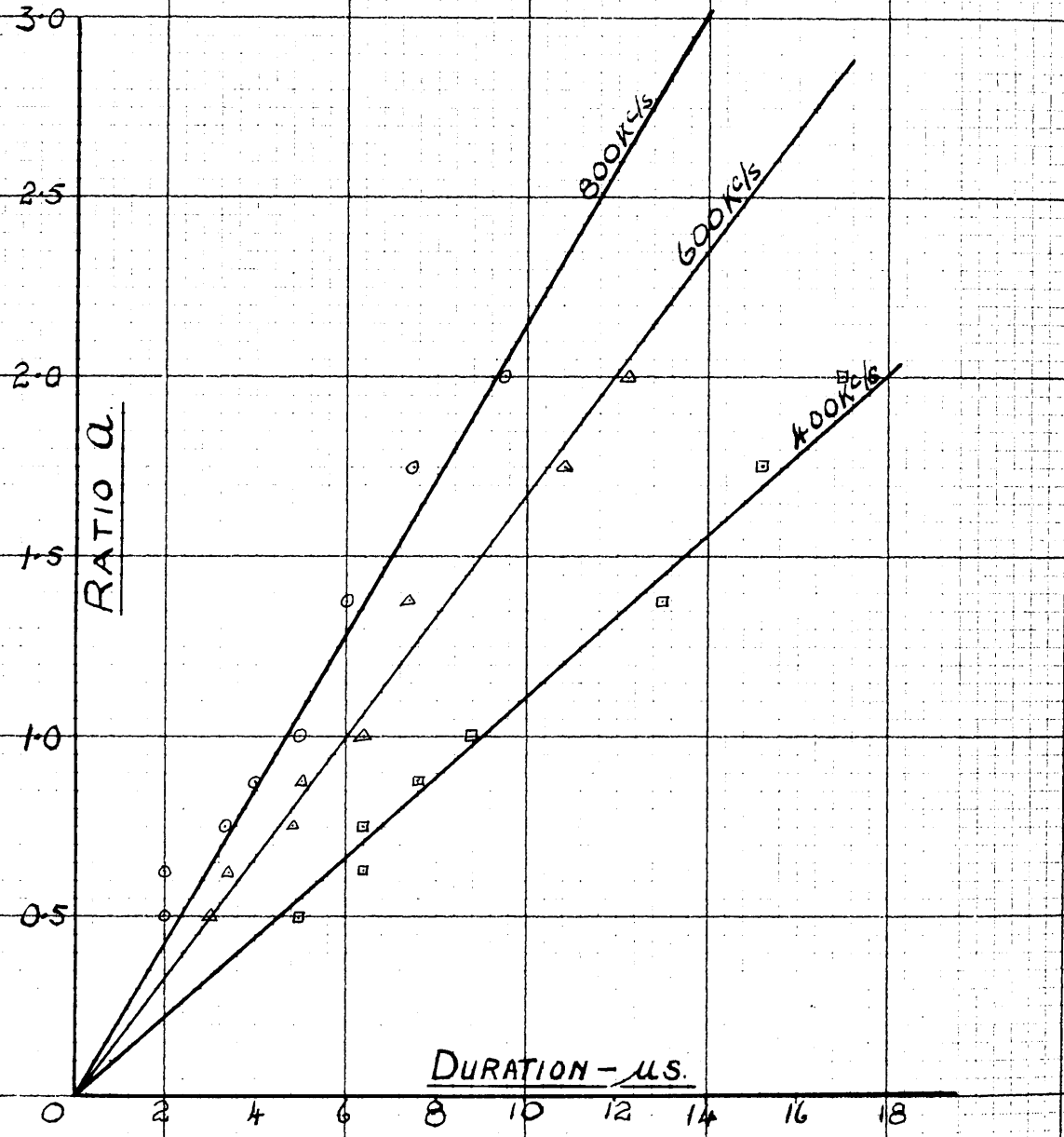
3·0
2·5
2·0
1·5
1·0
0·5
RATIO a.
800Kc/s
600Kc/s
400Kc/s
DURATION – μs.
0
2
4
6
8
10
12
14
16
18

GRAPH 5.2.

From the primary graphs of group (1), the duration of the transient in frequency was plotted against a^2. When plotted against a, for each value of b, the points were found to lie approximately on a straight line of a form -

$$T = B(b).\ a\ \mu sec.$$

where T is the transient duration and B(b) is some function of b, i.e. of frequency. These curves are shown in graphs 5.1 and 5.2 respectively. Within the range of b considered, it appears that to a close approximation B(b) is linear in b, being given by -

$$B(b) = 5.9b$$

whence $$T = 5.9ab\ \mu sec.$$

This simple relationship cannot be assumed to hold outwith the experimental range of b, but whatever B(b) is, from graph 5.1, T is seen to be directly proportional to a, for each of the three given values of b.

The results of group (2) are shown in graph 5.3 from which the variation of T is found for b values outwith the range considered above. It is immediately obvious from this graph that the relation between T and b is non-linear. In this graph, the curves have been extrapolated in both directions beyond the experimental range; such extrapolation is hardly justifiable in this purely experimental work. For frequencies within the experimental range above about 700 Kc/s, the curves

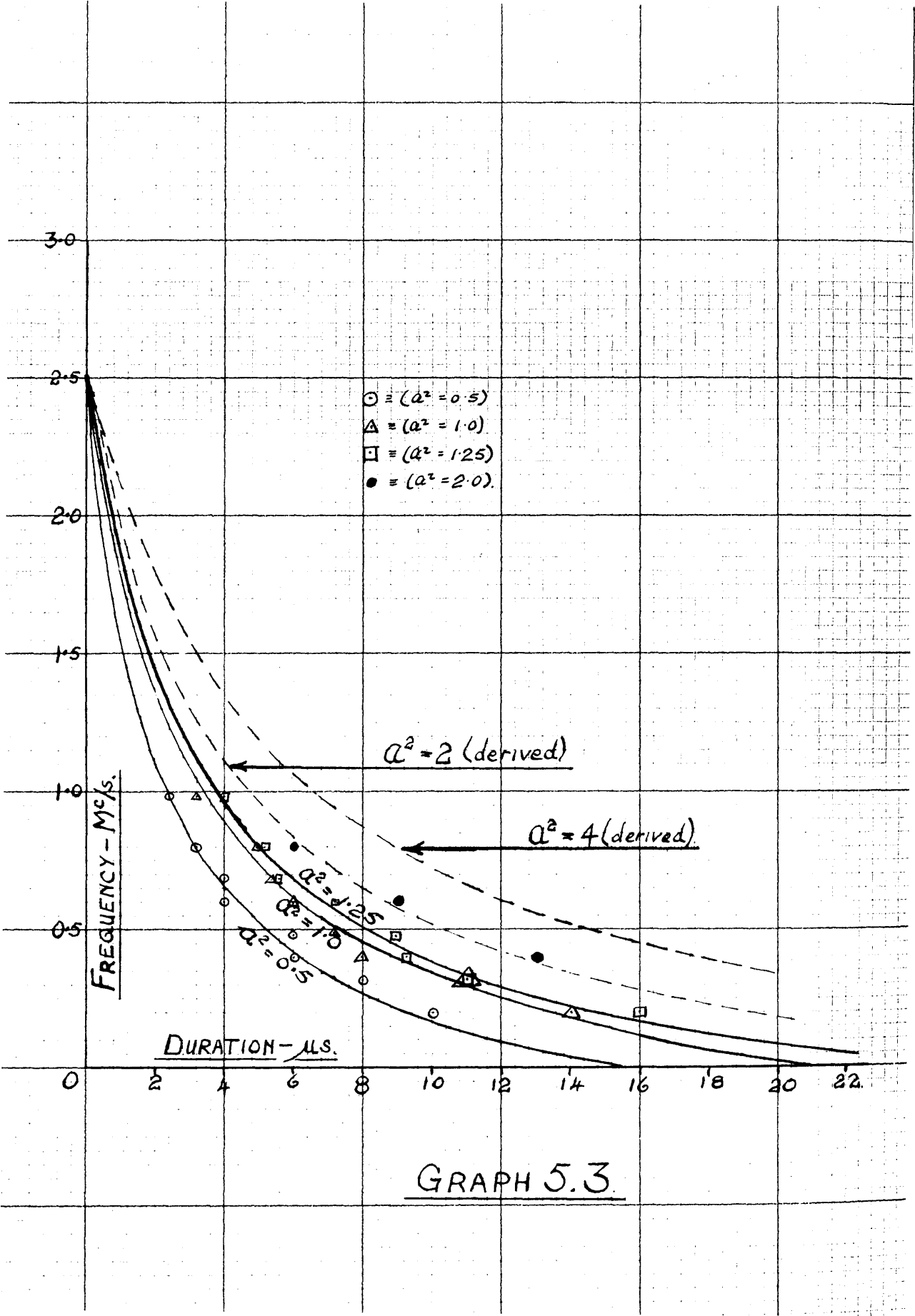
3·0
2·5
2·0
1·5
1·0
0·5
0
2
4
6
8
10
12
14
16
18
20
22
FREQUENCY – Mc/s.
DURATION – μs.
⊙ ≡ (a² = 0·5)
△ ≡ (a² = 1·0)
⊡ ≡ (a² = 1·25)
● ≡ (a² = 2·0).
a² = 2 (derived)
a² = 4 (derived)
a² = 1·25
a² = 1·0
a² = 0·5

GRAPH 5.3

show a tendency to converge, hence this convergence is continued with the result shown. For frequencies below 700 Kc/s within the range, the curves tend to run parallel, and all show a marked increase in linearity, hence the curves are drawn to continue in this manner and cut the zero frequency axis. Strictly this latter extrapolation is not correct, for theoretically any transient continues for all time; physically, the duration of a transient is purely arbitrary, depending only on the sensitivity of the measuring device used. Since these curves are a result of physical measurement, the transient will, in finite time, become sensibly zero. Therefore the curves are allowed to cut the zero frequency axis, indicating that with this method of measurement, for given a^2, as the frequency decreases (i.e. L and C increase) the frequency transient does not increase without limit. On the other hand, as frequency is increased, if extrapolation can be allowed, the curves appear to cut the T = 0 axis at the common point of 2.5 Mc/s. Now the switch pulse to the reactor valve had a rise-time of 0.2 μsecs., and following the work of Cawthra and Thomson[41] this rise-time may be considered as half of a sine-wave of period 0.4 μsec., i.e. of equivalent frequency 2.5 Mc/s. Since the rise-time is constant, this equivalent frequency is constant, and thus it may be said that there is no frequency

transient when the unmodulated oscillator frequency is equal to, or greater than, the equivalent switching frequency; for the unmodulated frequency less than the equivalent switching frequency, the duration of the frequency transient is as shown in graph 5.3. If this result may be applied in general to pulse modulation of frequency, it indicates that, for an equivalent modulating frequency less than the carrier frequency, the carrier frequency will follow the modulating waveform faithfully, but for an equivalent modulating frequency equal to or greater than the carrier frequency, there will be a certain amount of transient introduced; the resultant F -M signal will be distorted, and in the receiver a faithful reproduction of the modulating waveform is apparently impossible. This latter statement is rather hypothetical, since it could not be verified experimentally; such verification would be extremely difficult. The above finding is qualified later (pp. 109). Finally, for any given value of frequency, the duration of the transient is proportional to (a) within the accuracy of the graph. On this basis, with the curve for $a^2 = 1$ as reference, surves for $a^2 = 2$, $a^2 = 4$, were derived as shown. Three points on the $a^2 = 2$ curve were checked experimentally and found to be correct within 6%. This, in conjunction with graph 5.1 the duration of the frequency transient

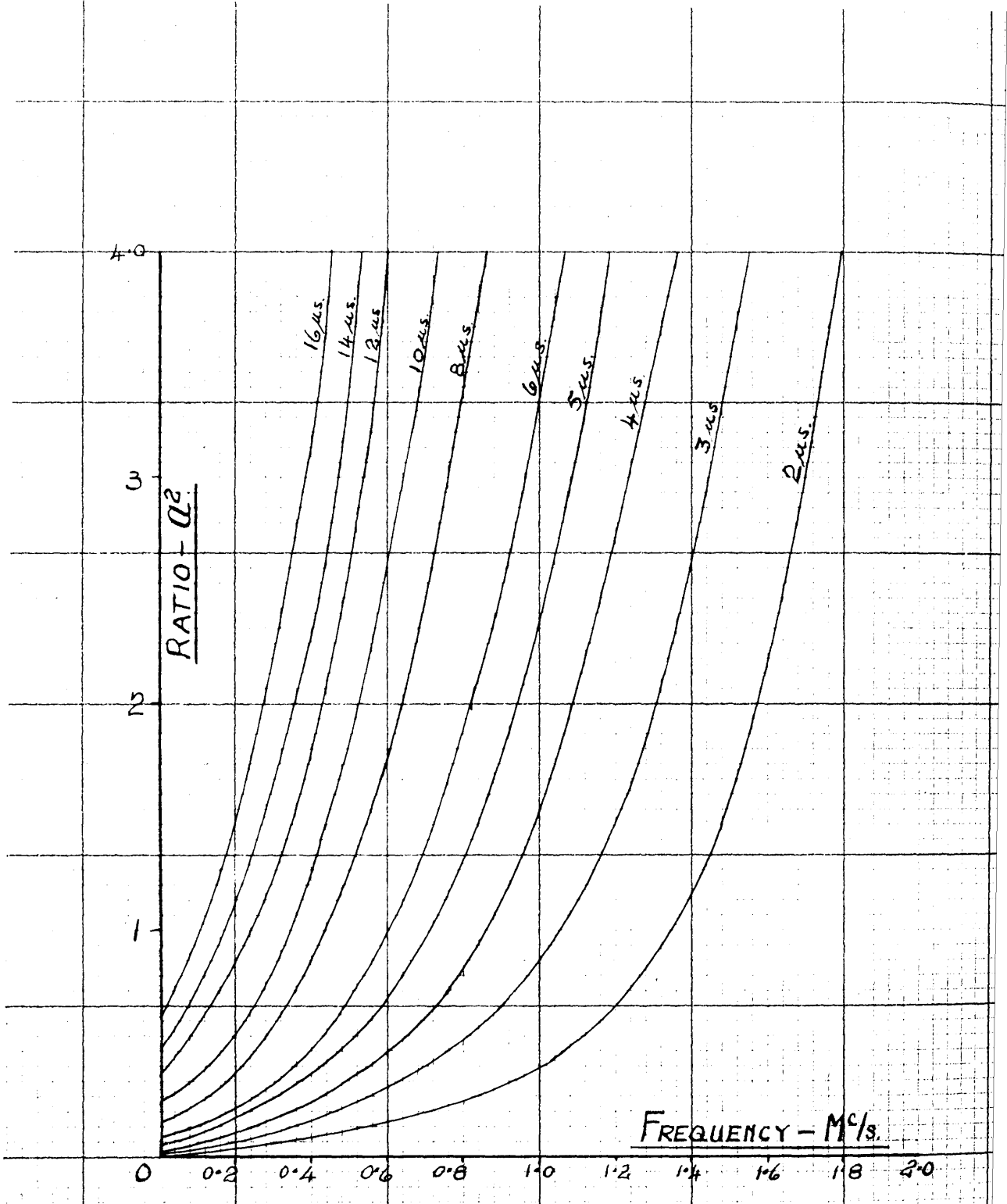
4·0
3
2
1
0
RATIO - Q²
16 μs.
14 μs.
12 μs.
10 μs.
8 μs.
6 μs.
5 μs.
4 μs.
3 μs.
2 μs.
FREQUENCY - Mc/s.
0·2
0·4
0·6
0·8
1·0
1·2
1·4
1·6
1·8
2·0

GRAPH 5.4.

for any a^2 and b values may be found. It is also noted in comparing 5.1 and 5.3 which were plotted from two separate groups of tests, that the agreement is within $\pm$ 7%.

To facilitate design, from 5.1 and 5.3 a family of constant duration curves can be constructed to axes of a^2 and frequency. This is done in graph 5.4 , any intermediate values of duration either being computed from 5.1 and 5.3, or more simply by using an interpolation formula and graph 5.4 . The use of this family of curves will be illustrated later, in predicting group (3) and (4) results. In telemetry, a normal accuracy of prediction of the gating period to one microsecond is ample, and hence this graph fully meets practical requirements. Graph 5.4 shows that a given change in a^2 has a proportionately similar effect on the frequency transient at low frequencies as at high. All the curves are contained in the area bounded by $a^2 = \infty$, f = 2.5 Mc/s, and all curves are asymptotic to this value of f. Graph 5.4 may now be discussed further since it presents graphs 5.1 and 5.3 in a form more amenable to analysis. When graph 5.4 is replotted on log-linear paper as in graph 5.4 (a), the frequency axis linear, the a^2 axis logarithmic, a family of straight lines is obtained for each value of T. Thus the relationship between f and log a^2 is linear,

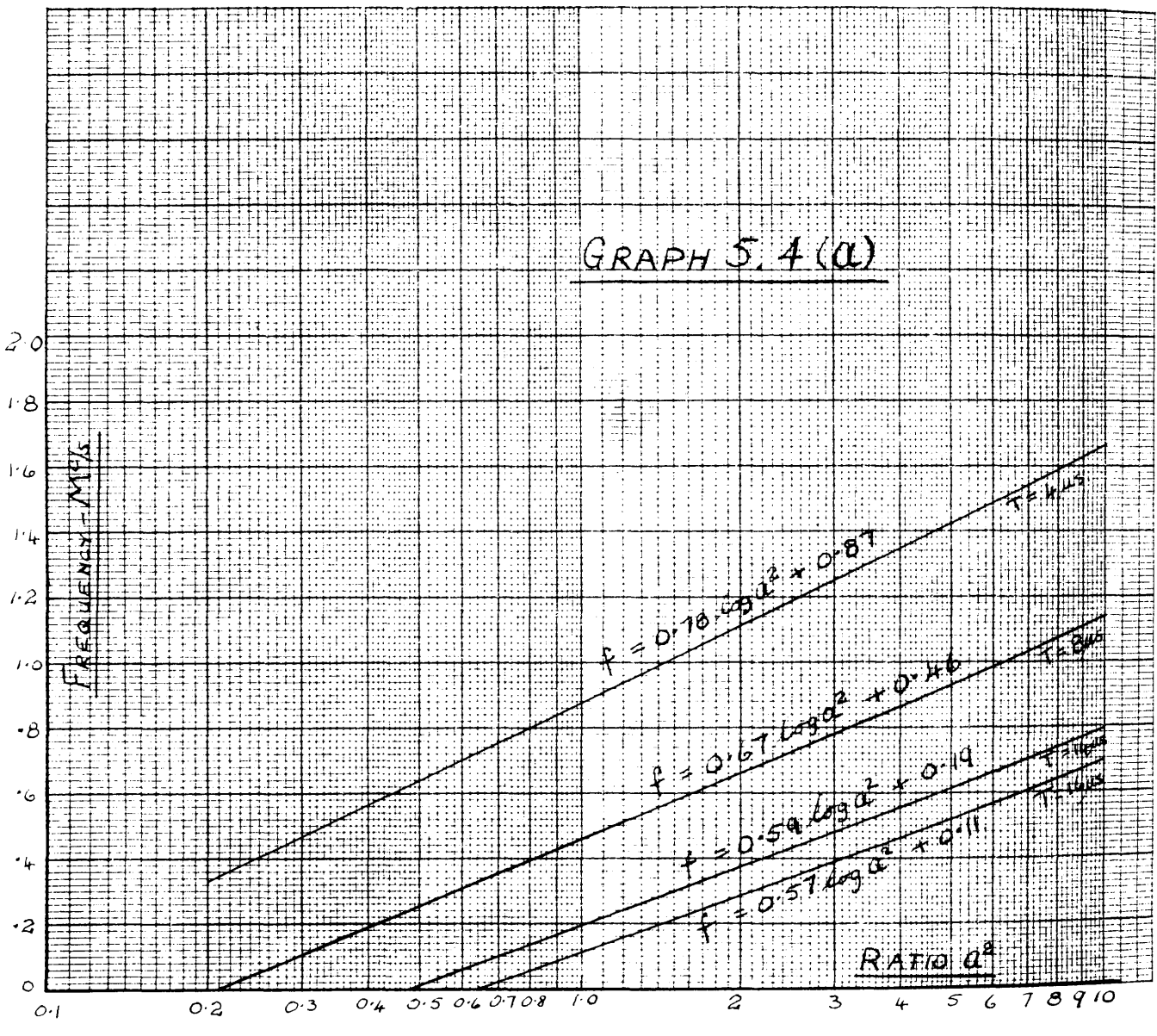
GRAPH 5.4(a)
FREQUENCY = M1/S
RATIO a²
f = 0·16 Log a² + 0·81
f = 0·67 Log a² + 0·46
f = 0·59 Log a² + 0·19
f = 0·57 Log a² + 0·11
T = 4 M²S
T = 2 M²S
T = 1 M²S
T = ½ M²S
2·0
1·8
1·6
1·4
1·2
1·0
·8
·6
·4
·2
0
0·1
0·2
0·3
0·4
0·5
0·6
0·7
0·8
1·0
2
3
4
5
6
7
8
9
10

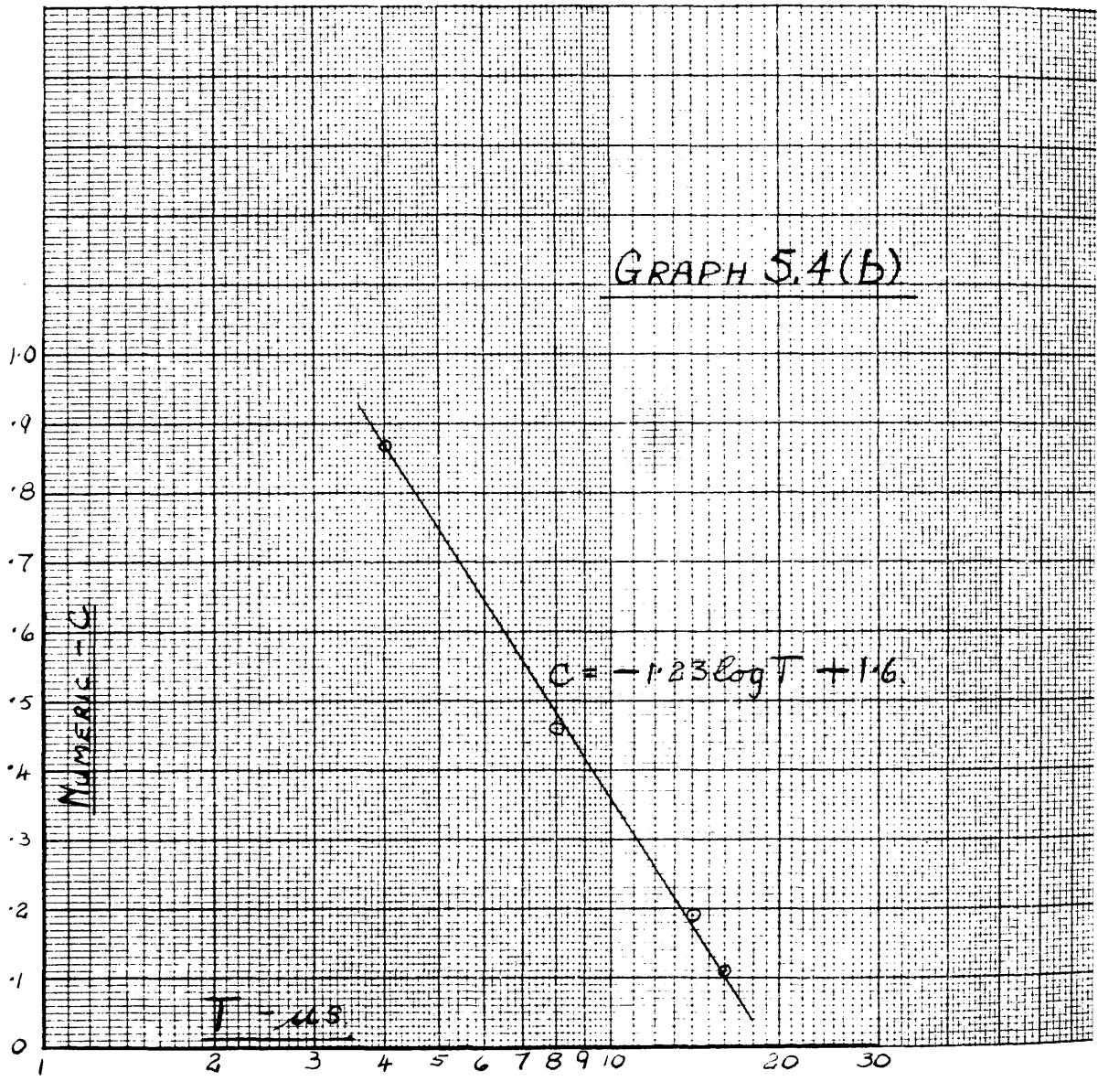
GRAPH 5.4(b)
C = −1·23 log T + 1·6
NUMERALS C
T − 44.5
1·0
·9
·8
·7
·6
·5
·4
·3
·2
·1
0
1
2
3
4
5
6
7
8
9
10
20
30

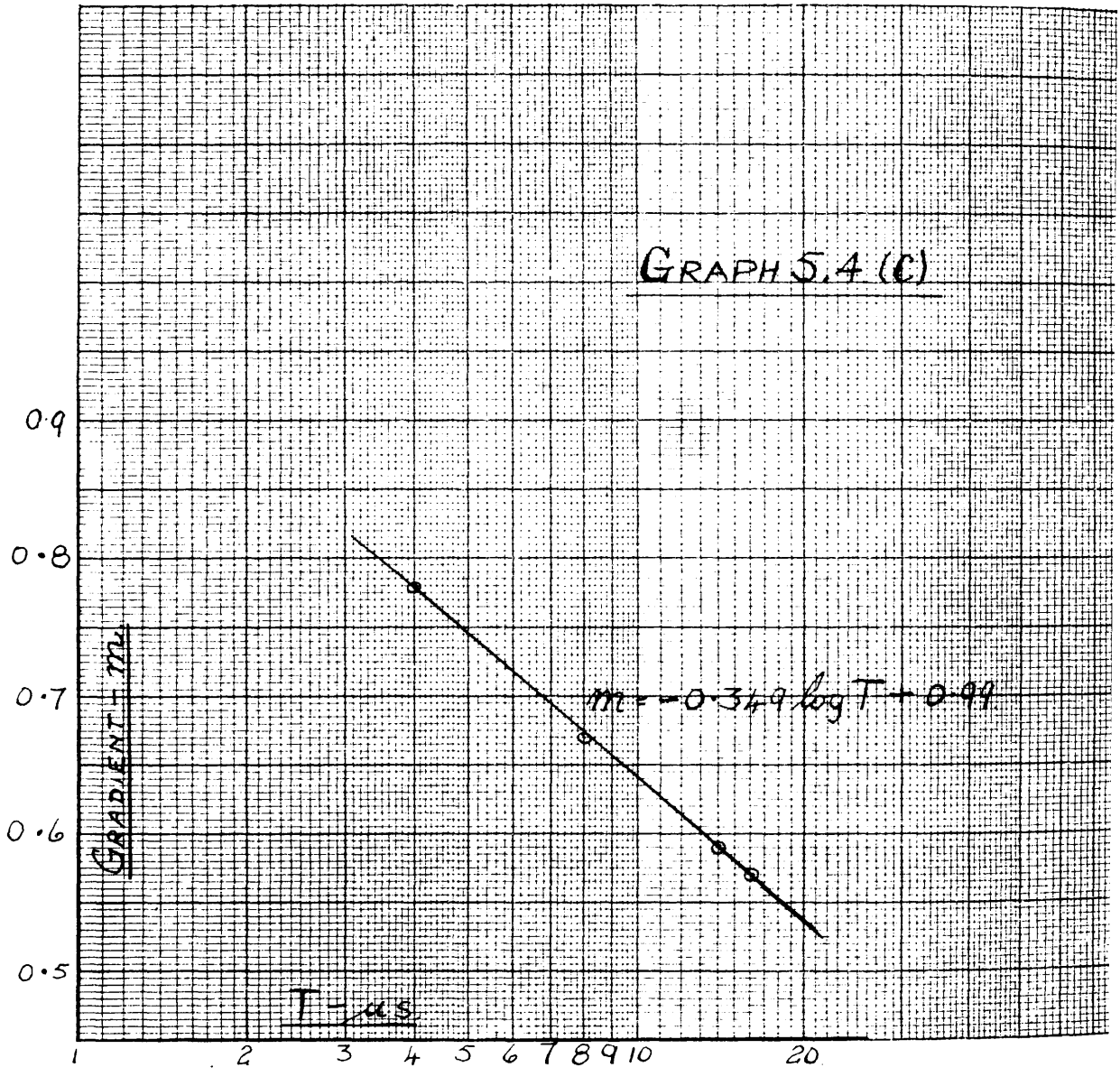
GRAPH 5.4 (C)
0·9
0·8
0·7
0·6
0·5
GRADIENT = m
m = -0·349 log T + 0·99
T - μs
1
2
3
4
5
6
7
8
9
10
20

i.e.,

$$f = m . \log (a)^2 + c,$$

for each line of constant T. For the lines shown in 5.4 (a), the gradient m and constant c were obtained. If now the several values of c are plotted against log T as in graph 5.4 (b), then it is seen that, to a close approximation

$$c = - m_1 . \log T + K.$$

The constants m_1 and k were evaluated as before, and gave

$$c = - 1.23 \log T + 1.6$$

$$= \log 39.8\, T^{-1.23}.$$

Finally, when m was plotted to log T it was found that, again, to a close approximation,

$$m = - 0.349 \log T + 0.99$$

$$= \log 9.77\, T^{-0.349}.$$

Since both m and c are now related to T, the expression for f becomes general, i.e.,

$$f = (0.99 - 0.349 \log T) . \log (a)^2 - 1.23 \log T + 1.6$$

$$= \log (a)^2 . \log 9.77\, T^{-0.349} + \log 39.8\, T^{-1.23}$$

This is the general, but approximate, function of the curves of graph 5.4. It is also the equation of the curves in 5.1 and 5.3 with f or a^2 constant respectively. Thus, in graph 5.1 for f = 0.8 Mc/s and $a^2 = 1$, using the first form of the equation,

$$0.8 = - 1.23 \log T + 1.6$$

i.e., $T = 4.5\ \mu$sec.

From 5.1, $T = 4.6\ \mu$secs.

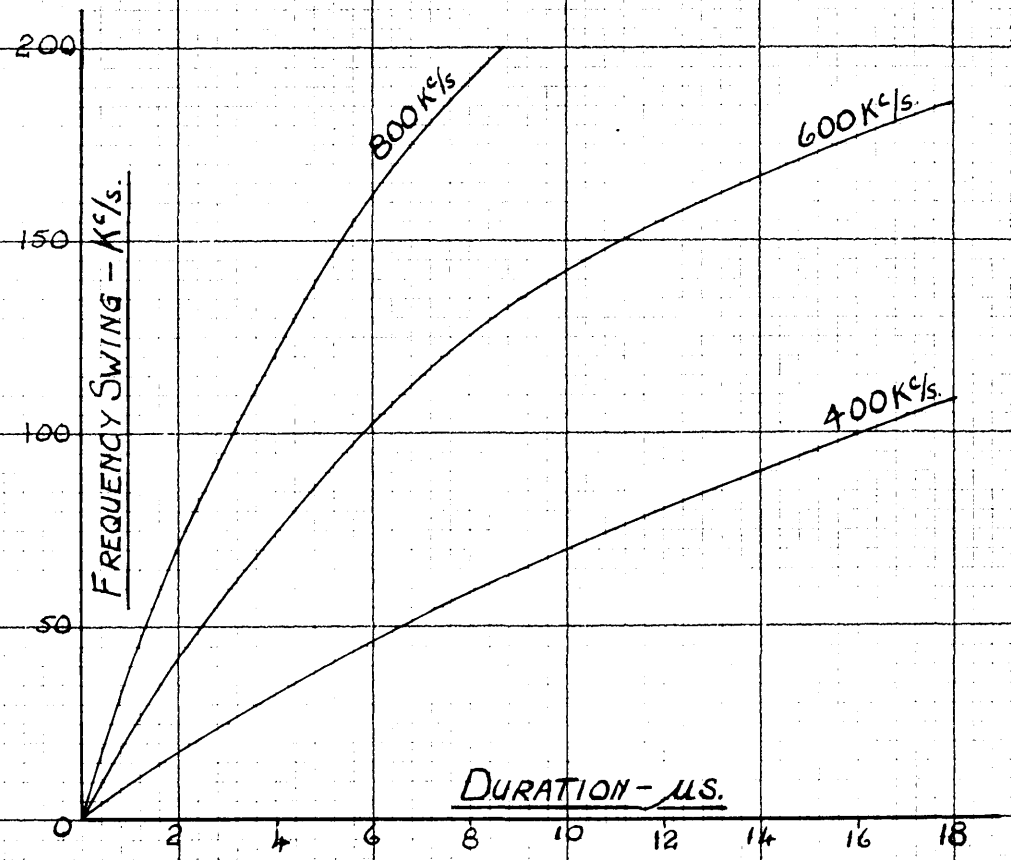
200
150
100
50
0
FREQUENCY SWING - Kc/s.
800 Kc/s
600 Kc/s.
400 Kc/s.
DURATION - μs.
2
4
6
8
10
12
14
16
18

GRAPH 5.5.

This shows good agreement between the curves and the derived formula, but if a^2 is made very small, in the order of 0.1, then the error in the formula becomes large, viz. at $a^2 = 0.1$, f = 0.6 Mc/s., from 5.4 T = 1.9μsec; but from the formula T is calculated to be 1.1μsec. Hence the general formula gives optimistic results, the error increasing with decreasing T and/or a^2. The accuracy for large T and a^2 cannot be discussed, since at frequencies under 200 Kc/s and over 1 Mc/s. the curves are extrapolated and not experimentally checked. The error must increase as f increases if the hypothesis of the limiting frequency of 2.5 Mc/s is to hold, for the equation can increase without limit, but for f < 1Mc/s the equation is correct.

Before considering further the dependence of the transient duration on the parameters a and b, attention is turned on graphs 5.5 to 5.7. The frequency swing is defined here as the difference in original and final steady-state frequencies, and graphs 5.5 and 5.6 refer to this quantity as obtained in group (1) tests. From 5.5 the frequency swing increases with increasing duration, but the transient duration is not related to frequency swing as it is to a. Comparison of 5.2 and 5.5 shows that the frequency swing increases slightly less rapidly than a for small T, but

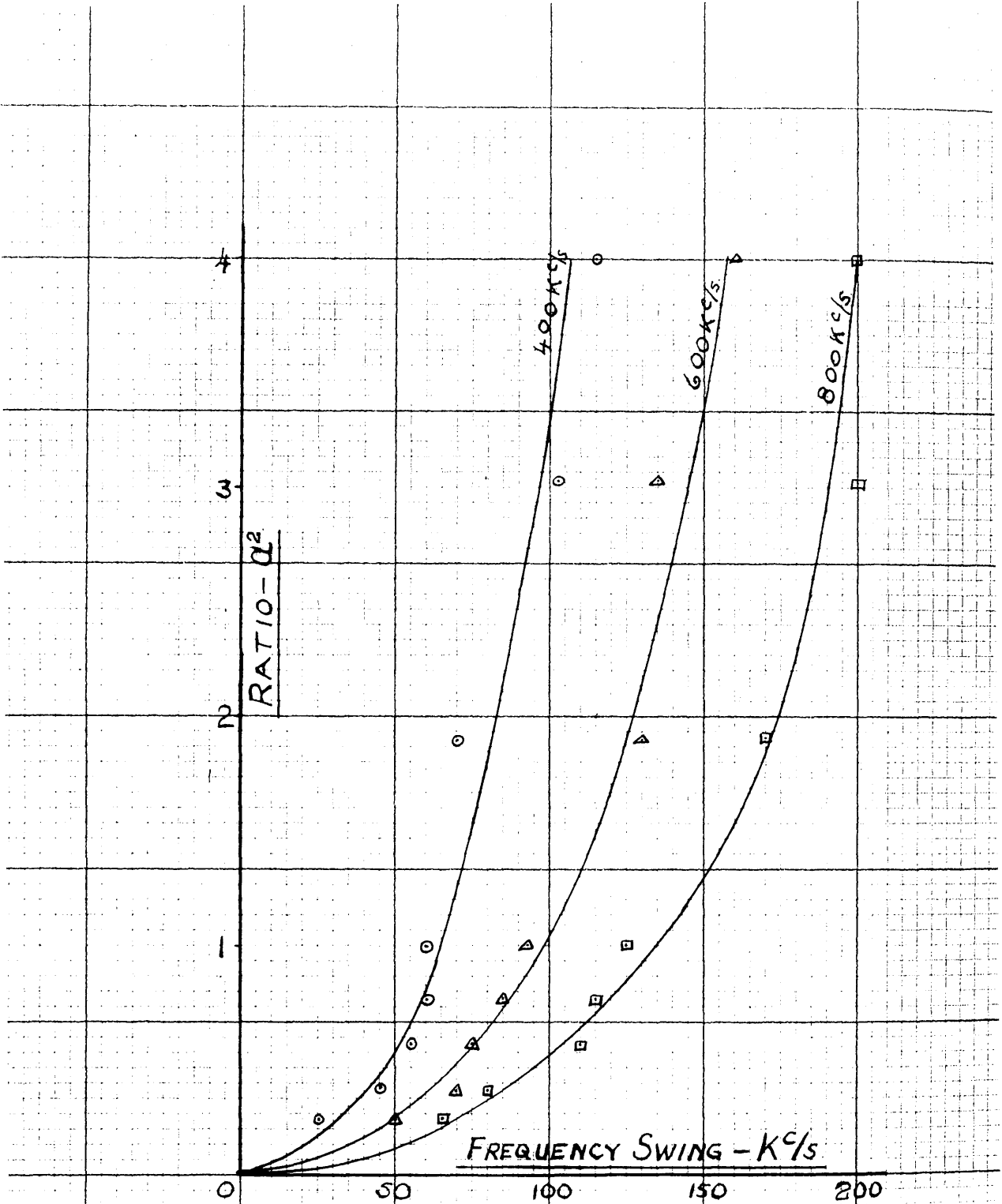
4
3
2
1
0
RATIO - a²
400 K c/s
600 K c/s
800 K c/s
50
100
150
200
FREQUENCY SWING - K c/s

GRAPH 5.6.

considerably less rapidly than a for large T, for the three values of b used. Graph 5.6 shows the relationship between frequency swing and a^2 for comparison with 5.1, and shows immediately the relative rates of increase of frequency swing and duration with a^2. Again, graph 5.7 shows the frequency swing to initial frequency obtained in group (2) tests. Here, over the range, the frequency swing is very closely a linear function of initial frequency. But graph 5.3 shows the duration is not a linear function of initial frequency except at large values of duration, where very approximate linearity is obtained. The dependence of the transient duration, T, on the parameters a, b, and the frequency swing δf, can now be investigated qualitatively. Graphs 5.1, 5.2, show that at a given frequency T appears to be a linear function of a, and an inverse function of frequency. But T may also be a function of δf, since δf increases with a. Thus, from group (1) tests, T may not depend simply on a, but may be of the form

$$T = F(\delta f).\, G(a) \,/\, H(f)_{f=\text{const.}}$$

for a constant frequency, the two additional functions combining to give the apparent dependence on (a) only. Now consider the evidence of group (2) tests. First, T appears to be proportional to a at all frequencies within the range. Secondly, for a given value of

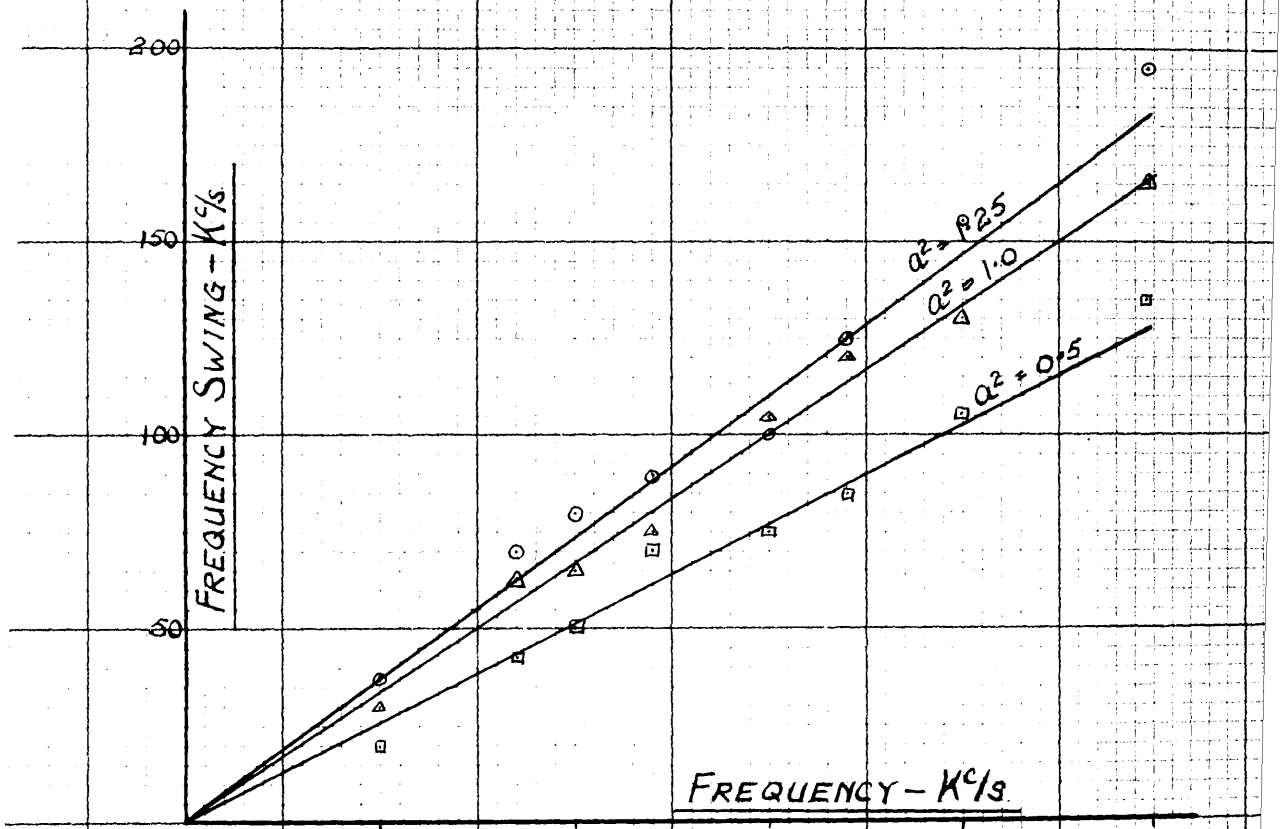
200
150
100
50
FREQUENCY SWING - K^c/s
a² = 2.5
a² = 1.0
a² = 0.5
FREQUENCY - K^c/s
0
200
400
600
800
1000

GRAPH 5.7.

a the duration T decreases with increasing frequency, i.e.

$$T \propto 1/H(f).$$

But from 5.7, δf increases with increasing frequency, i.e. δf increases for decreasing T. Thus, here, T may have the form,

$$T = G(a)_{a\,const.} / H(f).F(\delta f).$$

Since the values of T, δf, are equal for corresponding a^2 and f values in the two groups of tests, cf. 5.1, 5.3, 5.6 and 5.7, the two expressions for T can only be equal if

$$F(\delta f) = 1/F(\delta f).$$

Thus, for all a and b values

$$T = G(a) / H(f)$$
$$= G(a) . B(b)$$

i.e. the frequency swing does not influence the length of the frequency transient.

To sum up, it has been seen from 5.1, 5.2, that for constant b,

$$T = \text{Constant X } a,$$

with the constant depending on the particular value of b. Graph 5.3 showed the generality of this statement, and disclosed also that B(b) is a non-linear function of b in general, but tends towards linearity for large values of b, and, independently, for large values of a^2. It would seem that if only one curve on 5.3 is known, and its associated a^2 value, all other curves for $0 < a^2 < \infty$ can be drawn, and all such curves lie in

the strip between f = 0 and f = 2.5Mc/s, or, in terms of b, between b = ∞ and b = 0.239. For all b less than the latter figure, T = 0. For b = ∞ T has a finite value, which increases as a, and is only infinite when a is infinite. The effects of frequency transients are less noticeable at low frequencies than at high, and at low a^2 values than at high. In 5.3 , for $a^2 = 0.5$, at 100 Kc/s. the transient duration is 11.6μsecs. or about 1 cycle of the oscillator waveform. At 1 Mc/s. the transient duration is 2.4μsecs., or approximately two cycles of the final frequency of 870 Kc/s. For frequencies in the audio range, unless a^2 is very large indeed, the frequency transient will be over in less than one cycle and will be un-noticed.

Although δf has apparently no effect on transient duration, it does determine the maximum overshoot. From the primary graphs it was found that the ratio $e = \delta f/f$ in conjunction with the final steady-state frequency f_1, determines the overshoot. If f_2 is the minimum frequency attained, the overshoot is defined as

$$S = f_1 - f_2 ,$$

and the percentage overshoot becomes,

$$k = \frac{S}{f_1} \times 100\% .$$

From the primary graphs S was found to be

$$S = e . f_1 .$$

and therefore,

$$k = e \times 100\%$$

The minimum frequency attained then becomes,

$$f_2 = f_1 (1 - e)$$

and since the positive overshoot above f was always less than 10% the frequency range covered is, approximately,

$$f - f_2 = f - f_1 (1 - e)$$
$$= s + \delta f$$

Thus, in group (1) tests, graph 5.5 is actually a plot of e to duration, since each curve is drawn for a constant value of f. Although e increases with duration, the same remarks apply to e as to δf. Similarly, 5.7 is a plot of e to a different scale against frequency, and thus although e increases with frequency, since T is inversely proportional to some function of frequency, the greater initial frequency swings are more rapidly damped out. But from 5.3 when f = 2.5 Mc/s there is apparently no transient, and therefore the overshoot s must disappear at that value of f, i.e. f_2 coincides with f_1. The above expressions are therefore only true over the range of frequency used in the tests, since S must be a function of frequency. The behaviour of S near the critical frequency could not be investigated because of the circuit limitations described in Chapter 4, pp. 71. It is reasonable to expect that S will be a function not simply of the frequency f, but of the ratio

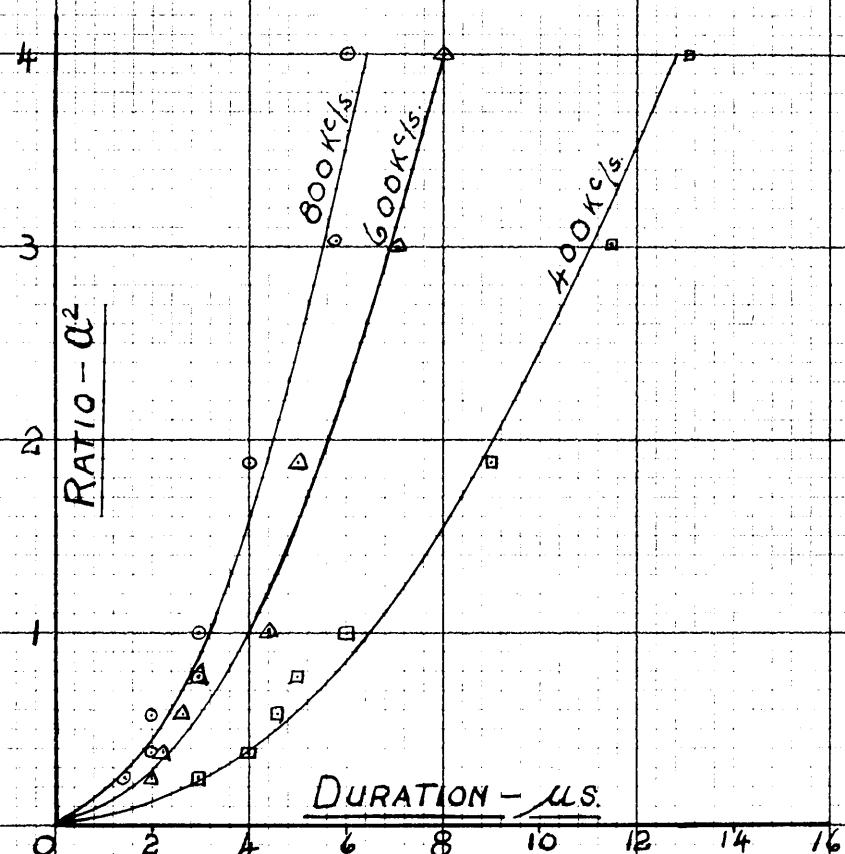
800 KC/S.
600 KC/S.
400 KC/S.
RATIO - a^2
DURATION - μS.
0
1
2
3
4
2
4
6
8
10
12
14
16

GRAPH 5.8

$f/f_{critical}$, or of $(f_{critical} - f)$, such that the magnitude of S is approximately ef_1 over the range investigated experimentally, but falling rapidly to zero as f approaches the critical value. Merely as a demonstration of the type of function required, if f and f(critical) are expressed in Kc/s., then one possible function is,

$$S = ef_1\left[1 - exp.K\{-(f_{crit} - f)\}\right]$$

where K is a positive constant. Thus if K = .01, at f = 1,500 Kc/s, the exponential power is 10, and is only 1/22,000 less than ef_1. Some function such as this, then, is envisaged for S, but in this case for f less than half f_{crit}. the value $S = ef_1$ is found to be a very close approximation.

Since the primary graphs in groups (1) and (2) are oscillatory in character, a mean line may be drawn on each graph. This line corresponds to the average frequency, i.e.

$$\frac{1}{t_2 - t_1}\int_{t_1}^{t_2} f_{seg}.\,dt.$$

The transient duration for the average frequency is considerably shorter than obtained previously, the segmental frequency latterly swinging equally above and below the final frequency. The curves relating to average frequency are shown in graphs 5.8 to 5.10. Comparing 5.8 with 5.1 the average frequency duration is also found to be proportional to (a), but the con-

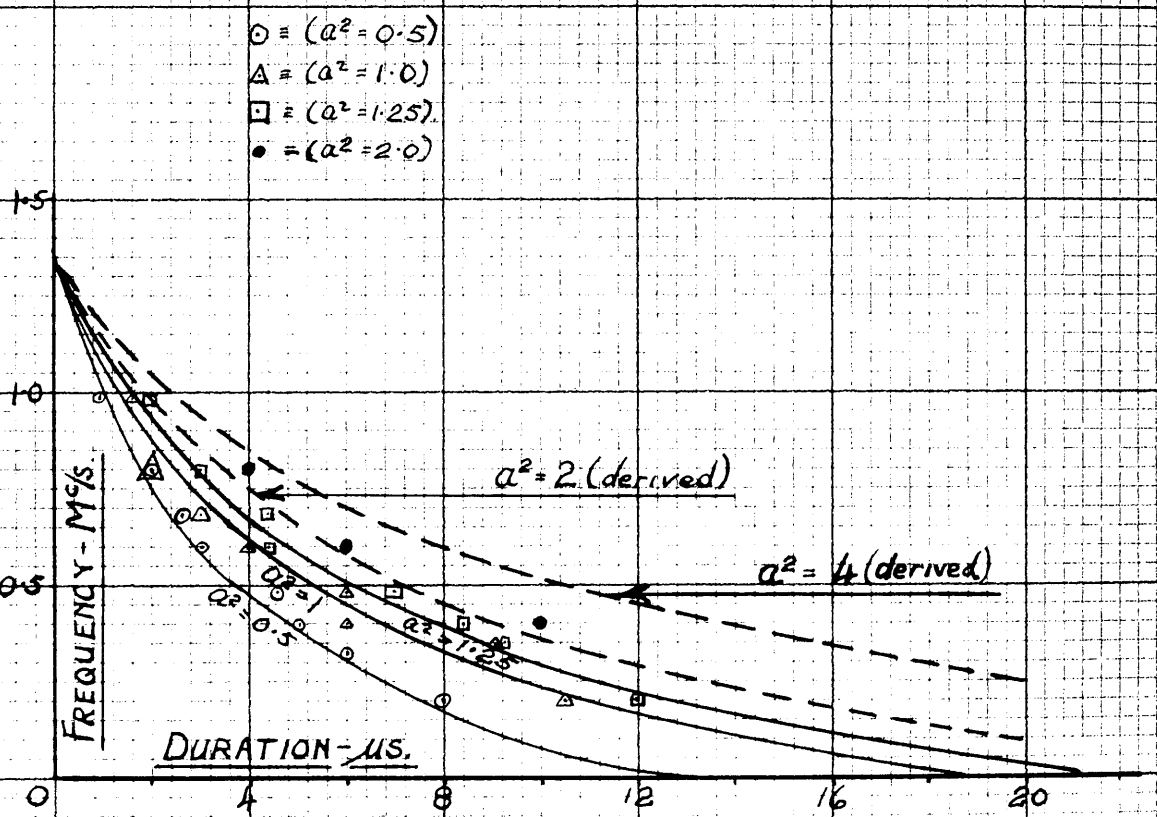
⊙ ≡ (a² = 0·5)
△ ≡ (a² = 1·0)
□ ≡ (a² = 1·25)
● ≡ (a² = 2·0)
1·5
1·0
0·5
0
FREQUENCY - Mc/s.
DURATION - μs.
4
8
12
16
20
a² = 2 (derived)
a² = 4 (derived)
a² = 1
a² = 0·5
a² = 1·25

GRAPH 5.9

stants of proportionality are much smaller than for corresponding curves in 5.1 . In 5.9 the average frequency duration curves for constant a^2 all cut the frequency axis at f = 1.35 Mc/s. However, if this point was taken as 1.25 Mc/s which lies within the limits of experimental and graphing errors, the average frequency would have no transient for a modulating (equivalent) frequency of less than twice the carrier frequency. If this is true, then any type of frequency discriminator would show no transient due to frequency for an equivalent modulating frequency equal to or less than twice the carrier. Over a fairly wide range of T, for any given a^2, T is approximately linearly proportional to frequency, the approximation becoming more accurate with increasing a^2 and T.

Graphs 5.9 and 5.3 jointly show an important point regarding the overshoot. The average frequency has no transient for f greater than approximately 1.25 Mc/s, but the transient in segmental frequency continues until f = 2.5 Mc/s. This implies that the segmental frequency overshoots its new value (f_1) to give an equal area, positive and negative about f_1, for all frequencies between 1.25 Mc/s and 2.5 Mc/s. For frequencies below 1.25 Mc/s, the area under the negative overshoot is greater than that under the positive overshoot and the average frequency has some

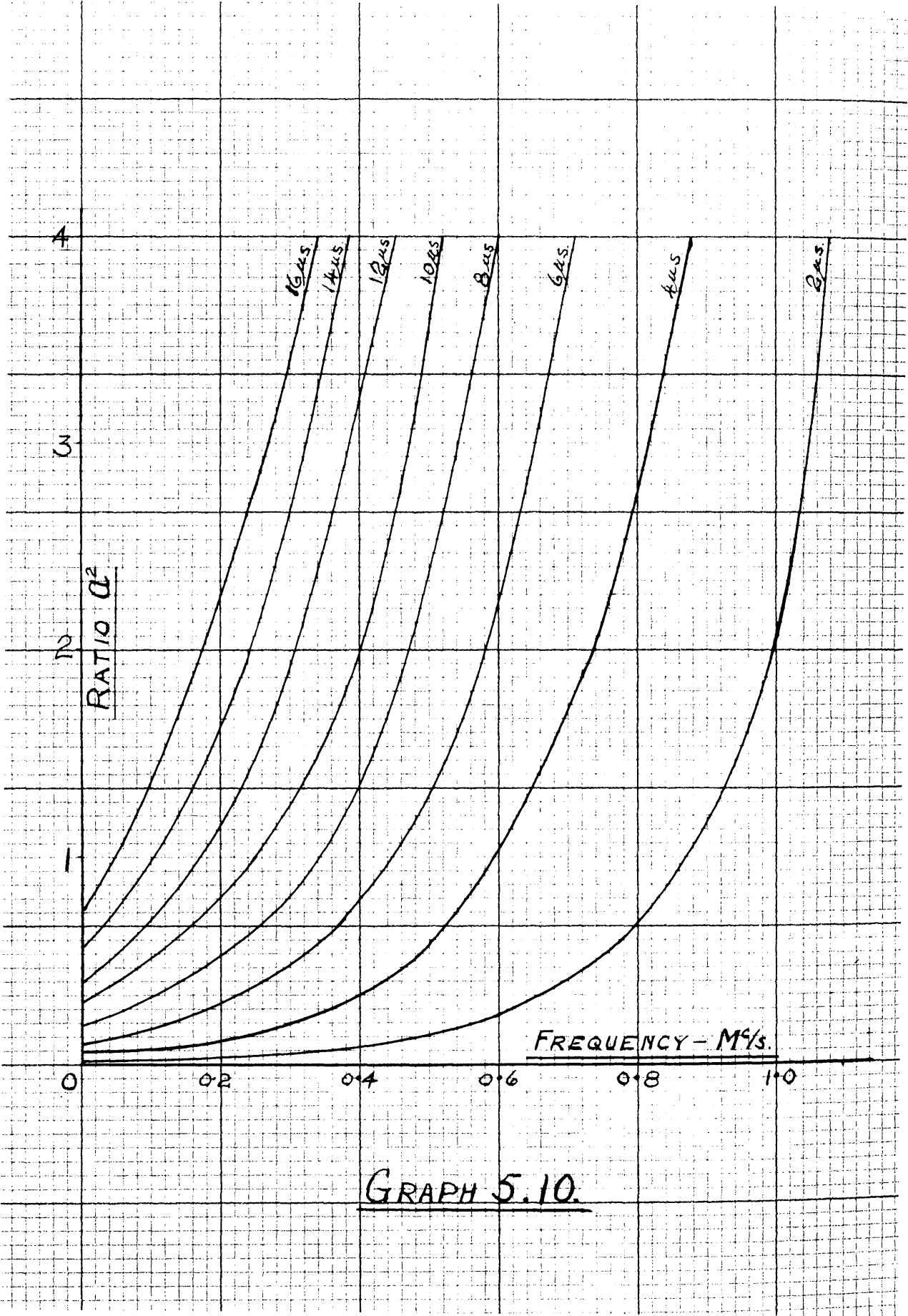
16μs
14μs
12μs
10μs
8μs
6μs
4μs
2μs
RATIO a²
FREQUENCY – Mc/s.
0
0·2
0·4
0·6
0·8
1·0
1
2
3
4

GRAPH 5.10.

transient. This is borne out by the primary graphs, where the area under the positive overshoots gradually increases with frequency; this gives some justification for the conclusions drawn from extrapolation.

This completes the conclusions drawn from test groups (1) and (2). These two groups appear to agree at common a^2 and f values on both the duration of the transient and the overshoot. For other values of a^2 and f test groups (3) and (4) are used, since in these groups both a^2 and f are varied simultaneously. If graphs 5.4 and 5.10 are correct it should be possible to predict the results of groups (3) and (4). Consider group (3) tests, commencing with the ratio $C/C_o = 0.75$. Here, theoretically, $C = 266.25 p$F. and $L_o = 200 \mu$H. throughout. Thus, $a^2 = 1/0.75$. The practical measurement of C gave $C = 268 p$F. and hence the actual value of a^2 was $1/0.755 = 1.325$. The initial frequency should be f = 690 Kc/s. Therefore, from graph 5.4 the duration of the frequency transient should be 6μsec. The measured value is 5.5μsec. which is 8.5% low. The initial frequency as measured was 710 Kc/s. and therefore the transient should be very slightly shorter than that expected. The measured final frequency f_1 is 569 Kc/s. and δf is 141 Kc/s., giving e = 0.19: therefore f_2 by calculation should be 460 Kc/s. The measured value of f_2 was 440 Kc/s. The predicted and measured values of

TABLE I.

By definition $T = a^2 T_o = a^2 \frac{L_o}{C_o}$ and here L_o is constant throughout, therefore $a^2 = C_o/C$.

Ratio $C/C_o = \frac{1}{a^2}$	Predicted		Measured		% Error.	
	Tμs.	f_2Kc/s	Tμs.	f_2Kc/s	T	f_2
0.75	6.0	460	5.5	440	-8.5	-4.4
0.875	6.0	435	6.3	415	+4.5	-5
1.0	6.0	413	6.4	390	+6.0	-3.5
1.125	6.0	396	6.5	405	+8.2	+2
1.25	6.0	382	5.5	369	-8.5	-3.4
1.375	6.0	372	5.5	349	-8.5	-6.2

TABLE II.

Here, C_o is constant and therefore $a^2 = \frac{L}{L_o}$

Ratio $\frac{L}{L_o} = a^2$	Predicted		Measured		% Error	
	Tμsec.	f_2Kc/s	Tμs.	f_2Kc/s	T	f_2
0.5	2.8	653	3.3	600	+18	-8
0.625	3.75	562	4.1	528	+ 9	-6
0.75	4.6	496	4.8	515	+ 5	+4
0.875	5.3	450	5.0	480	- 6	+6.5
1.0	6.0	413	5.7	394	- 5	-4.5
1.125	6.75	384	7.3	376	+ 8	-2
1.25	7.6	358	7.4	380	- 3	+6.2
1.375	8.3	337	7.7	315	-7	-6.5

T and f_2 are tabulated in Tables I and II for test groups (3) and (4) respectively, and show that the accuracy of prediction is within ± 10%, which is reasonable considering the number of sources of error involved in this method (see Chapter 5.3). From the Tables it would appear that graph 5.4 is correct, and that the various relationships obtained from groups (1) and (2) are essentially true.

Graph 5.4 can now be applied to a typical design for an oscilator for a telemetric system. The specification chosen is :-

To transmit nine data-carrying channels and one synchronising channel in a sequence-sampler F.M. system, the time lost per channel to be less than 5μsecs. The unmodulated frequency of the drive oscillator to be 500 Kc/s., and the maximum allotted data deviation -25 Kc/s. The sync. channel deviation to be -35Kc/s.

These figures are assumed to have been fixed by considerations irrelevant here, and an electronic type of commutator is also assumed such that the channel to channel switching is of approximately step function form. The oscillator in this system will be free running, and, as is usual in practice, may return to its unmodulated frequency between channels.

From Graph 5.4, at 500 Kc/s. a frequency transient of 3μsec. may be obtained if a^2 is dropped to 0.25. At

500 Kc/s. the value of b is

$$b = \frac{600}{500} = 1{\cdot}2,$$

$$\text{and } R_0 = \frac{b \times L_0}{b \times C_0} = \frac{1{\cdot}2 \times 200}{1{\cdot}2 \times 355}$$

$$= \frac{240}{426} \quad \frac{\mu H}{pF.}$$

Therefore, $R = a^2 R_0$, giving the required L and C as,

$$L = \sqrt{0{\cdot}25} \times 240 = 120 \mu H,$$

$$C = 426 / \sqrt{0{\cdot}25} = 952 pF.$$

The maximum frequency swing is -35Kc/s. Therefore, the minimum frequency f_1 = 465 Kc/s. and

$$\delta C \doteq C \left(f^2 / f_1^2 - 1 \right)$$

$$\doteq 148 pF.$$

It should be noted that if a^2 were made smaller to reduce the transient, C and δC would be much increased - δC in particular becoming too large to be practically obtainable. Thus, the value of a^2 cannot be decreased without limit. To obtain the actual value of injected capacitance required, the original capacitance of 952pF. is composed of 65pF. input capacitance from the reactor valve acting as a cathode follower, and 887pF. fixed capacitance. The new capacitance to produce the required frequency swing is (952 + 148)pF, or 1,100pF. Therefore the injected capacitance must be (1,100 - 887)

= 213pF., and this must be the value of the input capacitance of the reactor when the cathode follower valve is cut-off. The quickest method of calculating the required grid-cathode capacitor for the reactor is by trial and error. From a simple calculation, a value of C_{gk} of 250pF produces an input capacitance of 200pF. and input resistance of approximately 4K.Ohms. The additional 13pF. required could be obtained by trial and error methods of putting small fixed capacitors in parallel with the C_{gk} until the correct frequency swing is obtained; variable trimmers are not used in general due to their comparative frailty at the high accelerations obtained with missiles. Finally, the overshoot S will be

$$S = ef_1 = \frac{35}{500} \times 465 = 32 \text{ Kc/s},$$

giving the minimum frequency attained,

$$f_2 = (465 - 32)\text{Kc/s.}$$

$$\therefore 433 \text{ Kc/s.}$$

Thus, from the point of view of frequency transients the oscillator is fully designed. Using the circuit parameters as found above in the pulsed circuit on which the previous work had been carried out gave the following results:-

Transient duration = 3.5μsec. approximately,

frequency swing = 43Kc/s.

and maximum overshoot = 38 Kc/s.

These figures show that the transient is of the correct order, but due to the comparatively small frequency swing the finding of the end of the transient was difficult and open to error. The frequency swing was rather more than was expected, but this was a feature of all the tests, and was due to the effect on the injected (low) resistance and to the fact that the injected capacitance was a function of frequency, the actual capacitance injected at the lower frequency being rather more than the calculated value. The duration of the channel transmission may now be made as short as, say, 20μsec. with only the first 4μsec. rendered useless and removed in the receiver by gating. Allowing a 10μsec. inter-channel period for the oscillator to slide back to its unmodulated frequency, gives a total time per channel of 30μsec. Therefore, each channel is sampled for 16μsec. at a repetition speed of 3.3 Kc/s. Even doubling the sampling time still produces a very good system with a repetition speed of 2 Kc/s. i.e., the system will record data fluctuating at speeds up to 1 Kc/s. Naturally, the building of such a system would hinge on the development of the electronic commutator, but this is not difficult, and successful models have already been used.

In the fore-going design it should be noted that the unmodulated carrier frequency is correct but the

frequency swing is much greater than would normally be used in practice. The values used were so chosen to allow an experimental check to be carried out on the existing apparatus.

5.3 Discussion of Results.

A criticism of the equipment and method is relevant first of all.

The equipment used was per se as accurate as obtainable within the scope of the available laboratory measuring instruments. To summarise part of the content of chapter 4:-

Measurements of R, L, C, were taken on a standard bridge and/or Q-meter manufactured by Marconi Instruments, and the coils used in the test oscillator were the standard Q-meter coils supplied by the manufacturers. The calibration of the high-speed time-base was as accurate as could be obtained, although any error in this would be constant and would merely result in all the frequency scales being changed. The voltmeter used for observing the ordinates was calibrated on all its required ranges. The various delay lines, although not accurately calibrated, had their elements measured, and the delay of any section of a given line was compared with that of the other sections of the same line; where possible the lines were cross-checked one against another, i.e. 10 sections of the nominal 0.1μsec./section line

should give the same delay as one section of the 1μsec./ section delay line. All H.T. and heater voltages were monitored, but considerable difficulty was experienced due to main voltage drops of up to 20%. - in particular this drop affected the sensitivity of the Cossor Oscilloscope, and hence the equivalent speed of the time base (viz. chapter 4, pp 81.) Overall, the equipment was considered satisfactory.

The method of measurement of ordinates, and of computation of segmental frequency, is, however, open to large errors. As stated previously, the measurement of ordinates involves the point of intersection of three lines - the waveform being examined, the cursor lines (vertical) and the second beam of the oscilloscope which was used to measure the ordinate of the waveform at its intersection with the cursor lines. A number of readings taken at each of several ordinates showed that an accuracy better than $\pm$ 2½% could not be relied upon. Thus, since the angles θ_1 and θ_2 are computed from arc sine of ordinate/amplitude, the worst possible error in the difference ($\theta_2 - \theta_1$) is found to be approximately $\pm$10% for the order of differences used ($\approx 18^\circ$). A much more fundamental error is concerned with the amplitude A, which in all cases decreases by some 50%. This could be measured with much higher accuracy than the ordinates, being limited rather by the accuracy of reading

the voltmeter than by visual error on the oscilloscope. The peak value of such a waveform, however, is not necessarily the true length of the generating vector. Considering the exponentially degenerating waveform,

$$y = A_1 e^{-\alpha t} \sin \omega t.$$

Differentiating with respect to t and equating to zero for maxima shows that these occur when,

$$\frac{\alpha}{\omega} = \cot \omega t.$$

Thus, if $\alpha = \omega$, maxima occur when the generating vector is only 45° away from the base line: if $\alpha = 0$, there is no degeneration and the maxima occur when the vector is 90° from the base-line. This shows that although the peak voltage, A, was measured here, it was not the true length of the generating vector but the projection, on the vertical axis, of the true length. This error increases as α increases and ω decreases, but in the tests herein it never exceeded about 7%, for the values of α and ω used. The possible over-all error would therefore appear to be of the order of $\pm$ 15%; but it has been seen that the experimental results were accurate to within $\pm$ 10% and the above estimate is therefore pessimistic with regard to the conditions obtaining in practice.

The method is cumbersome, however, great labour being required in taking the initial readings, computation, and plotting: single points are not easily checked, and it

was found that very considerable eye-strain and fatigue were produced by the method of obtaining the ordinates. The segmental method in its present form is therefore unsuitable for an investigation of wide scope or high accuracy; it is also unsuitable for use with small percentage variations in frequency. It is, however, to the best of belief, the only method in existence whereby a waveform may be analysed experimentally in terms of instantaneous frequency, thereby allowing the existence of frequency transients to be shown.

It is recalled that the methods set out in Chapter 3 involving the measurement of the angle of the tangent to a point on a surve were dismissed partly because of the difficulty in obtaining this angle accurately. An optical method of obtaining this angle has been described[39] utilising a narrow base triangular prism with a small apex angle opposite the base. This optical method would be difficult to apply directly to an oscilloscope screen, and would still require the measurement of the ordinate at the tangent point, for,

$$-(\omega_{inst.})^2 = \frac{d^2y}{dt^2} / y,$$

at any ordinate y for any waveform whatever. The curve of dy/dt would have to be plotted against time to obtain $\ddot{y}$, and the overall accuracy would not be high. It is seen that it is possible for $\omega_{inst.}$ to be either real or complex, whereas the segmental frequency is always real;

whether or not $\omega_{inst.}$ would assume imaginary values remains to be proved. The optical method, however, does provide another means of attack on the problem, which may form the basis of future work on this subject.

A second more complicated, but very much more accurate, method which could be used is based on an elaboration of the present segmental idea. It was produced by McQueen[40] for a rather different purpose, and was a device such that the ordinate of a curve is measured at any instant of time; the only basic requirement is a pulsed repetitive waveform. Therein, a narrow strobe samples repetitively the ordinates of points on the waveform to be analysed, but although the time-separation of each successive strobe point is, say 0.01μ sec., the strobes occur at a relatively slow repetition frequency, which can be as low as a few hundred pulses per second. Thus the high frequency waveform is, in effect, drawn in replica on a very slow time-base. If the repetition frequency can be made so low, the electrical output could easily be made to actuate a mechanical device, such that the waveform could be mechanically differentiated twice. A simple pen tracer would give the actual waveform, thus allowing the computing of $\omega_{inst.}$ to a very high degree of accuracy. Due to its complexity, this method is hardly suitable for individual effort, but is feasible if, at any time,

the problem was considered to warrant such attention.

The results may be interpreted physically as follows.

From group (1) tests, i.e. constant initial frequency and variable L/C ratio the duration of the transient apparently increases as the average initial energy content of the oscillator tuned circuit decreases. But the lower the initial energy content (high L/C ratio) the greater was the change in energy. It has been found, however, that the duration does not depend on the frequency swing, which, related to the change in energy, was in all cases comparatively large. The frequency change had to be large, since the overall accuracy was low, and thus no results could be obtained with frequency changes small relative to the original frequency. It can only be concluded that, provided the change in energy is great enough, the duration of the resulting frequency transient depends only on the average initial content of the resonant circuit. The phase of the switching pulse with respect to the r.f. cycle, will almost certainly be of importance, at least in the case of the overshoot, but if the above conclusion is true then it will have no effect on transient duration. The accurate measurement of this phase is difficult in practical application, since obtainable pulses are inevitably round-cornered ramp functions at leading and trailing edges. A controlled rate of rise of the

switch pulse would allow investigation of the deduction of zero duration frequency transient for the ratio, (Original Frequency of oscillation/Equivalent modulating frequency) equal to, or greater than, unity (or two, if using average frequency).

Finally, it must be emphasized that all the above work and conclusions refer to the particular oscillator and reactor stage considered here, and taken as one unit; nowhere is it to be assumed that these findings apply to a resonant circuit in which the capacitance is instantaneously varied. The equivalent input circuit to the reactor stage used, is, during the leading edge of the switching pulse, dependent on the ia/vg characteristics of the two valves, where the non-linear portions of these characteristics are all-important. Thus, analysis is much too complex to be useful, since, in general, frequency modulation is brought about by a signal applied to the input of a reactor valve, and it is the resulting frequency changes at the oscillator output that are important. Further, in an oscillator employing coupled circuits the degree of coupling would certainly enter into the transient duration, and hence these results apply only to the general type of oscillator used herein, which has been used in practical radio-telemetry in modified free-running form.

CHAPTER 6.

GENERAL CONCLUSIONS.

With no theoretical verification available, it was assumed that a frequency-modulated oscillator was incapable of instantaneous variation of frequency. An experimental investigation of this assumption was carried out for an approximate step function modulating waveform; if the assumption was true, the frequency was expected to pass through a transient state before reaching the new steady-state value. The requirement was therefore to detect and measure a rapidly fluctuating frequency.

Most methods of frequency measurement were found to be inherently unsuitable. Methods involving the following of the test frequency by a subsidiary tone were discarded on the grounds of physical incapability of varying the latter at the required speed; also, the subsidiary tone itself may have a transient frequency response. Considering an abrupt frequency change as the instantaneous cessation of one frequency and application of another, an operational analysis of a parallel resonant circuit showed the inclusion of a transient term in the resultant output voltage function, which modified both the amplitude and phase of the steady-state solution. Any frequency sensitive circuit, which was also sensitive to

amplitude and/or phase, utilising such a resonant circuit was therefore unsuitable. Two such circuits are the Foster-Seeley Discriminator and the Ratio Detector, the former being both amplitude and phase sensitive, the latter only phase sensitive. Both circuits were rejected primarily on the above grounds, the necessary diode load time-constants forming a separate objection to their use. Of the bridge circuits considered, the Parallel-T feed-back amplifier was explored as the most useful of all; the Parallel-T circuit contains only resistance and capacitance, and its input and output circuits have a common terminal. The steady-state response of this circuit was similar to that of a resonant circuit; to utilise such a response to measure a frequency variation involved the use of the sloping side of the response curve. Under this condition, the sensitivity of the Parallel-T amplifier in terms of output voltage change per Kc/s change in input frequency, was found to be low. The gain, and hence sensitivity, of this amplifier could not be increased without limit, since the free transmission between output and input of all frequencies outwith a narrow band made stabilisation difficult. This is particularly true with a rapidly fluctuating input.

An attempt to measure the response of the above mentioned circuits to an abrupt change in frequency failed, and only a general conclusion could be drawn.

The Parallel-T amplifier gave a much more rapid response than the Discriminator, but the sensitivity of the latter was many times greater than that of the former. This test failed due to the impossibility of synchronisation between two local-oscillator frequencies and the repetition rate at which they were alternately switched to the circuit under test. This demonstrated most clearly the need for absolute synchronism in the system and a pulse controlled system was developed forthwith.

Since any frequency sensitive circuit possesses some electrical inertia, a more direct method of frequency measurement was sought using oscilloscopic techniques; in general, these permit the accurate determination of the time interval between any two points on a waveform. Time measuring techniques from the art of radar were investigated, and, although found inapplicable in themselves, led directly to the evolution of the segmental method of frequency analysis. Therein, from any segment of the waveform a particular value of frequency may be found, called the segmental frequency, which exists only for the particular segment under examination; the segmental frequency is the average value of the true instantaneous frequency over the segment. Therefore the segmental frequency may be found from the average angular velocity of the

generating vector, over the segment. It was demonstrated that this may be found from a variety of measurements upon the segment, all the methods, however, requiring some approximation or assumption. The particular method used was considered the most accurate, for no approximation was required, but the assumption was made that the amplitude of the generating vector could be found and that it varied smoothly throughout the transient period; this latter assumption is true in general, the amplitude decaying, say, as a simple or compound exponential function of time. Further, the only measurements required to be made on the segment, other than its time duration (which was essential to all methods) were the values of the ordinates at the extremities of the segment. All measurements were taken from the screen of an oscilloscope, which limited the accuracy to a maximum of $\pm$ 2½%. Also, the peak amplitude of a time-degenerative waveform as measured on an oscilloscope screen is not necessarily the true length of the generating vector. Therefore, the overall accuracy of the method was considered to be within $\pm$ 10%. Suitable equipment was designed for the isolation of short, successive, segments of the waveform to be analysed, the segments being displayed on an oscilloscope utilising a double-beam cathode-ray tube for measurement purpose.

For the purpose of this investigation, three dimensionless variables were defined. For a constant initial (unmodulated) frequency f_o, arbitrary values of tuning capacitance, C_o, and inductance, L_o were chosen, giving the ratio $R_o = L_o/C_o$; all other values of this ratio, denoted by R, were referred to R_o by,

$$R = \frac{a L_o}{C_o/a} = a^2 R_o, \quad 0 \leq a^2 \leq \infty.$$

Secondly, for constant $(a)^2$ and variable frequency f, all values of f were referred to f_o by the numeric b:-

$$f = \frac{1}{2\pi\sqrt{b.(aL_o).\frac{bC_o}{a}}} = \frac{f_o}{b}, \quad 0 \leq b \leq \infty.$$

Finally, the numeric $e = \delta f/f$ was defined, where δf was the difference between the initial steady-state frequency, f, and the final steady-state frequency, f_1. Analysis of the results was in terms of these positive numerics, a^2, b, and e.

For step function modulation, of rise-time approximately one tenth of the unmodulated waveform period, the frequency of the oscillator was found to pass through an oscillatory transient condition. For constant initial frequency, the duration, T, of the frequency transient was found to be a linear function of a: for constant $(a)^2$, T was found to be proportional to some function of b. From these latter results, by extrapolation, it appeared that no transient in

segmental frequency would be observed, for any value of $(a)^2$, for an equivalent modulating frequency less than the unmodulated frequency: in terms of average frequency, no transient would be observed for a modulating frequency less than twice the unmodulated frequency. These findings could not be verified experimentally due to limitations in the test equipment, but if they are correct they give the upper limit of the equivalent modulating frequency in any form of pulse-modulated F-M system, viz., frequency shift telegraphy, F-M television, and, of course, F-M telemetry. For the range of modulating frequency equal to, or up to twice, the unmodulated frequency, although the segmental frequency should be oscillatory, its average value should be constant; this was borne out by the trend of the primary graphs over the experimental range, thereby giving some justification for the conclusions drawn from the extrapolations. For decreasing frequency the transient duration appeared bounded, the limiting value of T depending on $(a)^2$. For audio frequencies the transient would be completed in less than one cycle of the final steady-state frequency (for step function modulation), and would pass unnoticed.

The dependence of T upon $(a)^2$ and b was most conveniently shown graphically, although an empirical

expression of good accuracy over the practical range of the variables was also derived. From the graphs, several other independent test results were predicted and an oscillator was designed to a given specification. The accuracy of prediction and design was found experimentally to be within ±10%. The results of independent test groups were also found to cross-check at common points within the stated accuracy.

The frequency swing, δf, had apparently no effect on the transient duration, but the numeric e determined the overshoot in frequency; if f_1 was the final steady-state frequency, the minimum frequency attained by the transient was given by $(1 - e)f_1$, over the experimental range. It was deduced that this relationship may not be applied outwith the given range.

It is concluded, from physical considerations of the oscillator circuit and modulation used, that provided the change in the energy content of the resonant circuit is great enough, the duration of the resulting frequency transient depends only on the average initial energy content of this circuit.

The object of this experimental investigation has thus been fulfilled. The existence of frequency transients has been shown and their dependence on circuit parameters has been explored within the limits of the method used. The results have been found to

cross-check on common points, and used to design an experimental circuit whose actual performance agreed with that predicted. Since the method was already so laborious, it was felt that more detailed investigation on one particular oscillator-reactor unit, or general investigation on a variety of oscillator-reactor circuits, would yield very little profitable result, and was not justified.

The immediate usefulness of the results of this work is in the art of radio-telemetry, as has been shown. In the future, they may be applicable to any system of F-M television, which is envisaged just now, or to any form of frequency-shift telegraphy requiring larger frequency changes than are used now. In general, the results are applicable to any form of pulse-modulated F-M system.

In conclusion, this work is not presented with any degree of finality, but rather as a primary investigation into a phenomenon which can be of importance, and which appears to have had no attention paid to it previously, possibly by reason of the unusual experimental and analytical work that is involved.

APPENDIX I. The Transient Response of a Parallel L,C,R, Network.

Consider a parallel connection of R, L, C, fed from a constant current source, e.g. a pentode valve.

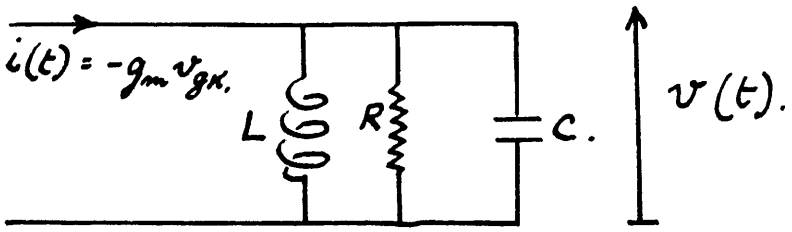

The differential equation for the voltage v(t) is :-

$$i(t) = \frac{v(t)}{R} + \frac{1}{L}\int v(t)dt + C\frac{d}{dt}v(t).$$

Assuming v(t) is zero at time t = o, the Laplace Transform of the above is :-

$$i(p) = \frac{v(p)}{R} + \frac{1}{L}\cdot\frac{v(p)}{p} + C\,p\,v(p).$$

whence

$$v(p) = \frac{i(p)}{C}\cdot\frac{p}{(p+\frac{1}{2CR})^2 + \frac{1}{LC} - \frac{1}{4C^2R^2}}$$

$$= \frac{i(p)}{C}\cdot\frac{p}{(p+\alpha)^2 + \omega_0^2}$$

where i(p) and v(p) are $\mathcal{L}$ i(t) and $\mathcal{L}$ v(t) respectively, and

$$\alpha = \frac{1}{2CR}\ ,\quad \omega_0^2 = \frac{1}{LC} - \alpha^2.$$

Now let $i(t) = I \sin(\omega t + \theta).\ U(t)$.

$$\therefore\ i(p) = \frac{I.\omega\cos\theta}{p^2+\omega^2} + \frac{I.p\sin\theta}{p^2+\omega^2}$$

$$i.e.,\ v(p) = \frac{I}{c}\cdot\cos\theta.\ \frac{p\,\omega}{\left[(p+\alpha)^2+\omega_o^2\right]\left[p^2+\omega^2\right]}$$

$$+\frac{I}{c}\cdot\sin\theta.\ \frac{p^2}{\left[(p+\alpha)^2+\omega_o^2\right]\left[p^2+\omega^2\right]}$$

$$= V_1(p) + V_2(p).$$

Hence the Bromwich Integral becomes,

$$v(t) = \frac{1}{2\pi j}\int_{c-j\infty}^{c+j\infty} v(p).e^{pt}\,dp.$$

$$= \frac{1}{2\pi j}\int_{c-j\infty}^{c+j\infty} V_1(p)\,e^{pt}\,dp + \frac{1}{2\pi j}\int_{c-j\infty}^{c+j\infty} V_2(p)\,e^{pt}\,dp.$$

$$= I_1 + I_2.$$

Considering I_1 and I_2 as contour integrals, they may be evaluated by summing their residues at the poles of V_1 and V_2. These latter functions each yield four first order poles occurring at,

$$p = -\alpha \pm j\omega_o,$$

$$p = \pm j\omega.$$

both V_1 and V_2 having poles at these values of p. Considering I_1 alone, two of the residues will be multiplied by the exponential $e^{-\alpha t}.\ e^{\pm j\omega_o t}$. These two residues will form the transient term in the solution of I_1 due to the time degenerative factor $e^{-\alpha t}$. The other two residues of I_1 will be

multiplied by $e^{\pm j\omega t}$, and will form the steady state solution. The same reasoning applies exactly to I_2.

The admittance of the circuit to a cisoidal source is,

$$Y = \frac{1}{R} + \frac{1}{j\omega L} + j\omega C.$$

$$= \frac{C}{j\omega}\left[\frac{j\omega}{CR} - \omega^2 + \frac{1}{LC}\right].$$

$$= \frac{C}{j\omega}\left[\omega_0^2 + (\alpha + j\omega)^2\right].$$

$$\therefore Z = \frac{j\omega}{C} \cdot \frac{1}{\omega_0^2 + (\alpha + j\omega)^2}$$

$$= \frac{1}{C} \cdot \frac{j\omega}{a + jb} \quad \text{where} \begin{cases} a = \alpha^2 + \omega_0^2 - \omega^2, \\ b = 2\alpha\omega \end{cases}$$

$$= \frac{\omega}{C\sqrt{(a^2+b^2)}} \cdot \left[\frac{b}{\sqrt{(a^2+b^2)}} + j\frac{a}{\sqrt{(a^2+b^2)}}\right].$$

whence,

$$\cos\phi = \frac{b}{\sqrt{(a^2+b^2)}} \; ; \; \sin\phi = \frac{a}{\sqrt{(a^2+b^2)}},$$

$$|Z| = \frac{\omega}{C\sqrt{(a^2+b^2)}}.$$

Writing the residues of I_1 and I_2 for the steady-state solution gives,

$$p = +j\omega; \; A_1 = \frac{j\omega}{C} \cdot \frac{I\cos\theta}{(\alpha + j\omega)^2 + \omega_0^2} \cdot \frac{e^{j\omega t}}{2j}$$

$$- \frac{\omega}{C} \cdot \frac{I\sin\theta}{(\alpha + j\omega)^2 + \omega_0^2} \cdot \frac{e^{j\omega t}}{2j}.$$

$$= \frac{j\omega}{c} \cdot \frac{I\cos\theta}{a+jb} \cdot \frac{e^{j\omega t}}{2j} - \frac{\omega}{c} \cdot \frac{I\sin\theta}{a+jb} \cdot \frac{e^{j\omega t}}{2j}$$

$$p = -j\omega_j \; A_2 = \frac{j\omega}{c} \cdot \frac{I\cos\theta}{(\alpha - j\omega)^2 + \omega_0^2} \cdot \frac{e^{-j\omega t}}{2j}$$

$$+ \frac{\omega}{c} \cdot \frac{I\sin\theta}{(\alpha - j\omega)^2 + \omega_0^2} \cdot \frac{e^{-j\omega t}}{2j}$$

$$= \frac{j\omega}{c} \cdot \frac{I\cos\theta}{a - jb} \cdot \frac{e^{-j\omega t}}{2j} + \frac{\omega}{c} \cdot \frac{I\sin\theta}{a - jb} \cdot \frac{e^{-j\omega t}}{2j}$$

Hence, since the steady state solution is the sum of the residues,

$$A_1 + A_2 = \frac{\omega I\cos\theta}{c} \left[\frac{b+ja}{a^2+b^2} \cdot \frac{e^{j\omega t}}{2j} + \frac{ja-b}{a^2+b^2} \cdot \frac{e^{-j\omega t}}{2j} \right]$$

$$+ \frac{\omega I\sin\theta}{c} \left[\frac{a+jb}{a^2+b^2} \cdot \frac{e^{-j\omega t}}{2j} - \frac{a-jb}{a^2+b^2} \cdot \frac{e^{j\omega t}}{2j} \right].$$

$$= I|Z|\cos\theta \left[\frac{b}{\sqrt{(a^2+b^2)}} \sin\omega t + \frac{a}{\sqrt{(a^2+b^2)}} \cos\omega t \right]$$

$$+ I|Z|\sin\theta \left[\frac{b}{\sqrt{(a^2+b^2)}} \cos\omega t - \frac{a}{\sqrt{(a^2+b^2)}} \sin\omega t \right]$$

$$= I|Z|\cos\theta \left[\cos\varphi \sin\omega t + \sin\varphi \cos\omega t \right]$$

$$+ I|Z|\sin\theta \left[\cos\varphi \cos\omega t - \sin\varphi \sin\omega t \right]$$

$$= I|Z| \left[\cos\theta . \sin(\omega t + \varphi) + \sin\theta . \cos(\omega t + \varphi) \right]$$

$$= I|Z| \sin(\omega t + \theta + \varphi).$$

This is the expected final steady state term.

The transient terms are best manipulated separately, and hence dealing with I_1 first, the relevant residues are :-

$$p = -(\alpha + j\omega_0);\ A_3 = \frac{\alpha + j\omega_0}{2j\omega_0} \cdot \frac{I\cos\theta}{c.} \cdot \frac{\omega e^{-(\alpha+j\omega_0)t}}{(\alpha+j\omega_0)^2 + \omega^2}$$

$$p = -(\alpha - j\omega_0);\ A_4 = \frac{-(\alpha - j\omega_0)}{2j\omega_0} \cdot \frac{I\cos\theta}{c.} \cdot \frac{\omega e^{-(\alpha-j\omega_0)t}}{(\alpha-j\omega_0)^2 + \omega^2}.$$

But,

$$(\alpha + j\omega_0)^2 + \omega^2 = \alpha^2 + \omega^2 - \omega_0^2 + j2\alpha\omega_0 = f + jg.$$

$$\therefore (\alpha - j\omega_0) + \omega^2 = f - jg.$$

Also,

$$a + jb = \alpha^2 + \omega_0^2 - \omega^2 + j2\alpha\omega.$$

$$\therefore a^2 + b^2 = f^2 + g^2.$$

$$\text{and } |Z| = \frac{\omega}{c} \cdot \frac{1}{\sqrt{(f^2+g^2)}},$$

$$\cos\phi = \frac{b}{\sqrt{(a^2+b^2)}} = \frac{g}{\sqrt{(f^2+g^2)}} \cdot \frac{\omega}{\omega_0}$$

$$\text{i.e., } \frac{g}{\sqrt{(f^2+g^2)}} = \frac{\omega_0}{\omega} \cdot \cos\phi.$$

Similarly,

$$\sin\phi = \frac{a}{\sqrt{(a^2+b^2)}} = \frac{f}{\sqrt{(f^2+g^2)}} + \frac{2\omega_0^2}{\sqrt{(f^2+g^2)}} - \frac{2\omega^2}{\sqrt{(f^2+g^2)}}.$$

$$= \frac{f}{\sqrt{(f^2+g^2)}} + \frac{\omega_0^2}{\alpha\omega}\cos\phi - \frac{\omega}{\alpha}\cos\phi.$$

$$\therefore \frac{f}{\sqrt{(f^2+g^2)}} = \sin\phi + \frac{\omega}{\alpha}\left(1 - \frac{\omega_0^2}{\omega^2}\right)\cos\phi.$$

Using these identities and summing A_3 and A_4 gives,

$$A_3 + A_4 = e^{-\alpha t}\frac{I\cos\theta}{C}\left[\frac{\alpha\omega}{2j\omega_0}\cdot\frac{e^{-j\omega_0 t}}{f+jg} + \frac{\omega}{2}\cdot\frac{e^{-j\omega_0 t}}{f+jg} - \frac{\alpha\omega}{2j\omega_0}\cdot\frac{e^{j\omega_0 t}}{f-jg} + \frac{\omega}{2}\cdot\frac{e^{j\omega_0 t}}{f-jg}\right].$$

$$= \frac{e^{-\alpha t}\cdot\omega I\cos\theta}{C(f^2+g^2)}\left[\frac{\alpha}{\omega}\left(-f\sin\omega_0 t - g\cos\omega_0 t\right) + \left(f\cos\omega_0 t - g\sin\omega_0 t\right)\right]$$

$$= I|Z|e^{-\alpha t}\cos\theta\left[\sin\phi\cos\omega_0 t + \frac{\sin\omega_0 t}{\omega_0}\left(\alpha\sin\phi + \omega\cos\phi\right)\right].$$

which is the resulting transient term from I_1.

Now writing the residues for I_2 at the same poles gives :-

$$p = -(\alpha+j\omega_0);\quad A_5 = -\frac{I\sin\theta}{2j\omega_0 C}\cdot\frac{(\alpha+j\omega_0)^2 e^{-(\alpha+j\omega_0)t}}{(\alpha+j\omega_0)^2+\omega^2}.$$

$$p = -(\alpha-j\omega_0);\quad A_6 = \frac{I\sin\theta}{2j\omega_0 C}\cdot\frac{(\alpha-j\omega_0)^2 e^{-(\alpha-j\omega_0)t}}{(\alpha-j\omega_0)^2+\omega^2}.$$

Here, in the numerators,

$$(\alpha+j\omega_0)^2 = \alpha^2 + j2\alpha\omega_0 - \omega_0^2 = (f+jg) - \omega^2$$

$$(\alpha-j\omega_0)^2 = \alpha^2 - j2\alpha\omega_0 - \omega_0^2 = (f-jg) - \omega^2$$

Hence, since the denominators are $2j\omega_0 C.(f\pm jg)$, rationalising and adding A_5 and A_6 gives,

$$A_5 + A_6 = \frac{I\sin\theta e^{-\alpha t}}{2j\omega_0 C}\left[\frac{f^2+g^2-\omega^2(f+jg)}{f^2+g^2}\cdot e^{j\omega_0 t} - \frac{f^2+g^2-\omega^2(f-jg)}{f^2+g^2}\cdot e^{-j\omega_0 t}\right].$$

$$= \frac{I\sin\theta e^{-\alpha t}}{2j\omega_0 C}\left[e^{j\omega_0 t} - \frac{\omega^2(f+jg)}{f^2+g^2}e^{j\omega_0 t} - e^{-j\omega_0 t} + \frac{\omega^2(f-jg)}{f^2+g^2}e^{-j\omega_0 t}\right]$$

$$= \frac{I \sin\theta . e^{-\alpha t}}{\omega_0 C.} \sin\omega_0 t - \frac{\omega I \sin\theta e^{-\alpha t}}{c\sqrt{(f^2+g^2)}} \cdot \left[\frac{\omega}{\omega_0} \cdot \frac{f + jg.}{\sqrt{(f^2+g^2)}} e^{j\omega_0 t} \right.$$

$$\left. - \frac{\omega}{\omega_0} \cdot \frac{f - jg.}{\sqrt{(f^2+g^2)}} e^{-j\omega_0 t} \right]$$

$$= \frac{I \sin\theta . e^{-\alpha t}}{\omega_0 C.} \sin\omega_0 t - I|z| e^{-\alpha t} \sin\theta \left[\cos\omega_0 t . \cos\theta . \right.$$

$$\left. + \frac{\omega}{\omega_0} . \sin\omega_0 t \left\{ \sin\phi + \frac{\omega}{\alpha}\left(1 - \frac{\omega_0^2}{\omega^2}\right)\cos\phi \right\} \right].$$

This is the transient term resulting from I_2. Hence the full transient term is the summation of $(A_3 + A_4 + A_5 + A_6)$.

$$A_3 + A_4 + A_5 + A_6 = \frac{I e^{-\alpha t}}{\omega_0 C} \sin\theta \sin\omega_0 t - I|z| e^{-\alpha t} \left[\cos\theta \sin\phi \cos\omega_0 t \right.$$

$$+ \sin\theta \cos\phi \cos\omega_0 t + \frac{\omega}{\omega_0} \sin\theta \sin\phi \sin\omega_0 t$$

$$+ \frac{\alpha}{\omega_0} \cos\theta \sin\phi \sin\omega_0 t + \frac{\omega}{\omega_0} \cos\theta \cos\phi \sin\omega_0 t$$

$$\left. + \frac{\omega^2}{\alpha \omega_0}\left(1 - \frac{\omega_0^2}{\omega^2}\right)\cos\phi . \sin\theta . \sin\omega_0 t \right].$$

Now the last term in the brackets gives,

$$\frac{\omega^2}{\alpha \omega_0}\left(1 - \frac{\omega_0^2}{\omega^2}\right)\cos\phi = \frac{\omega}{\omega_0} \cos\phi . \left[\frac{\omega^2 - \omega_0^2}{\alpha \omega} \right]$$

$$= \frac{\omega}{\omega_0} . \frac{b}{\sqrt{(f^2+g^2)}} . \frac{\omega^2 - \omega_0^2}{b/2.}$$

$$= \frac{\omega}{\omega_0} . \frac{2(\omega^2 - \omega_0^2)}{\sqrt{(f^2+g^2)}.}$$

$$= \frac{\omega}{\omega_0} . \frac{(-2a)}{\sqrt{(a^2+b^2)}.} + \frac{\omega}{\omega_0} . \frac{2\alpha^2}{\sqrt{(a^2+b^2)}.}$$

$$= - \frac{2\omega}{\omega_0} \sin\phi + \frac{\alpha}{\omega_0} \cos\phi .$$

Hence the last term becomes,

$$\frac{\omega^2}{\alpha\omega_0^2}\left(1-\frac{\omega_0^2}{\omega^2}\right)\cos\phi\sin\theta\sin\omega_0 t = -2\frac{\omega}{\omega_0}\cdot\sin\phi.\sin\theta.\sin\omega_0 t + \frac{\alpha}{\omega_0}\cos\phi.\sin\theta.\sin\omega_0 t.$$

Thus grouping the terms, the transient solution for the circuit is,

$$v_t = \frac{Ie^{-\alpha t}}{\omega_0 C}\sin\theta.\sin\omega_0 t - I|z|e^{-\alpha t}\left[\cos\omega_0 t.\sin(\theta+\phi) + \frac{\omega}{\omega_0}\cdot\sin\omega_0 t.\cos(\theta+\phi) + \frac{\alpha}{\omega_0}\cdot\sin\omega_0 t.\sin(\theta+\phi)\right],$$

which is the required result.

Although the form of the result presented above has been found by others, mainly by classical calculus analysis, the result normally obtained from an operational analysis is composed of complex and conjugate impedance terms, yielding little information without considerable interpretation. Therefore, the novel method of manipulation of the residues shown above was developed to obtain the simplest result, and clarify the procedure. It also facilitates the modification required for the special case of $\omega = \omega_0$, when a second order pole is obtained.

BIBLIOGRAPHY.

CHAPTER 1.

1. 'Telemetering from V2 Rockets' Heeren (and others); Electronics, March, April 1947.

2. 'Electronic Commutating for Telemetering', Rauch; Electronics, February 1947.

3. 'Frequency Modulation'. Balth van der Pol; Proc.I.R.E. Vol.18. July 1930 pp.1194

4. 'The Fundamental Principles of Frequency Modulation'. Balth van der Pol; Journ.I.E.E. III.1946 pp.153

5. 'Theory and Application of Mathieu Functions' (book) McLaghlan; Oxford Univ. Press, 1947.

6. 'Sinusoidal Variation of a Parameter in a Simple Series Circuit', Maginnis; Proc. I.R.E. January, 1941.

7. 'Notes on Modulation'. Brainerd; Proc.I.R.E. March 1940.

8. 'Frequency Modulation' (book) Hund; McGraw Hill, New York 1942.

9. 'Trigonometric Components of a Frequency Modulated Wave' Cambi; Proc. I.R.E. January 1948.

10. 'On Superregeneration of an ultra short-wave Receiver' Ataka; Proc. I.R.E. August 1935.

11. 'Further studies of oscillatory circuits having periodically varying Parameters'. Barrow, Smith and Bauman; Journ. Frank Inst. March and April 1936.

12. 'Solution of Mathieu's Equation' Brainerd & Weygandt; Phil. Mag. Vol.30 December 1940.

13. 'Stability of Oscillations in Systems obeying Mathieu's Equation', Brainerd; Journ.Frank Inst., February 1942.

14. 'On Parametric Excitation', Minorsky; Journ. Frank Inst., July 1945.

15. 'Solution of the Mathieu Equation'. Gray, Mortin and Brainerd; Trans. A.I.E.E. Vol.67,1948; pp.429.

16. 'A New Electrical method of Frequency Analysis, and its Application to Frequency Modulation'. Barrow; Proc. I.R.E. Vol.20, October 1932.

17. 'Frequency Modulation and the Effects of a Periodic Capacity Variation in a non-dissipative Oscillatory Circuit'. Barrow; Proc. I.R.E., Vol.21 August 1933.

18. 'On the Oscillations of a Circuit having a Periodically Varying Capacitance'. Barrow; Proc. I.R.E. Vol.22, February 1934.

19. 'The Optimum Performance of a Wave Analyser', Barber; Electronic Engineering, Vol.21, May 1949.

CHAPTER 2.

20. 'Transients in Frequency Modulation', Salinger; Proc. I.R.E. pp. 378, 1942.

21. 'Carrier Frequency Amplifiers', Eaglesfield; Wireless Engineer, Vol.23. April 1946. pp.97

22. 'Radio Frequency Electrical Measurements' (book), Brown; McGraw-Hill, New York, 1938.

23. 'A New Type of Selective Circuit and some Applications'. Scott; Proc. I.R.E., Vol.26, February 1938.

24. 'Bridged-T and Parallel-T Null Circuits for Measurements at Radio Frequencies'. Tuttle; Proc.I.R.E. January 1940.

25. 'Design of Parallel-T Networks for R-C Oscillators' Lynch and Robertson; A.W.A. Tech. Rev., September 1946.

26. 'Parallel-T R-C Networks'. Wolf; Proc. I.R.E. September 1946.

27. 'Parallel-T Bridge Amplifier', Millman; Journ. I.E.E. III January 1947.

28. 'Automatic Tuning, Simplified Circuits and Design Practice', Foster and Seeley; Proc. I.R.E., March 1937.

29. 'Automatic Frequency Control', Travis; Proc. I.R.E. October 1935.

30. 'Theory of the Discriminator Circuit for Automatic Frequency Control', Roder; Proc.I.R.E. May 1938.

31. 'The Ratio Detector'. Seeley & Avins; R.C.A. Review, Vol.8. June 1947, pp.201.

32. 'F.M. Ratio Detector'. Peters; Communications, November 1945.

CHAPTER 4.

33. 'Pulse Modulated Oscillator', Easton; Electronics, March 1947.

34. 'The Multivibrator, Applied Theory and Design', Shenk; Electronics, 17, January, February and March 1944.

35. 'Cathode-coupled Multivibrator', Glegg; Proc. I.R.E. June 1950.

36. 'Reactance Valve Frequency Modulator', Williams; Wireless Engineer, August 1943.

37. 'Reactance Modulator Theory', Butler; Wireless Engineer, March 1948.

38. 'The Cathode Follower', Parker; Electronic Engineering,1948. pp. 12, 55, 92, 126.

CHAPTER 5.

References 4, 5, 6, 7, 11 and 17 as for Chapter 1, and,

39. 'Drawing Tangents and Normals to Plane Curves'. Harker; Engineering Vol.161, March 1946 pp.209.

40. 'Monitoring of High Speed Waveforms'. McQueen; Electronics, October 1952.

41. 'Bandwidth of a Sinusoidal Carrier, Frequency-Modulated by a Rectangular Wave with half Sine-wave Build-up', Cawthra and Thomson; Journ I.E.E. III, 98 January 1951.